Moment Resistance of Strong-Axis Open-Section Beam-to-Column Welded Steel Joints

Final Report

Luis Simões da Silva
Jorge Conde
Filip Ljubinković
João Pedro Martins
Francisca Santos
Fernando Freire
Juan Aguiar

December, 2024

This Report has been developed in the framework of a collaboration between ISISE (Institute for Sustainability and Innovation in Structural Engineering) and IDEA StatiCa. This project has been funded jointly by both entities.

The University of Coimbra University of Coimbra (UC) is a reference in higher education and R&D in Portugal, due to the quality of the courses taught at its eight colleges and to the advances achieved in pure and applied research in various scientific domains and on technology-related areas. ISISE – Institute for Sustainability and Innovation in Structural Engineering is a Research, Development & Innovation Centre formed in 2007 that focuses on the Structural and Functional Performance of Construction Works.

This document reports on the results of the study. It is complemented by 8 appendices that detail individual results. The full report is formed by the following documents:

1. REPORT (this document).
2. APPENDIX I (summary of relevant tables and figures).
3. APPENDIX II (FE results – BR-S275-EPPL).
4. APPENDIX III (FE results – BB-S275-EPPL).
5. APPENDIX IV (FE results – FR-S275-EPPL).
6. APPENDIX V (FE results – BF-S275-EPPL).
7. APPENDIX VI (FE results – BR-S235-EPPL).
8. APPENDIX VII (FE results – BR-S355-EPPL).
9. APPENDIX VIII (FE results – BR-S275-QUAD).

Each of the Appendices II to VIII corresponds to a specific cluster of the study. More details can be found in Section 2.4 of the current document.

Executive Summary

This report presents a thorough analysis of welded beam-to-column steel joints with a specific focus on the column web in shear component, using properly validated, high-quality 3D-FEM models. The study comprises strong-axis moment-resisting welded open-section beam-to-column joints, with and without transverse stiffeners, covering one-sided and two-sided joints located at either an intermediate (internal) or last story (roof), and, for internal joints, with different levels of column axial load. The study comprises a wide range of situations in terms of column slenderness, joint aspect ratio, joint configuration, stiffeners, axial force, and moment ratio (for two-sided joints). FE-relevant aspects, such as material model, analysis type, mesh density, initial imperfections, etc. are also considered.

The current study supplements a previous one (hereinafter referred to as 'Phase I') in the following ways:

1. The set list has been expanded to include cases with 30% and 70% axial load (in Phase I only 50% axial load was included).
2. The steel grades include S235, S275 and S355 (in Phase I only S275 was contemplated).
3. Welded columns are discussed (in Phase I only rolled columns were considered).
4. A comprehensive study on the differences between GMNA and MNA has been included (in Phase I this was done only for some sets).
5. A comprehensive study on the influence of the material constitutive law has been included (in Phase I this was done only for some sets).
6. The influence of fillet welds on the joint behavior is studied (not discussed in Phase I).

This report includes all results of Phase I and can be used as a stand-alone document.

Objectives

The objective of this study is the assessment of strong-axis bending-moment resistance of welded joints in one- and two-sided beam-to-column configurations with open-section members (beams and columns), including the influence of transverse stiffeners, using: i) European design rules, ii) FEA (3D solid elements) and iii) IDEA StatiCa; and the comparison of results obtained by each method.

Methodology

1. Assess the design resistance of the web panel component for a wide range of welded beam-to-column joints through high-quality 3D FEM models, used subsequently as benchmark cases.
2. Compare the joint resistance with CBFE models (IDEA StatiCa), based on shell elements.
3. Discuss the possibility of improving the features and default options offered by IDEA StatiCa to ensure that a realistic and safe value of resistance is obtained.
4. Compare the joint resistance with results obtained from design expressions provided in Eurocode 3, current and forthcoming versions.
5. Assess the differences in moment resistance produced by the 5% equivalent plastic strain criterion adopted by IDEA StatiCa to define the 'design resistance' on the moment-rotation

curve, versus other common criteria (such as the relaxation of the secant stiffness to 1/3 of the initial stiffness).

Questions addressed

- What is the scatter of results?
- What is the influence of the different parameters (slenderness, aspect ratio, bending moment ratio, transverse stiffeners, axial force, etc.) on these results?
- What is the influence of the column web components on these results?

Exclusions

No reliability assessment of program results is carried out, as it is outside the scope of this study.

Summary of conclusions

The analysis of the Abaqus results has highlighted the following conclusions:

1. Regarding the 5% equivalent plastic strain criterion, it has been shown that, for this type of joint, it produces resistance results like those obtained from the same numerical model with a reduction of secant stiffness to 1/3 of the initial stiffness.
2. Initial imperfections play a minor role in the behavior of the joints analyzed; however, geometrical non-linearity (2nd order analysis) should be included, particularly in cases where the axial load is present.
3. Inclusion of strain hardening results in a small average increase of 4% in resistance, however, it has a large effect, about 44% on average, on the joint rotation.

The following comments are relevant for implementation in IDEA StatiCa:

1. IDEA StatiCa with the program's default mesh (version 23.1) and MNA (materially non-linear analysis) provides resistances which are larger than those obtained with Abaqus. On average, 6% larger for rolled columns with butt welds, and about 11% for welded columns with butt or fillet welds. For rolled columns with fillet welds the results are, on average, identical to those of Abaqus. The peak deviations observed for an individual case are 22% (rolled columns with butt welds) and 53% (welded columns with butt welds).
2. IDEA StatiCa with a refined mesh (halving the size of the default mesh) and GMNA (geometrically and materially non-linear analysis) provides resistances which are in good accordance (within ±5% on average) to the Abaqus results. The peak deviations observed for an individual case are 15% (rolled columns with butt welds), 5% (rolled columns with fillet welds), 27% (welded columns with butt welds) and 14% (welded columns with fillet welds).
3. The influence of initial imperfections was studied for one-sided internal joints and found to be negligible.
4. Purely material non-linear analysis without 2nd order effects leads to unconservative results in case of axial force on the column. Therefore, it is recommended that the geometrically non-linear analysis is activated by default in the program.
5. The mesh size plays an essential role in the accuracy of results. A potential approach to estimate the converged value could be based on an automated process that halves the mesh size and applies the Richardson extrapolation to the moment resistance obtained with both values.

6. The material model implemented by IDEA StatiCa (with E/1000 strain hardening slope) results in an average of 3% increase in moment resistance when compared to the results obtained with elastic perfectly plastic material.

Table of contents

1 Welded Beam-to-Column Joints 19
1.1 Introduction and motivation 19
1.2 Organization of the study 20
1.3 Welded Beam-To-Column Joints 20
1.4 Structural Analysis 22
1.4.1 One-sided joint, internal configuration 22
1.4.2 Two-sided joint, internal configuration 25
1.4.3 One-sided joint, roof configuration 27
1.4.4 Two-sided joint, roof configuration 28
1.4.5 Transverse stiffeners 28
1.4.6 Second-order effects 28
1.4.7 Welded columns 29
2 Methods 31
2.1 Component Method and Design Codes 31
2.1.1 The Component Method 31
2.1.2 Eurocode 3 31
2.2 FE solid models 36
2.2.1 Model description 36
2.2.2 Model validation and verification 42
2.3 CBFE models 46
2.3.1 Modeling and analysis using Python script 46
2.3.2 Model definition 46
2.3.3 Type of analysis 50
2.3.4 Geometrically non-linear analysis (GMNA) 53
2.3.5 Results extraction in case of axially loaded columns 54
2.3.6 Mesh size and Richardson extrapolation 55
2.4 Numerical Study 56
2.4.1 Scope of study and case selection 56
2.4.2 Materials 62
2.4.3 Limitations and assumptions of the study 62
2.4.4 Analysis 63
2.4.5 Post-processing and data extraction 63
3 Summary of Results 73
3.1 Generalities 73
3.1.1 Assessment metrics 73
3.1.2 Statistics 74
3.1.3 Terminology and color code 74
3.1.4 Exclusions 75
3.2 Results for rolled columns (clusters BR and FR) 76

3.2.1 Influence of material model 76
3.2.2 Influence of imperfections 76
3.2.3 Influence of steel grade 77
3.2.4 Influence of joint configuration 78
3.2.5 Influence of axial load 79
3.2.6 Influence of fillet welds 87
3.2.7 Stiffness 91
3.2.8 LBA study 94
3.3 Results for welded columns (clusters BB and BF) 102
3.3.1 Influence of joint configuration 102
3.3.2 Influence of axial load 103
3.3.3 Influence of fillet welds 110
3.3.4 Stiffness 113
4 Summary and Conclusions 117
4.1 Summary 117
Other relevant conclusions 118
4.2 Implementations for IDEA StatiCa 119
References 121

List of Figures

Fig. 1.1 – Problems treated in the study. 21
Fig. 1.2 – Section notation. 22
Fig. 1.3 – Statics of the one-sided joint at an internal story. 23
Fig. 1.4 – Lever arm for plastic sections. 23
Fig. 1.5 – Deformation of the one-sided joint at an internal story. 25
Fig. 1.6 – Statics of the two-sided joint at the internal story. 26
Fig. 1.7 – Deformation of the two-sided joint at an internal story. 27
Fig. 1.8 – Statics of the one-sided joint at the roof. 27
Fig. 1.9 – Deformation of one-sided joint at the roof. 28
Fig. 2.1 – Geometry of welds. 32
Fig. 2.2 – Geometry of beam-column fillet welds. 35
Fig. 2.3 – Solid model description. 36
Fig. 2.4 – Geometries contemplated in the numerical study. 37
Fig. 2.5 – EPPL, QUAD and E1000 material models for steel S275. 37
Fig. 2.6 – Crack locations for an unstiffened joint. 38
Fig. 2.7 – Boundary conditions and loads for the FE solid model. 39
Fig. 2.8 – Mesh sensitivity analysis for FE solid models. 40
Fig. 2.9 – FE mesh for the solid core – stiffened joint. 41
Fig. 2.10 – Initial geometric imperfections for FE solid models. 42
Fig. 2.11 – Material properties for tests from (Klein, 1985). 43
Fig. 2.12 – Material properties for tests from (Jordão, 2008). 43
Fig. 2.13 – Geometric imperfections for validation models. 44
Fig. 2.14 – Experimental vs numerical results for tests from (Klein, 1985). 44
Fig. 2.15 – Experimental vs numerical results for tests from (Jordão, 2008). 45
Fig. 2.16 – Python Scripting. 47
Fig. 2.17 – Mesh control in IDEA StatiCa. 48
Fig. 2.18 – Mesh control in IDEA StatiCa. 48
Fig. 2.19 – IDEA Connections. 49
Fig. 2.20 – Horizontal stiffener plate geometry. 50
Fig. 2.21 – Von Mises Stress distribution. 51
Fig. 2.22 – LBA analysis in IDEA StatiCa 23.1. 52
Fig. 2.23 – IDEA StatiCa 23.1 Moment-rotation curve. 52
Fig. 2.24 – IDEA StatiCa 23.1 Stiffness analysis boundary conditions. 53
Fig. 2.25 – GMNA activation in IDEA StatiCa 23.1 API. 53
Fig. 2.26 – GMNA activation in IDEA StatiCa 23.1. 53
Fig. 2.27 – Developer version activation. 54
Fig. 2.28 – Algorithm implemented to obtain the real moment resistance. 54
Fig. 2.29 – Layout for FE models. 57
Fig. 3.1 – LBA analysis. α_{cr} vs χ. 96
Fig. 3.2 – SET01 - buckling shapes. 98
Fig. 3.3 – SET02 (n = 50%) - buckling shapes. 99
Fig. 3.4 – SET03 - buckling shapes. 100

Fig. 3.5 – SET04 (n = 50%) - buckling shapes..... 101

List of Tables

Table 2.1. Comparison of EC3-1-8 and FprEC3-1-8 component expressions for welded joints. 33
Table 2.2. Correlation factors β_w for fillet welds. 34
Table 2.3. Worst and average aspect ratio for every joint layout (worst case). 41
Table 2.4. Geometry of the selected welded joints for validation. 42
Table 2.5. Selection of cases. 59
Table 2.6. Definition of sets. 60
Table 2.7. Definition of clusters. 61
Table 2.8. Resistance values for weld study. 72
Table 3.1. Thresholds for statistics. 75
Table 3.2. Color code for classification of ratios. 75
Table 3.3. Rolled columns, S275 (cluster BR). Influence of material model QUAD vs EPPL. .. 77
Table 3.4. Rolled columns, EPPL (cluster BR). Influence of steel grade. 78
Table 3.5. Rolled columns, S275 (cluster BR-S275), EPPL material model. Failure modes. 81
Table 3.6. Ratios for unstiffened rolled columns, S275 (cluster BR-S275), EPPL 82
Table 3.7. Ratios for stiffened rolled columns, S275 (cluster BR-S275), EPPL 83
Table 3.8. Ratios rolled columns, axial load, S275 (cluster BR-S275), EPPL. EN, FprEN. 84
Table 3.9. Ratios, rolled columns, axial load, S275 (cluster BR-S275), EPPL. IS MNA. 85
Table 3.10. Ratios rolled columns, axial load, S275 (cluster BR-S275), EPPL. IS GMNA. 86
Table 3.11. Rolled columns with fillet welds, S275 (cluster FR-S275), EPPL. Failure modes. .. 88
Table 3.12. Ratios rolled columns, fillet welds, S275 (cluster FR-S275), EPPL. EN, FprEN. 88
Table 3.13. Ratios for rolled columns, fillet welds, S275 (cluster FR-S275), EPPL. IS, MNA. . 89
Table 3.14. Ratios rolled columns, fillet welds, S275 (cluster FR-S275), EPPL. IS, GMNA. 90
Table 3.15. Initial stiffness ratios, rolled columns, S275 (BR-S275), EPPL. EN, FprEN. 92
Table 3.16. Initial stiffness ratios, rolled columns, fillet welds, S275 (FR-S275), EPPL. EN, FprEN. 93
Table 3.17. Initial stiffness ratios, rolled columns, S275 (FR-S275), EPPL. EN, FprEN vs IS. . 94
Table 3.18. Statistics of χ_{def} for different ranges of α_{cr}. 97
Table 3.19. Statistics of χ_{ref} for different ranges of α_{cr}. 97
Table 3.20. Statistics of χ_{rich} for different ranges of α_{cr}. 97
Table 3.21. Time ratios (GMNA/MNA). 101
Table 3.22. Time ratios (Refined/Default). 102
Table 3.23. Welded columns, S275 (cluster BB-S275), EPPL material model. Failure modes 104
Table 3.24. Ratios, unstiffened welded columns, no axial load, S275 (BB-S275), EPPL. 105
Table 3.25. Ratios, stiffened welded columns, no axial load, S275 (cluster BB-S275), EPPL. 106
Table 3.26. Ratios, welded columns, axial load, S275 (cluster BB-S275), EPPL. EN, FprEN. 107
Table 3.27. Ratios, welded columns, axial load, S275 (cluster BB-S275), EPPL. IS MNA. 108
Table 3.28. Ratios, welded columns, axial load, S275 (cluster BB-S275), EPPL. IS GMNA... 109
Table 3.29. Failure modes for welded columns with fillet welds, S275 (cluster BF-S275)..... 110
Table 3.30. Ratios, welded columns, fillet welds, S275 (BF-S275), EPPL. EN, FprEN. 111
Table 3.31. Ratios, welded columns, fillet welds, S275 (BF-S275), EPPL. IS MNA. 112
Table 3.32. Ratios welded columns, fillet welds, S275 (BF-S275), EPPL. IS GMNA. 113
Table 3.33. Initial stiffness ratios, welded columns, S275 (BB-S275), EPPL. EN, FprEN. 115
Table 3.34. Initial stiffness, welded cols., fillet welds, S275 (BF-S275), EPPL. EN, FprEN. .. 115

Notation

The following conventions are used throughout the text:

- *Italics* denote variables.
- **Bold** denotes matrices or vectors.
- The subscripting system of Eurocodes is used. Different subscripts added to the same variable are separated with commas (example: $M_{pl,Rd}$). If the subscript is a variable or index it is italicized (example: F_i). Otherwise, it is not (example: F_{Rd}).

Acronyms and abbreviations

BCW	Beam–column weld
BB	Cluster BB (butt-welded beam, butt-welded column)
BCW	Beam-column weld
BF	Cluster BF (butt-weld beam, welded column with fillet welds)
BFC	Beam Flange and Web in Compression
BR	Cluster BR (butt-weld beam, rolled column)
BWT	Beam Web in Tension
CBFEM	Component-Based Finite Element Method
CFB	Column flange in bending
CM	Component Method
CWP	Column Web Panel
CWC	Column Web in Compression
CWT	Column Web in Tension
CWS	Column Web in Shear
FB	Cluster FB (fillet-welded beam, butt-welded column)
FE	Finite Element
FEM	Finite Element Method
GMNA	Geometrically and Materially Non-linear Analysis
GMNIA	Geometrically and Materially Non-linear Analysis with Imperfections
I	Internal joint (joint at internal story)
IS	IDEA StatiCa
MNA	Materially Non-linear Analysis
R	Roof joint (joint at roof)
T	Stiffened joint
U	Unstiffened joint
WP	Web Panel
1S	One-sided joint
2S	Two-sided joint

Symbols

Latin Uppercase

A	Area, cross-section area
A_{CWS}	Area of the column web in shear component
A_d	Area of the flat part of the web panel

A_{f1}	Area of one flange
AR_a	Average aspect ratio of a FE element
AR_w	Worst aspect ratio of a FE element
A_{vc}	Column shear area
A_{vz}	Shear area as defined in EN 1993-1-1:2005 (strong axis bending)
A_w	Area of the web (total area minus flange area)
A_{wp}	Web panel
E	Elastic modulus of steel
E_{sh}	Post-yield modulus of steel
F	Force
G	Shear modulus of steel
I	Second moment of inertia of the cross-section
$L_{eff,w,i}$	Effective length of weld *i*
L_c	Total length of column between supported points
M	Bending moment
M_1, M_2	Moment applied at side 1, 2
$M_{BCW,R}$	Moment resistance limited by the BCW component
$M_{CFB,R}$	Moment resistance limited by the CFB component
$M_{CWC,R}$	Moment resistance limited by the CWC component
$M_{CWS,R}$	Moment resistance limited by the CWS component
$M_{CWT,R}$	Moment resistance limited by the CWT component
$M_{j,b1,Ed}$	Applied design beam moment on side 1 (measured at beam-column intersection)
$M_{j,b2,Ed}$	Applied design beam moment on side 2 (measured at beam-column intersection)
$M_{pl,fb,Rd}$	Plastic bending moment resistance of the beam flange (assumed equal to stiffener)
$M_{pl,fc,Rd}$	Plastic bending moment resistance of the column flange
M_R	Moment resistance
$M_{R,FprEN}$	Moment resistance obtained with FprEN 1993-1-8:2023
$M_{R,EN}$	Moment resistance obtained with EN 1993-1-8:2005
$M_{R,FEM,5\%}$	Moment resistance obtained with FEM using the 5% plastic strain criterion
$M_{R,IS,GMNA,def}$	Moment resistance obtained with IDEA StatiCa, GMNA, default mesh
$M_{R,IS,GMNA,ref}$	Moment resistance obtained with IDEA StatiCa, GMNA, refined mesh
$M_{R,IS,GMNA,rich}$	Moment resistance obtained with IDEA StatiCa, GMNA, Richardson extrapolation
$M_{R,IS,MNA,def}$	Moment resistance obtained with IDEA StatiCa, MNA, default mesh
$M_{R,IS,MNA,ref}$	Moment resistance obtained with IDEA StatiCa, MNA, refined mesh
$M_{R,IS,MNA,rich}$	Moment resistance obtained with IDEA StatiCa, MNA, Richardson extrapolation
$M_{y,wp}$	Yield moment of web panel
N_E	Applied axial load on the column
$N_{pl,Rk}$	Plastic axial resistance of the column
S_j	Joint stiffness
$S_{j,ini}$	Initial joint stiffness
$S_{j,sec}$	Secant joint stiffness (at moment resistance)
$S_{j,tan}$	Tangent joint stiffness (at moment resistance)
$V_{wp,Rd}$	Design shear resistance of web panel (due only to the column web)
$V_{wp,add,R}$	Added design shear resistance of web panel (due to column flanges and stiffeners)

W	Plastic modulus of the cross-section

Latin Lowercase

a	Geometrical distance between external face of beam flange and column support.
a	Weld throat of fillet weld
a_b	Weld throat
a_c	Weld throat of fillet weld between column flange and column web
a_f	Weld throat of fillet weld between beam flange and column
a_w	Weld throat of fillet weld between beam web and column
$a_{w,i}$	Weld throat of fillet weld i
b	Flange width
b_{fb}	Beam flange width
b_{fc}	Column flange width
b_{eff}	Effective width
$b_{eff,CWC}$	Effective width of the CWC component
$b_{eff,CWT}$	Effective width of the CWT component
d	Width of the flat part of an I section ($h - 2 \cdot t_f - 2 \cdot r$)
d_c	Width of the flat part of the column
d_{B1}	Corrected displacement at centroid of bottom beam flange of beam 1
d_{FEM}	Displacement obtained by FEM
$d_{FEM,B1}$	Displacement obtained by FEM at centroid of bottom beam flange of beam 1
$d_{FEM,T1}$	Displacement obtained by FEM at centroid of top beam flange of beam 1
d_{RJ}	Elastic displacement of the column excluding joint region at centroid of beam flange
d_{T1}	Corrected displacement at centroid of bottom beam flange of beam 1
f_u	Tensile strength
f_{ub}	Tensile strength of beam
f_{uc}	Tensile strength of column
f_y	Yield strength
f_{yb}	Yield strength of beam
f_{yc}	Yield strength of column
h	Height of the cross-section
h_b	Beam height
h_c	Column height
h_{ic}	Clear distance between column flanges
h_{ib}	Clear distance between beam flanges
k	Stiffness
k_{CWC}	Stiffness of CWC component
k_{CWS}	Stiffness of CWS component
k_{CWT}	Stiffness of CWT component
k_{wc}	Factor for interaction of CWC with normal stress
m_r	Ratio between applied moment on sides 2 and 1 (0 for one-sided joints).
n	Ratio of applied to plastic axial load on column
n_c	Sides of the joint (1 for one-sided joints, 2 for two-sided joints)
r_{method}	Ratio of resistance calculated by 'method' to benchmark Abaqus resistance

r	Root radius of rolled section between web and flange
r_b	Root radius of beam
r_c	Root radius of column
s_{method}	Ratio of stiffness calculated by 'method' to benchmark Abaqus stiffness
t	Thickness
t_{fb}	Beam flange thickness
t_{fc}	Column flange thickness
t_{wb}	Beam web thickness
t_{wc}	Column web thickness
u	Displacement
z_b	Beam lever arm (distance between centroids of flanges)
$z_{w,i}$	Lever arm of weld i

Greek Symbols

α_{cr}	Buckling factor
β	Transformation parameter
β_w	Correlation factor for welds
γ_{M0}, γ_{M1}, γ_{M2}	Partial safety factors
ε	Strain
$\varepsilon_{pl,eq}$	Plastic equivalent strain
$\varepsilon_{pl,eq,max}$	Maximum plastic equivalent strain
λ	Mechanical slenderness
λ_p	Mechanical slenderness of the web panel
μ	Friction coefficient
ν	Poisson's ratio
χ	Ratio of resistance obtained by GMNA to resistance obtained by MNA
ρ	Buckling factor for CWC
σ	Stress
$\sigma_{com,Ed}$	Axial stress in the column web panel
ϕ_j	Joint rotation
$\phi_{j,ap}$	Apparent joint rotation (measured directly from FEM)
$\phi_{j,R}$	Joint rotation when the applied moment is the joint moment resistance
$\phi_{y,wp}$	Panel zone yielding distortion
ω	Factor for interaction of CWC and CWT with shear

1 Welded Beam-to-Column Joints

1.1 INTRODUCTION AND MOTIVATION

Most steel structures are formed by linear elements, which must be assembled through their connecting points by joints. Therefore, joints are instrumental in resistance, stiffness, ductility, reliability, robustness, economy, ease of erection, disassembly, and reuse of steelwork.

The study of the behavior of joints has been and still is a major research topic. However, joints are complex objects, formed by many different elements. The Component Method (CM) is a well-established and simple procedure to assess the resistance and stiffness of steel joints, based on the identification of the joint basic active components, the subsequent assessment of their force-displacement characteristics, and finally, the assemblage of the individual properties of these components using appropriate rigid links and linear spring component models. The method is conceptually general but has only been validated by experimental work for the standard cases that are covered by design codes.

In the last years, the Component Based Finite Element Method (CBFEM) has appeared as an automated alternative to the CM. In the current formulation of CBFEM implemented in the commercial software IDEA StatiCa, shell and linear elements are used to model plates, bolts, and welds; this simplification intends to overcome computational restraints in terms of time and memory allotment. Advances in the speed and capacity of computers make it possible nowadays to analyze joints using high-quality 3D (volumetric) Finite Element Models (3D-FEM), including material and geometrical non-linearity, as well as a complex definition of material models, contact, preload, etc.

One of the most common components in steel joints is the Column Web in Shear (CWS). It appears, for instance, in the beam-to-column assemblage, probably the most recurrent joint in structural steelwork. The resistance and stiffness of this component strongly depend on the ratio of applied bending moments at both sides; the component is usually critical for unbalanced moments, for which the extreme case is one-sided joints. For this reason, the joint is often reinforced with stiffeners or doubler plates in the web. Restrictions for the consideration of these elements in the resistance and stiffness of the joint are given in the current and upcoming version of the European Standard, with a large economic impact on the joint design and fabrication. Therefore, it is of interest to find out if some of these restrictions can be relaxed. An additional issue is the contribution of the Vierendeel-type frame formed by the column flange and stiffeners to the shear resistance of the column web panel. Analytical evidence shows that this is only possible after very large levels of deformation have been reached.

A proper characterization of the component resistance and stiffness is desirable, including the effect of transverse stiffeners. This characterization should be based on physical experiments, which can be expanded using well-calibrated 3D-FEM models. Such models are the most complete and updated possibility to analyze these joints and constitute a proper benchmark for the verification of other methodologies, including CM, CBFEM, and code prescriptions.

This approach is followed in this study, where a systematic analysis of a specific joint typology is carried out, using high-quality FE models as a benchmark for comparison of other existing design methods, such as the Component Method (as implemented in the Eurocodes), and CBFEM (as implemented in the software IDEA StatiCa).

The choice of the joint which is the object of this study (welded open-section beam-to-column) is based on several aspects:

- It is one of the most common joints in steel construction.
- It is well characterized in the Eurocode.
- It is widely studied, both experimentally and analytically.
- It does not include bolts and contacts.

Bolts, welds, and contacts are possibly the most complex elements in the FE modeling of joints. Avoiding bolts and contacts greatly simplifies modeling. Welds cannot be avoided. However, given that the study does not target the full characterization up to rupture, but the determination of a design moment resistance, they can be treated in simplified ways which are described below.

1.2 Organization of the study

The layout of this work is the following:

- In this Chapter the main concepts regarding the welded joints contemplated in the study are presented, including the notation used throughout the text, and some analytical approaches to tackle their resistance and stiffness.
- Chapter 2 presents the methods used in the study: Component Method as implemented in Eurocode 3, FE solid models, and CBFE models. It also describes in detail the numerical study.
- Chapter 3 presents and discusses the results of the study.
- Chapter 4 summarizes the conclusions of the study.

1.3 Welded Beam-To-Column Joints

The study focuses on welded beam-to-column moment-resisting joints between open-section profiles on the strong axis. The problems tackled in the study are summarized in **Fig. 1.1**, and can be divided into two major topics:

- One-sided joints (referred to as 1S).
- Two-sided joints (referred to as 2S).

The joint can be placed on:

- Internal stories (referred to as I), (1S-I, 2S-I).
- Roof (referred to as R), (1S-R, 2S-R).

The joints can be

- Unstiffened (U), (1S-I-U, 2S-I-U, 1S-R-U, 1S-R-U).
- Stiffened (T), (1S-I-T, 2S-I-T, 1S-R-T, 1S-R-T).

Furthermore, the column types can be

- Hot-rolled.
- Welded (also called built-up).

In the latter case, the connection between the column flange and column web can be rolled (R), butt weld (B), or fillet weld (F). Regarding the beam-column welds, butt welds (B) and fillet welds (F) are possible.

The column web panel is the part with largest influence on the joint resistance and stiffness. The study comprises different aspect ratios and shear capacities of the column web panel. The columns shown in **Fig. 1.1** are typically hot-rolled or welded double-T open-section profiles, with cross-section as shown in **Fig. 1.2**(a)-(b). They can be seen as formed by three parts: flanges, flange-web transition area, and web panel. The transition area can be rolled, **Fig. 1.2**(a) or welded, **Fig. 1.2**(b), and it generally includes a portion of the flange, a portion of the web, and either radius of accordance (rolled) or the welds (welded). The web panel itself is comprised of the flat part of the web (between transition areas). The height of this part, d_c, (not to be confused with the free height between flanges h_{ic}) is a critical magnitude because the buckling of the web is mainly governed by the slenderness:

$$\lambda_{wp} = d_c / t_{wc}, \tag{1.1}$$

and its resistance and stiffness are dependent on d_c and t_{wc}. The beams included in the study, **Fig. 1.2**(c), are also hot-rolled sections, but for simplicity, they are modeled without the root radius.

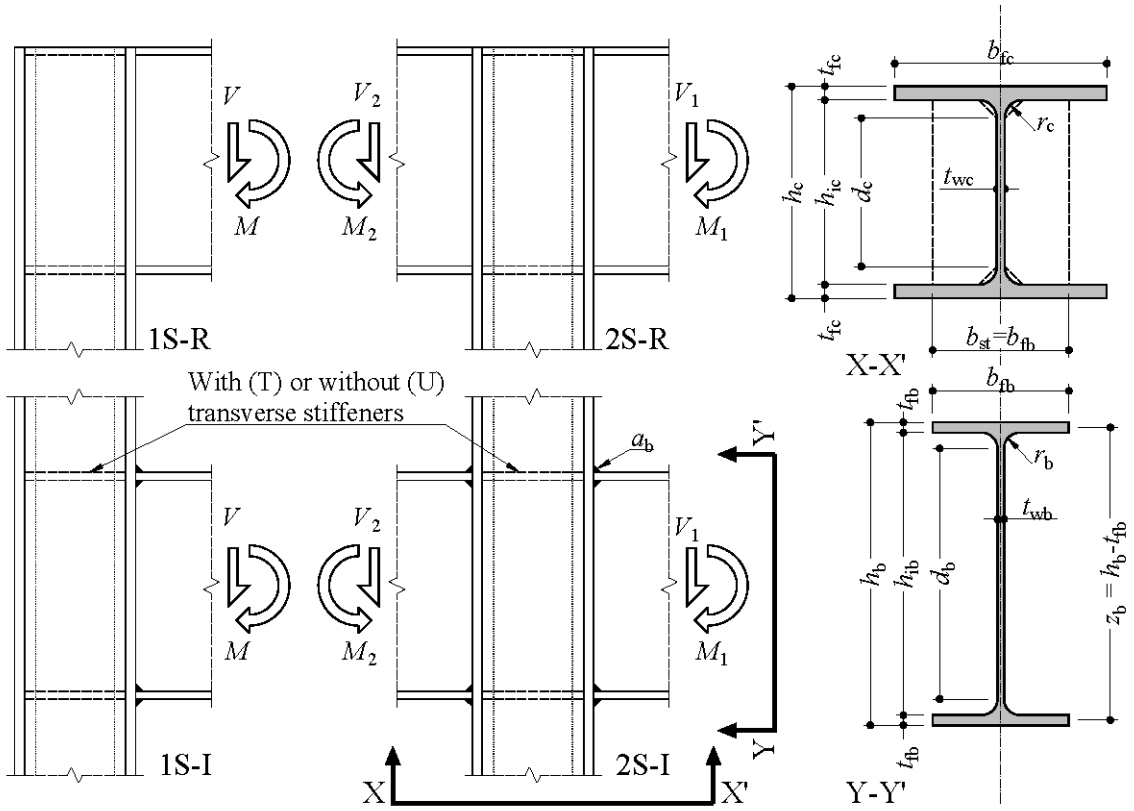

Fig. 1.1 – Problems treated in the study.

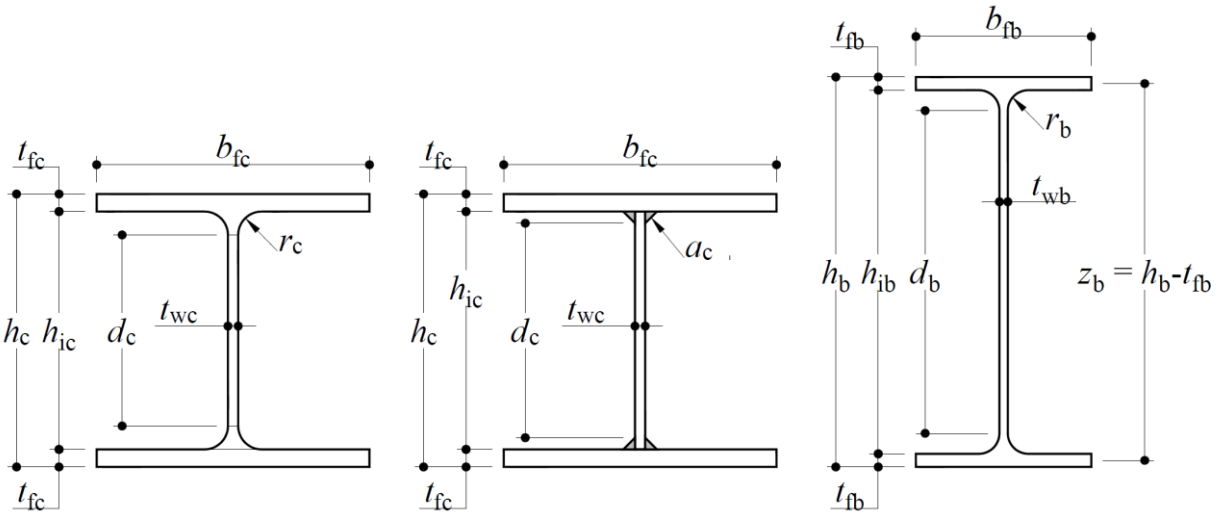

(a) (b) (c)

Fig. 1.2 – Section notation.
(a) hot-rolled column; (b) welded column; (c) hot-rolled beam.

1.4 STRUCTURAL ANALYSIS

In this Section, the statics of the joints are discussed for the configurations treated in this study.

1.4.1 One-sided joint, internal configuration

Fig. 1.3 shows the statics of the layout for the one-sided (1S) joint in an internal (I) story configuration. The basic case consists of a column of length L_c, with the joint symmetrically located. The bending moment M is applied on the beam stub and can be converted to two opposite forces:

$$F_b = \frac{M}{z_b}, \tag{1.2}$$

where z_b is the distance between centroids of beam flanges,

$$z_b = h_b - t_{fb}, \tag{1.3}$$

hereinafter referred to as *joint lever arm*, see **Fig. 1.2**(c).

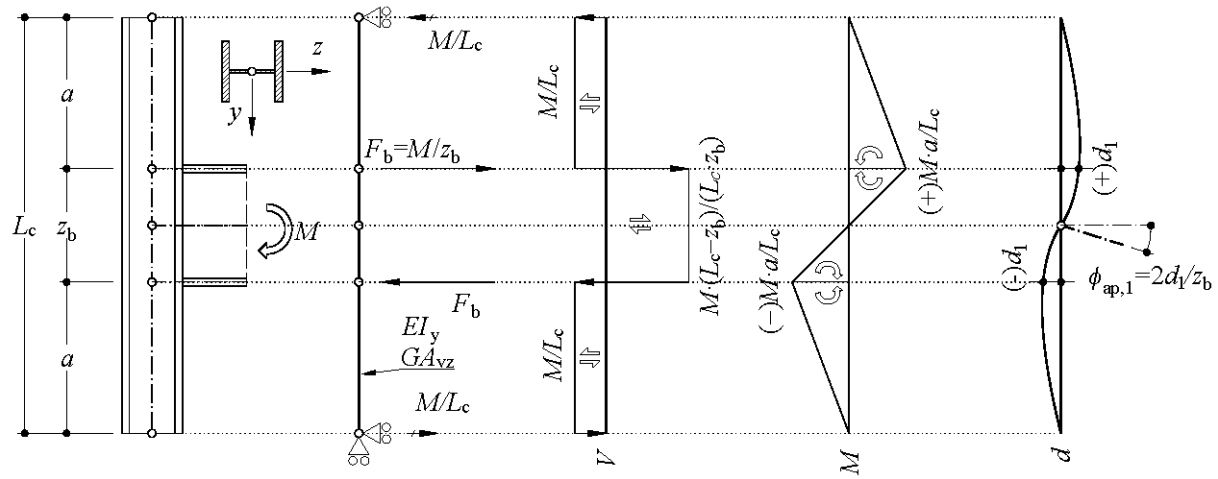

Fig. 1.3 – Statics of the one-sided joint at an internal story.

This expression is not exact, because the lever arm depends on the level of plasticity of the beam cross-section. For a fully yielded beam, the moment resistance is

$$M_{\mathrm{R}} = W_{\mathrm{pl,y}}\, f_{\mathrm{y}}, \tag{1.4}$$

and the axial capacity of the half section is

$$N_{\mathrm{R}} / 2 = A\, f_{\mathrm{y}} / 2, \tag{1.5}$$

therefore

$$z_{\mathrm{b,exact}} = 2W_{\mathrm{pl,y}} / A. \tag{1.6}$$

The ratio between this $z_{\mathrm{b,exact}}$ and z_{b} (given by Eq. (1.3)) is shown in **Fig. 1.4** for IPE and HE sections as a function of h. This ratio is systematically below 1, with a mean value of 0.80 for IPE and 0.85 for HE. As a result, expression (1.2) overestimates F_{b}. Notwithstanding this, the use of z_{b} is widespread in the literature. It must be considered that F_{b} is used mainly for verifications of the CWC and CWT components. In that sense, it is conservative, as it assumes the total force to act at the level of the flange, whereas, in reality, this force is spread over a larger length including the web. However, for cases governed by these components, it results in over-conservativeness.

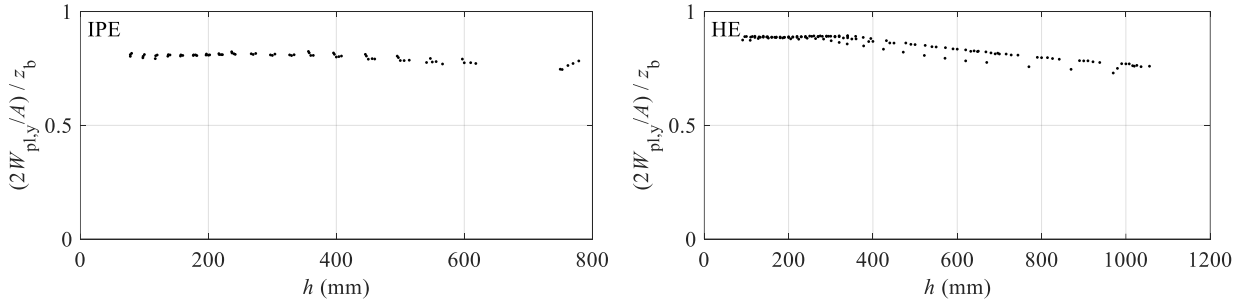

(a) (b)

Fig. 1.4 – Lever arm for plastic sections.
(a) IPE; (b) HE.

In **Fig. 1.3** no shear force is applied, so the joint deformation is entirely due to the moment. However, the shear force V_{cw} acting on the joint's column web panel is not the total force F_b, but only a fraction:

$$V_{cw} = M\frac{L_c - z_b}{L_c\, z_b} = \frac{M}{z_b}\left(1-\frac{z_b}{L_c}\right) = F_b\left(1-\frac{z_b}{L_c}\right). \tag{1.7}$$

The fraction of the bending moment that produces shear on the joint's column web panel is:

$$M_{cw} = M\left(1-\frac{z_b}{L_c}\right). \tag{1.8}$$

Thus, if the joint shear resistance is V_R, the resisting bending moment is:

$$M_R = \frac{V_R z_b}{1-\frac{z_b}{L_c}}, \tag{1.9}$$

which is always larger than the standard value $V_R \cdot z_b$. Notice that Eq. (1.7) is equivalent to considering the column shear on the verification, as per EN 1993-1-8:

$$\frac{M}{z_b} - \frac{V_T + V_B}{2}, \tag{1.10}$$

where V_T is the top column shear and V_B is the bottom column shear.

When the joint is analyzed with a FEM model, the displacements include the flexibility of the column outside the joint. For the joint analysis, this deformation must be eliminated. For the system shown in **Fig. 1.5**(a), infinite bending and shear stiffness are assumed for the joint region, and the corresponding displacements at the level of the beam flange can be found by applying the unit displacement theorem as:

$$d_{FFRRFF} = M\frac{z_b\, a^3}{3L_c^2 EI_y} + M\frac{z_b\, a}{L_c^2 GA_{vz}}, \tag{1.11}$$

where EI_y is the bending stiffness and GA_{vz} is the shear stiffness; the first part on the right term is the bending deformation and the second part is the shear deformation. The subscript for the displacement reads 'FFRRFF'; the first group of two letters refers to the bottom column bending stiffness and shear stiffness; the second group refers to the joint bending stiffness and shear stiffness; and the third group refers to the top column bending stiffness and shear stiffness; 'F' stands for flexible and 'R' for rigid. Subtracting this term from the FEM displacements, the column flexibility is excluded from the analysis:

$$d_{jT} = d_{FEM,T} - d_{FFRRFF}, \tag{1.12}$$

$$d_{jB} = d_{FEM,B} + d_{FFRRFF}, \tag{1.13}$$

where $d_{FEM,T}$ (assumed positive) is the displacement at the top beam flange centroid level obtained from FEM, and bottom $d_{FEM,B}$ (assumed negative) is the displacement at the bottom beam flange centroid level obtained from FEM. If the bending deformability is added for the central part:

$$d_{FFFRFF} = d_{FFRRFF} + M\frac{z_b^2 a^2}{6L_c^2 EI_y}, \tag{1.14}$$

and the corresponding values of deformation at beam top and bottom centroids due only to the joint shear deformability are:

$$d_{\mathrm{jVT}} = d_{\mathrm{FEM,T}} - d_{\mathrm{FFFRFF}}, \tag{1.15}$$

$$d_{\mathrm{jVB}} = d_{\mathrm{FEM,B}} + d_{\mathrm{FFFRFF}}. \tag{1.16}$$

If the shear deformability of the central part is added to (1.11):

$$d_{\mathrm{FFRFFF}} = d_{\mathrm{FFRRFF}} + M\frac{2a^2}{L_c^2 GA_v}, \tag{1.17}$$

The corresponding values of deformation at beam top and bottom centroids due only to the joint bending deformability can be found as:

$$d_{\mathrm{jMT}} = d_{\mathrm{FEM,T}} - d_{\mathrm{FFRFFF}}, \tag{1.18}$$

$$d_{\mathrm{jMB}} = d_{\mathrm{FEM,B}} + d_{\mathrm{FFRFFF}}. \tag{1.19}$$

The apparent rotation ϕ_{ap} is defined as the rotation measured from the horizontal, see **Fig. 1.5**(b), and can be found as:

$$\phi_{\mathrm{j,ap}} \approx \frac{d_{\mathrm{jT}} - d_{\mathrm{jB}}}{z_{\mathrm{b}}}, \tag{1.20}$$

where d_{jB} is assumed to be negative. To characterize the joint rotation, it must also include the component due to the rotation of the column, as shown in **Fig. 1.5**(b). That is,

$$\phi_j \approx \frac{d_{\mathrm{jT}} + d_{\mathrm{jB}}}{z_{\mathrm{b}}} + \frac{d_{\mathrm{jT}} + d_{\mathrm{jB}}}{2a} = (d_{\mathrm{jT}} + d_{\mathrm{jB}})\left(\frac{1}{z_{\mathrm{b}}} + \frac{1}{2a}\right). \tag{1.21}$$

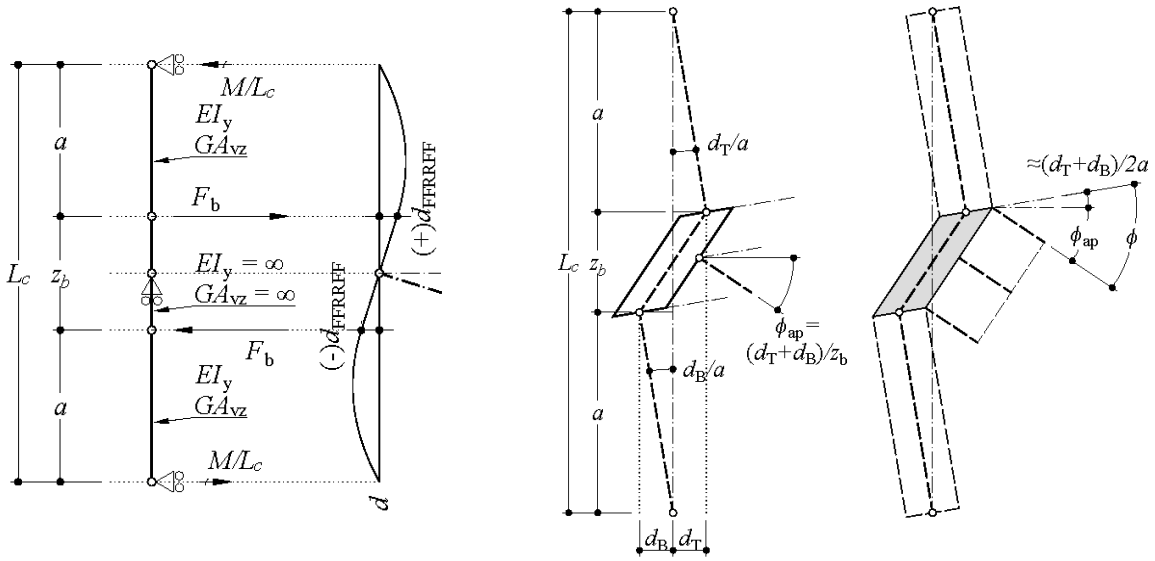

(a) (b)

Fig. 1.5 – Deformation of the one-sided joint at an internal story.

1.4.2 Two-sided joint, internal configuration

The previous equations apply for the two-sided joint, with the following nuances: first, the moment that produces bending and shear deformation in the joint is the net moment *M*, calculated as:

$$M = M_1 - M_2 = M_1(1 - m_r), \tag{1.22}$$

where M_1 is the largest bending moment (in absolute value) and M_2 is the bending moment acting on the opposite side, see **Fig. 1.6**(a); the sign for both bending moments is considered positive when they produce tension in the top part of the joint (as in the figure). M_1 is always considered positive. M_2 can be positive or negative, but always $M_2 \le M_1$. Using M as defined in Eq. (1.22), the equations derived in the previous Section 1.4.1 can be used, particularly Eqs. (1.11), (1.12), and (1.13) provide the corrected top and bottom displacements excluding the out-of-joint elastic column deformability.

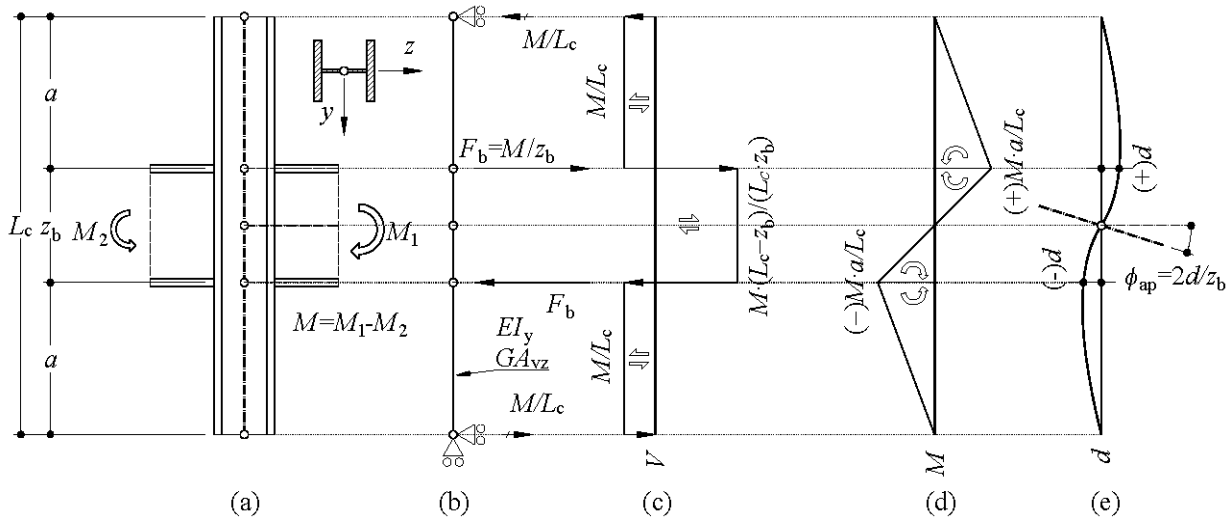

Fig. 1.6 – Statics of the two-sided joint at the internal story.

Likewise, as seen in **Fig. 1.7**, the joint rotation can be found as:

$$\phi_{j,1} \approx \frac{d_{jT,1} + d_{jB,1}}{z_{b,1}} + \frac{d_{jT,1} + d_{jB,1}}{2a} = (d_{jT,1} + d_{jB,1})\left(\frac{1}{z_{b,1}} + \frac{1}{2a}\right). \tag{1.23}$$

A similar equation can be written for side 2, replacing the subscript ‘1’ by ‘2’.

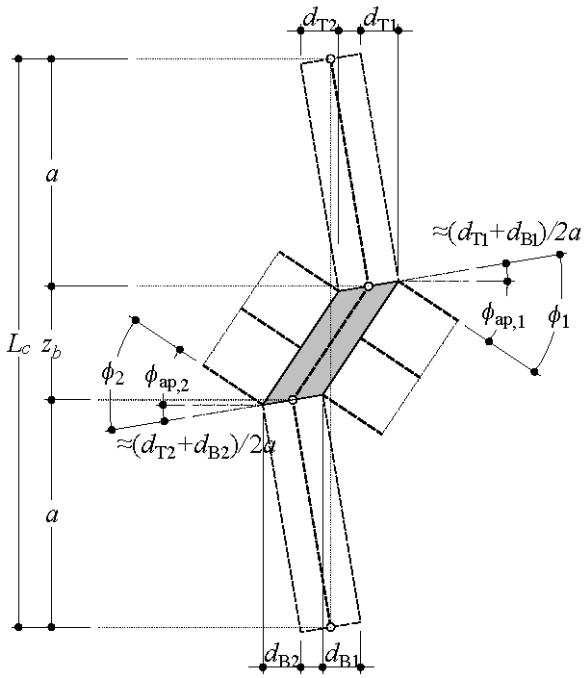

Fig. 1.7 – Deformation of the two-sided joint at an internal story.

1.4.3 One-sided joint, roof configuration

For the roof joint, the static layout is slightly different, as can be seen in **Fig. 1.8**. The beam neutral axis is horizontally supported, to allow for a simple support at the column bottom, which simulates an inflection point (no bending moment) in the column deformation. The maximum shear force at the joint is only dependent on M and z_b. Eqs. (1.7)–(1.9) read:

$$V_{cw,roof} = F_b. \tag{1.24}$$

$$M_{cw,roof} = M. \tag{1.25}$$

$$M_{R,roof} = V_R z_b. \tag{1.26}$$

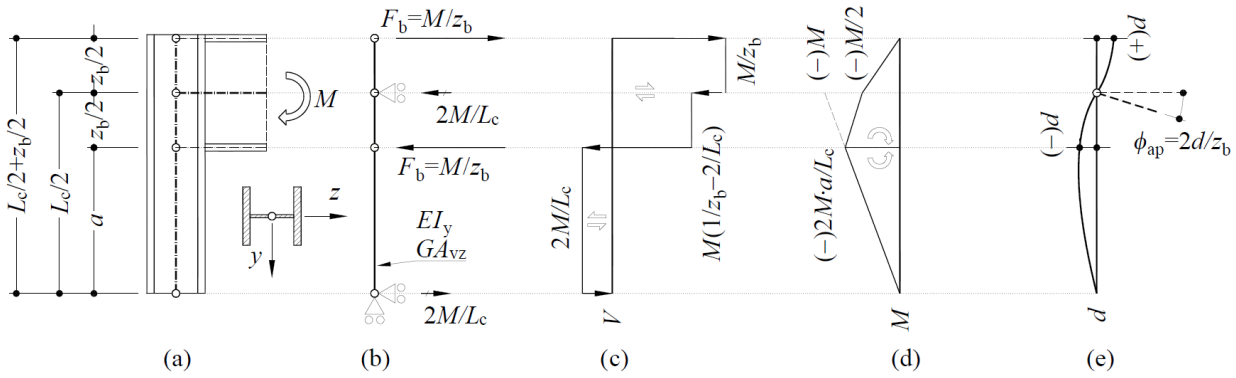

Fig. 1.8 – Statics of the one-sided joint at the roof.

The displacements obtained from FEM contain all deformability terms. To focus on joint deformation, Eqs. (1.12) and (1.13) can be used with the deformation d_{FFRRFF} obtained from **Fig. 1.8** as:

$$d_{\text{FFRRFF,roof}} = M\,\frac{2\,z_b\,a^3}{3L_c^2 EI_y} + M\,\frac{2z_b\,a}{L_c^2 GA_{vz}}, \tag{1.27}$$

which is exactly two times the same value for the internal story.

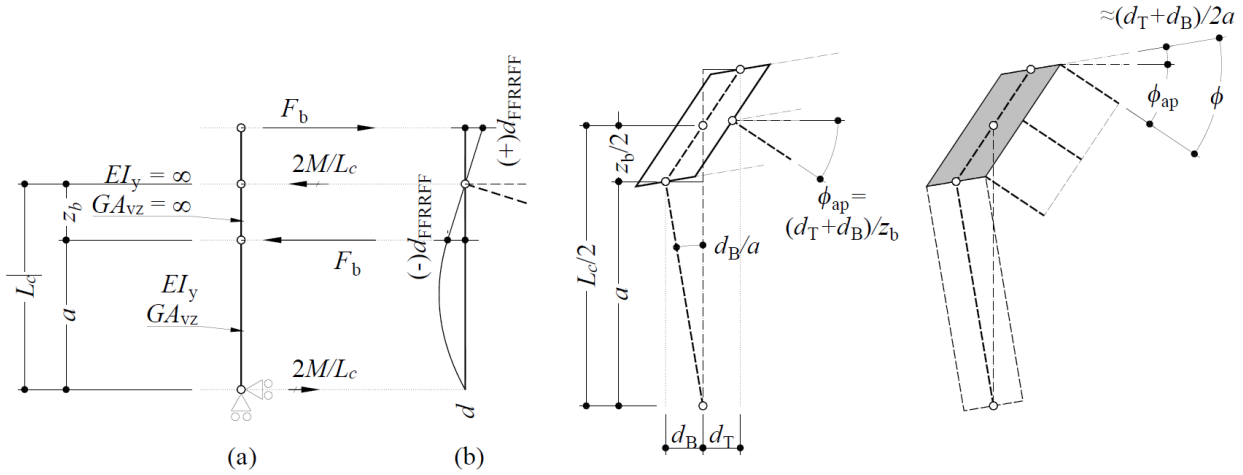

Fig. 1.9 – Deformation of one-sided joint at the roof.

Considering the joint bending stiffness, the displacement is:

$$d_{\text{FFFRFF,roof}} = d_{\text{FFRRFF,roof}} + M\,\frac{z_b^2(L_c^2 + 2L_c a + 8a^2)}{24L_c^2 EI_y}, \tag{1.28}$$

and, if the joint shear stiffness is considered:

$$d_{\text{FFRFFF,roof}} = d_{\text{FFRRFF,roof}} + M\,\frac{(L_c^2 - 2L_c z_b + 2z_b^2)}{2L_c^2 GA_v}. \tag{1.29}$$

Using these expressions, Eqs. (1.15), (1.16), (1.18), (1.19) can be applied.

1.4.4 Two-sided joint, roof configuration

The equations from the previous sub-section 1.4.3 (one-sided joint, roof configuration) can be used with the moment M given by Eq. (1.22). The joint rotation is given by Eq. (1.23).

1.4.5 Transverse stiffeners

The presence of transverse stiffeners does not change the joint analytical behavior, so all the previous equations can be applied.

1.4.6 Second-order effects

The expressions presented in the previous sub-sections do not consider second-order effects. However, the Finite Element Analysis (FE) performed in the study (GMNIA, geometrically non-linear analysis with imperfections) includes these effects. Thus, the displacements obtained from FEA are second-order displacements, typically larger than the first-order displacements. To obtain

the joint rotation, first-order displacements are subtracted from second-order displacements, which is not consistent, unless second-order effects are negligible.

To evaluate if this is the case, first and second-order analyses are performed, and the results are compared as described in Section 2.4.

1.4.7 Welded columns

The expressions presented in the previous sub-sections can be used for welded columns if the geometrical and mechanical properties are corrected as follows:

$$h_{ic} = h_c - 2t_{fc}, \tag{1.30}$$

$$d_c = h_c - 2t_{fc} - 2\sqrt{2}a_c, \tag{1.31}$$

$$A_c = 2t_{fc}b_{fc} + h_{ic}t_{wc}, \tag{1.32}$$

$$A_{vc} = h_{ic}t_{wc}. \tag{1.33}$$

$$I_y = 2\frac{b_c t_{fc}^3}{12} + \frac{h_{ic}^3 t_{wc}}{12} + 2b_c t_{fc}\left(\frac{h_c - t_{fc}}{2}\right)^2, \tag{1.34}$$

2 Methods

The purpose of this study is to perform a comparison of resistance predicted by different methods used in current practice, namely:

- Component Method (CM) as implemented in European design codes (Eurocode 3, part 1-8, current and forthcoming versions); and
- Component-Based Finite Element Method (CBFEM) as implemented in the software IDEA StatiCa.

The benchmark for comparison is the resistance predicted by sophisticated 3D Finite Element Models (FEM), performed using Abaqus, and properly validated against lab experiments. A numerical study is designed to perform this comparison in a meaningful way for a large dataset of connections representative of current practice, under the scope of this work. This Chapter introduces the methods used in the present investigation and then provides a complete description of the numerical study.

2.1 Component Method and Design Codes

2.1.1 The Component Method

The component method (CM) is a well-established general procedure to determine the main structural properties (resistance and stiffness) of a joint (Simões da Silva, 2008). The method is based on the identification of the joint active components, subsequent assessment of their individual structural properties, and creation of a joint model assembling the individual components by means of rigid links and springs. A detailed explanation of the CM is given in (Jaspart and Weynand, 2016). The most widespread application of the CM can be found in part 1-8 of Eurocode 3, hereinafter referred to as EC3-1-8 (CEN, 2005b), or its revision, hereinafter referred to as FprEC3-1-8 (CEN, 2023). The component verification according to these codes is discussed in the next subsection.

2.1.2 Eurocode 3

EC3-1-8 presents CM-based expressions for strong-axis, open-section, welded, and beam-column joints. According to the code, the joint resistance is limited by the most restrictive of the following individual components: column web panel in shear (CWS), column web in transverse compression (CWC), column web in transverse tension (CWT), column flange in transverse bending (CFB), beam flange and web in compression (BFC), or beam-column welds (BCW). The joint stiffness is dependent on the individual stiffnesses of the CWS, CWT, and CWC. The CWC and CWT components can be disregarded if a transverse stiffener is placed, aligned with the beam flange, in the compression or tension zone, respectively (no rules are given for verification of the stiffeners, which should be addressed using parts 1 and 5 of Eurocode 3). The transverse stiffeners, together with the column flanges, increase the resistance of the CWS component through Vierendeel frame action. The joint is divided into a panel zone and either one (one-sided joints 1S) or two (two-sided joints 2S) connections. For a two-sided joint, the demand on the CWS component is dependent on

the bending moments applied on both sides. This is considered using a transformation parameter β, applied to one connection, which is dependent on the bending moment ratio between both connections. FprEC3-1-8 is based on a similar rationale but includes some adjustments based on recent numerical studies (Corman, 2022; Jaspart *et al.*, 2022).

The EC3-1-8 and FprEC3-1-8 expressions are summarized and compared for hot-rolled and welded columns in **Table 2.1**. The main differences between both codes are i) the definition of the column shear area A_{CWS} (CWS); ii) the strength contribution of the column flange and transverse stiffeners (CWS); and iii) the definition of the web panel slenderness and buckling expressions (CWC). The BCW component is dependent on the type of weld:

- For butt welds with overmatching electrodes, it can be assumed that the full resistance of the weakest element connected is achieved. If the butt weld is not oversized, **Fig. 2.1**(b)-(c) (the filler material is contained within the geometrical boundaries of the plates conforming the connection), the weakest of both materials (beam, column) will dictate the design resistance of the connection. However, the filler material should be selected based on the strongest material connected.
- For fillet welds, **Fig. 2.1**(a), each weld will contribute to the overall bending moment resistance according to its individual resistance in the beam axis direction, considering as lever arm the distance of the weld to the compression center of the connection (midplane of the beam bottom flange), see **Fig. 2.2**. The resistance of the weld must be calculated using the properties of the weakest material (beam, column) connected. However, the filler material should be selected based on the strongest material connected.

In the verification by the Eurocode of the column web components in joints with fillet welds, the following assumptions are made:

- The effective length of any fillet weld is considered equal to its geometrical length, i.e., no reduction of the length is considered.
- For fillet welds, contact is assumed between the welded plates. Therefore, the resistance of the weld is only critical in tension. In compression, the full capacity of the plates can be transferred.
- For welded columns with butt welds, the capacity of the column components is not limited by the welds.
- For welded columns with fillet welds, the column web in tension (CWT) resistance is limited by the resistance of the welds joining the column flange to the column web. The CWC resistance is not limited, because of plate contact.

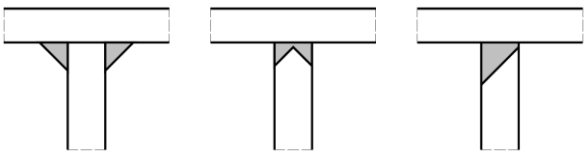

(a) (b) (c)

Fig. 2.1 – Geometry of welds.

Table 2.1. Comparison of EC3-1-8 and FprEC3-1-8 component expressions for welded joints.

	EC3-1-8	**FprEC3-1-8**
Conditions in this study	One- or double-sided joints, hot-rolled or welded open sections (H, I), strong-axis, welded connections. With or without transverse stiffeners. For double-sided joints, equal beam height. For stiffened joints, transverse stiffeners in both tension and compression zones, aligned with beam flanges, $f_{yst} = f_{yb}$, $t_{st} = t_{fb}$, $b_{st} = b_{fb}$.	
Limits	$d_c / t_{wc} \le 69\sqrt{235\text{MPa} / f_{yc}}$	$h_{ic} / t_{wc} \le 60\sqrt{235\text{MPa} / f_{yc}}$
CWS	**Resistance**: $M_{CWS,Rd} = z_b \left(V_{wp,Rd} + V_{wp,add,Rd}\right) / \beta$, $V_{wp,Rd} = 0.9 A_{CWS} f_{yc} / \gamma_{M0} \sqrt{3}$ $z_b = h_b - t_{fb}$, $\beta_1 = \left\lvert 1 - M_{j,b2,Ed} / M_{j,b1,Ed} \right\rvert \le 2$, $\beta_2 = \left\lvert 1 - M_{j,b1,Ed} / M_{j,b2,Ed} \right\rvert \le 2$	
	Hot-rolled col.: $A_{CWS} = A - 2bt_{fc} + (t_{wc} + 2r_c)t_{fc}$ Welded column: $A_{CWS} = h_{ic} t_{wc}$.	Hot-rolled column: $A_{CWS} = h_c t_{wc}$ Welded column: $A_{CWS} = h_{ic} t_{wc}$
	Unstiffened joint: $V_{wp,add,Rd} = 0$ Stiffened joint: $V_{wp,add,Rd} = 4M_{pl,fc,Rd} / z_b$	Unstiffened joint: $V_{wp,add,Rd} = 4M_{pl,fc,Rd} / z_b$, Stiffened joint: $V_{wp,add,Rd} = (4M_{pl,fc,Rd} + 2n_c M_{pl,fb,Rd}) / z_b$
	n_c = 1 (one-sided) or 2 (double-sided), $M_{pl,fb,Rd} = 0.25 b_{fb} t_{fb}^2 f_{yb}$, $M_{pl,fc,Rd} = 0.25 b_{fc} t_{fc}^2 f_{yc}$	
	Stiffness: $k_{CWS} = 0.38 A_{CWS} / (\beta z_b)$	
CWT CWC	**CWT Resistance:** hot-rolled: $M_{CWT,Rd} = z_b \, \omega \, b_{eff,CWT} t_{wc} f_{yc} / \gamma_{M0}$, Welded: $M_{CWT,Rd} = z_b \, \omega \, b_{eff,CWT} \min\left\{t_{wc} f_{yc} / \gamma_{M0}; 2a_c f_{u,w,Rd} / \sqrt{2}\right\}$, $f_{u,w,Rd} = f_{uc} / (\beta_{wc} \gamma_{M2})$, β_{wc} listed in **Table 2.2** according to column steel grade **CWC Resistance**: $M_{CWC,Rd} = z_b \min\left\{\rho \, \omega \, k_{wc} \, b_{eff,CWC} t_{wc} f_{yc} / \gamma_{M1}; \omega \, k_{wc} \, b_{eff,CWC} t_{wc} f_{yc} / \gamma_{M0}\right\}$ $b_{eff,CWT} = t_{fb} + 2\sqrt{2} a_b + e(t_{fc} + s)$; $b_{eff,CWC} = t_{fb} + 2\sqrt{2} a_b + 5(t_{fc} + s)$ e = 5 (internal) or 2.5 (roof); $s = r_c$ (hot-rolled) or $a_c\sqrt{2}$ (welded) $k_{wc} = \begin{cases} \sigma_{com,Ed} \le 0.7 f_{yc} & \rightarrow k_{wc} = 1 \\ \sigma_{com,Ed} > 0.7 f_{yc} & \rightarrow k_{wc} = 1.7 - \sigma_{com,Ed} / f_{yc} \end{cases}$ $\begin{cases} 0 \le \beta \le 0.5, & \rightarrow \omega = 1, \\ 0.5 < \beta < 1, & \rightarrow \omega = \omega_1 + 2(1-\beta)(1-\omega_1), \\ \beta = 1, & \rightarrow \omega = \omega_1, \\ 1 < \beta < 2, & \rightarrow \omega = \omega_1 + (\beta - 1)(\omega_2 - \omega_1), \\ \beta = 2, & \rightarrow \omega = \omega_2. \end{cases}$ with $\begin{cases} \omega_1 = \dfrac{1}{\sqrt{1 + 1.3 (b_{eff,CWT} t_{wc} / A_{CWS})^2}} \\ \omega_2 = \dfrac{1}{\sqrt{1 + 5.2 (b_{eff,CWT} t_{wc} / A_{CWS})^2}}, \end{cases}$	
	$\bar{\lambda}_p = 0.932 \sqrt{\dfrac{b_{eff,CWC} \, d_{wc} \, f_{yc}}{E \, t_{wc}^2}}$	$\bar{\lambda}_p = 0.932 \sqrt{\dfrac{\omega \, k_{wc} \, b_{eff,CWC} \, d_{wc} \, f_{yc}}{E \, t_{wc}^2}}$

	$\begin{cases}\bar{\lambda}_p \le 0.72 & \rightarrow \rho = 1 \\ \bar{\lambda}_p > 0.72 & \rightarrow \rho = (\bar{\lambda}_p - 0.2)/\bar{\lambda}_p^2\end{cases}$	$\begin{cases}\bar{\lambda}_p \le 0.673 & \rightarrow \rho = 1 \\ \bar{\lambda}_p > 0.673 & \rightarrow \rho = (\bar{\lambda}_p - 0.22)/\bar{\lambda}_p^2\end{cases}$
	Stiffness: unstiffened joints $k_{CWC} = 0.7 b_{eff,CWC} t_{wc}/d_{wc}$, $k_{CWT} = 0.7 b_{eff,CWT} t_{wc}/d_{wc}$ stiffened joints, $k_{CWC} = k_{CWT} = \infty$.	
CFB	Joint needs stiffeners if $b_{eff} \ge b_b f_{yb}/f_{ub}$ **Resistance** (only for unstiffened joints): $M_{CFB,Rd} = z_b b_{eff} t_{fb} f_{yb}/(\beta \gamma_{M0})$ $b_{eff} = t_{wc} + 2s + 7k t_{fb}$, $k = t_{fc} f_{yc}/(t_{fb} f_{yb}) \le 1$; $s = r_c$ (hot-rolled) or $a_c\sqrt{2}$ (welded)	
BCW	**Resistance** (full penetration butt welds): $M_{BCW,Rd} = W_{pl,b} f_{w,Rd}$, $W_{pl,b}$ is the strong-axis plastic modulus of the beam footprint on the column, $f_{w,Rd} = \min\{f_{yc}, f_{yb}\}/\gamma_{M0}$ **Resistance** (fillet welds, directional method): $M_{BCW,Rd} = (f_{u,w,Rd}/\sqrt{2})\sum_i L_{eff,w,i} a_{w,i} z_{w,i}$, $L_{eff,w,i}$, $a_{w,i}$, $z_{w,i}$ are the effective length, throat and lever arm (measured to centre of compression) of fillet weld *i*, see **Fig. 2.2**; $f_{u,w,Rd} = \min\{f_{uc}/\beta_{wc}, f_{ub}/\beta_{wb}\}/\gamma_{M2}$. β_{wc}, β_{wb} are correlation factors depending on the column or beam material, **Table 2.2**.	

NOTE: See notation in **Fig. 1.1** and **Fig. 1.2**.

Table 2.2. Correlation factors β_w for fillet welds.

Steel grade	S235	S275	S355	S460	S690
EN 1993-1-8	0.80	0.85	0.90	1.00	1.00
FprEN 1993-1-8	0.80	0.85	0.90	0.85	1.10

ACIV - Associação para o Desenvolvimento da Engenharia Civil - **UNIVERSIDADE DE COIMBRA** – NIF 505448173
Departament of Civil Engineering - FCTUC * Rua Luís Reis Santos | Pólo II da Univ. Coimbra | 3030-788 COIMBRA
ISISE UC – Institute for Sustainability and Innovation in Structural Engineering

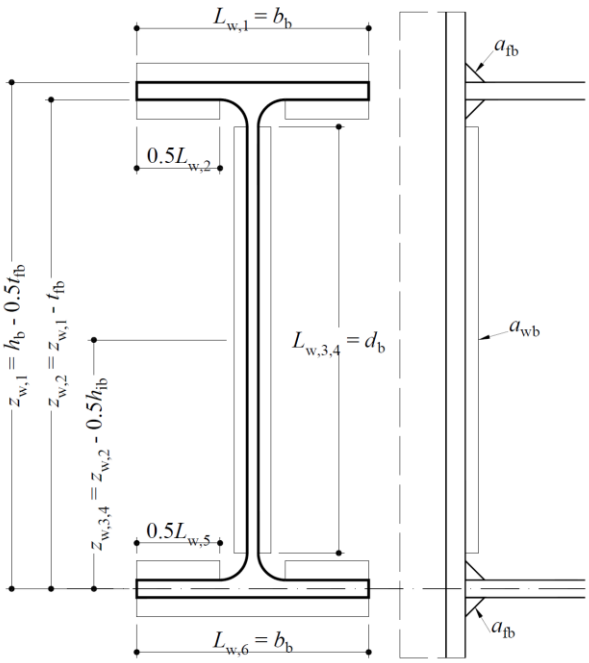

Fig. 2.2 – Geometry of beam-column fillet welds.

2.1.2.a EC3-1-8 (EN 1993-1-8:2005)

Using the expressions in **Table 2.1**, the values of moment resistance limited by the joint components as per EC3-1-8 are $M_{CWS,R,EN}$, $M_{CWC,R,EN}$, $M_{CWT,R,EN}$, $M_{CFB,R,EN}$, $M_{BCW,R,EN}$, where the subscript 'EN' is used to refer to the current version EC3-1-8. The moment resistance of the joint (referred to as the moment applied on side 1), is assessed as follows:

$$M_{R,EN} = \min\left\{M_{CWS,R,EN}; M_{CWC,R,EN}; M_{CWT,R,EN}; M_{CFB,EN,R}; M_{BCW,EN,R}\right\}. \quad (2.1)$$

When assessing the moment resistance due to the web panel on the internal configuration, proper account should be taken of the shear forces in the column, as indicated by Eq. (1.8).

The joint initial stiffness defined by EC3-1-8 and referred to as side 1 can be obtained from the stiffness components $k_{CWS,EN}$, $k_{CWC,EN}$, $k_{CWT,EN}$, as:

$$S_{j,ini,EN} = E\, z_b^2 \left(k_{CWS,EN}^{-1} + k_{CWC,EN}^{-1} + k_{CWT,EN}^{-1}\right)^{-1}, \quad (2.2)$$

and the secant stiffness $S_{j,sec,EN}$ is defined as 1/3 of the previous value.

2.1.2.b FprEC3-1-8 (FprEN 1993-1-8:2023)

The previous equations can be used for $M_{R,prEN}$, $S_{j,ini,prEN}$, and $S_{j,sec,prEN}$, just replacing the EN components by those obtained with the FprEC3-1-8 expressions ($M_{CWS,R,prEN}$, $M_{CWC,R,prEN}$, $M_{CWT,R,prEN}$, $M_{CFB,R,prEN}$, $M_{BCW,R,prEN}$, $k_{CWS,prEN}$, $k_{CWC,prEN}$, $k_{CWT,prEN}$):

$$M_{R,prEN} = \min\left\{M_{CWS,R,prEN}; M_{CWC,R,prEN}; M_{CWT,R,prEN}; M_{CFB,prEN,R}; M_{BCW,prEN,R}\right\}. \quad (2.3)$$

Again, when assessing the moment resistance due to the web panel on the internal configuration, proper account should be taken of the shear forces in the column, as indicated by Eq. (1.8).

The joint initial stiffness is given by:

$$S_{j,ini,prEN} = E\, z_b^2 \left(k_{CWS,prEN}^{-1} + k_{CWC,prEN}^{-1} + k_{CWT,prEN}^{-1}\right)^{-1}, \quad (2.4)$$

The joint secant stiffness $S_{j,sec,prEN}$ is taken as 1/3 of the previous value.

2.2 FE SOLID MODELS

2.2.1 Model description

2.2.1.a Introduction

Sophisticated numerical models were developed using the commercial FE software Abaqus (Simulia, 2021). Among the several types of analysis available, the most complex one has been selected, i.e., geometrically, and materially nonlinear analysis with initial imperfections included (GMNIA). The advanced numerical model described in this section follows the requirements and recommendations given in prEN 1993-1-14 (CEN, 2022), highlighting the assumptions adopted.

2.2.1.b Geometry

The FE solid model comprised a solid core region connected to shell parts on the members' extremities, see **Fig. 2.29**. The length of the members within the solid core part was defined as 1.25 times the depth of the member for each side, which corresponds to the standard value adopted on IDEA StatiCa software. The first assumption is that this adopted length results in a realistic behavior of the model. This is in line with the well-known Saint-Venant principle. It is important to acknowledge that the model continues beyond this region, albeit with shell elements instead of solid elements, therefore the link between both types of elements must be solved by imposing a nodal constraint. **Fig. 2.3** describes the geometry of the numerical model created on Abaqus.

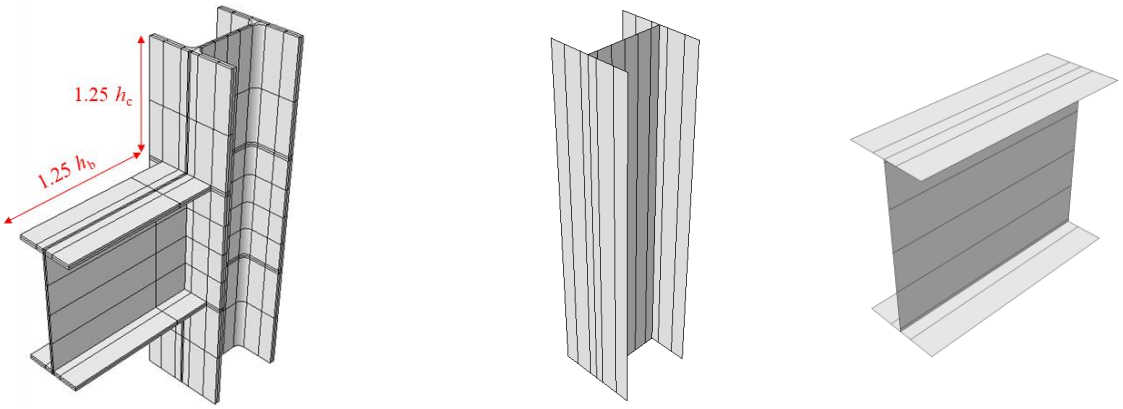

(a) (b) (c)

Fig. 2.3 – Solid model description.
(a) Solid core; (b) Column part (shell); c) Beam part (shell).

For the sake of simplicity, the beam root radius was not modeled. Different geometries were included in this study, see Section 1.3. Beam-to-column welds can be butt welds (B) or fillet welds (F); and the column cross section can be rolled (R), welded with butt welds (B), or welded with fillet welds (F). **Fig. 2.4** shows the different geometries analyzed, where the first letter indicates the beam-to-column weld, and the second letter indicates the column cross-section type.

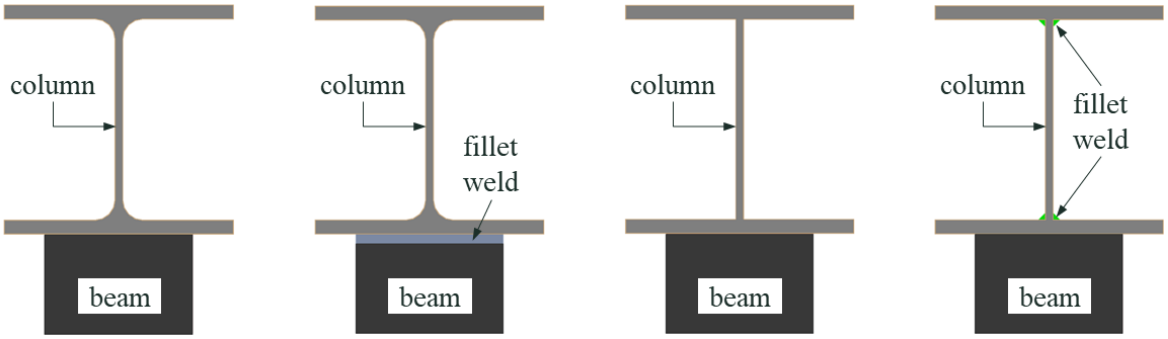

Fig. 2.4 – Geometries contemplated in the numerical study.
(a) BR; (b) FR; c) BB; d) BF.

For stiffened joints, the stiffeners were adopted with the same width and thickness as the beam flange. The chamfer of the stiffeners was kept with the same size as the column root radius. In welded columns, the same chamfer dimension was kept. Stiffener welds were modeled as butt welds for geometries BR, BB, and BF; and as fillet welds for geometry FR.

2.2.1.c Material models

Three different material models were considered in this study: i) the theoretical elastic-perfectly plastic material law (EPPL), ii) the quad-linear material model (QUAD) from prEN 1993-1-14 (CEN, 2022); iii) an elastic-perfectly plastic with post-yield stiffness of E/1000 (E1000) which reproduces the material model utilized in IDEA StatiCa. The converted true material properties were included in the numerical model, as depicted in **Fig. 2.5**. The Poisson's ratio ν and Young's modulus of steel E were taken as 0.3 and 210GPa, respectively. For joints with transverse stiffening, the material of the stiffeners was the same as the column. Fillet welds were always modeled with the QUAD material model.

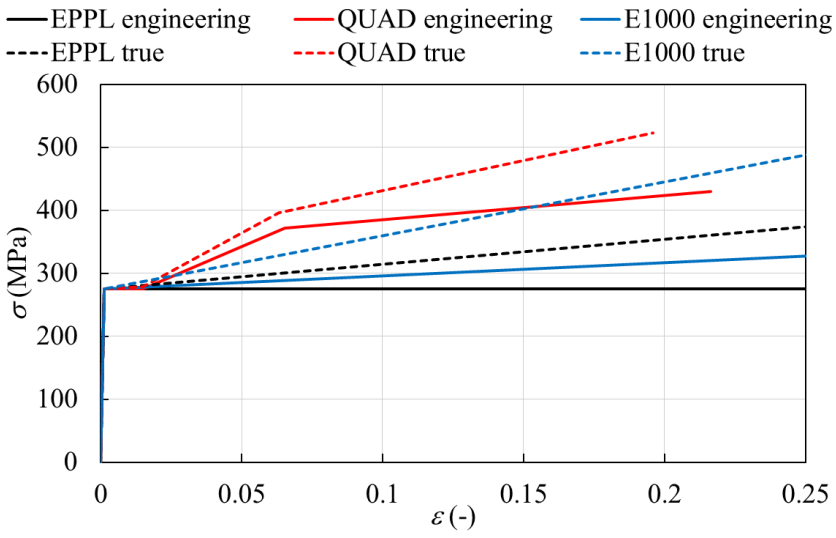

Fig. 2.5 – EPPL, QUAD and E1000 material models for steel S275.

2.2.1.d Analysis type

Regarding the analysis type, the *"Static, General"* procedure was applied, considering the nonlinear effects of large deformations and displacements ("*Nlgeom*"). The initial, minimum, and maximum increment sizes were set as 0.001, 1E-10, and 0.005, respectively. The maximum number of increments was set as 10,000.

2.2.1.e Modeling of welds

Modeling of welds using FE methods can be rather complex. To capture the actual behavior, some weld models require the inclusion of material damage/fracture, heat-affected zone, residual stresses, and very fine meshes (below 1 mm in size). It is not the objective of this study to cover metallurgical aspects of welding, but to check the influence of the weld geometry on the mechanical behavior of welded joints. Therefore, a simplified model for the welds has been developed.

For joint geometries BR and BB, only full penetration butt welds with no oversize were considered. Consequently, the welds were not explicitly modeled, no contact was included in the model and the weld was simulated by direct connection of the corresponding nodes on welded parts.

For joint geometries FR and BF, the geometry of the fillet welds was explicitly modeled. General contact was applied in the model with "hard" contact pressure-overclosure, and penalty friction formulation (friction coefficient μ of 0.2). A seam (crack) was assigned on the interface of plates joined by fillet welds to simulate the separation/contact between plates. **Fig. 2.6** depicts the crack location for joint geometries with fillet welds. It is worth noting that the cracks have been assigned exclusively to the solid core.

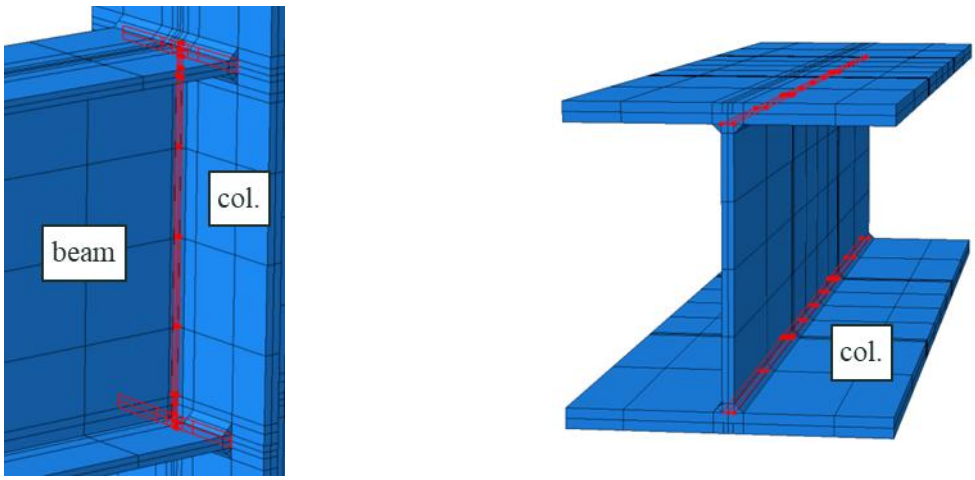

(a) (b)

Fig. 2.6 – Crack locations for an unstiffened joint.
(a) Geometry FR; (b) Geometry BF.

2.2.1.f Constraints and boundary conditions

The nodes in the extremities of the column and beams were constrained to the motion of a reference point through rigid-body constraints. Shell parts were coupled to the solid core through shell-to-solid couplings. Pinned boundary conditions were applied to the column ends, and the beam end

was fixed to move in the out-of-plane direction. The load was introduced through a bending moment M_1 on the beams and a concentrated force N_2 on the column. **Fig. 2.7** summarizes the boundary conditions and applied loads for different joint layouts, see also Section 2.4.1.

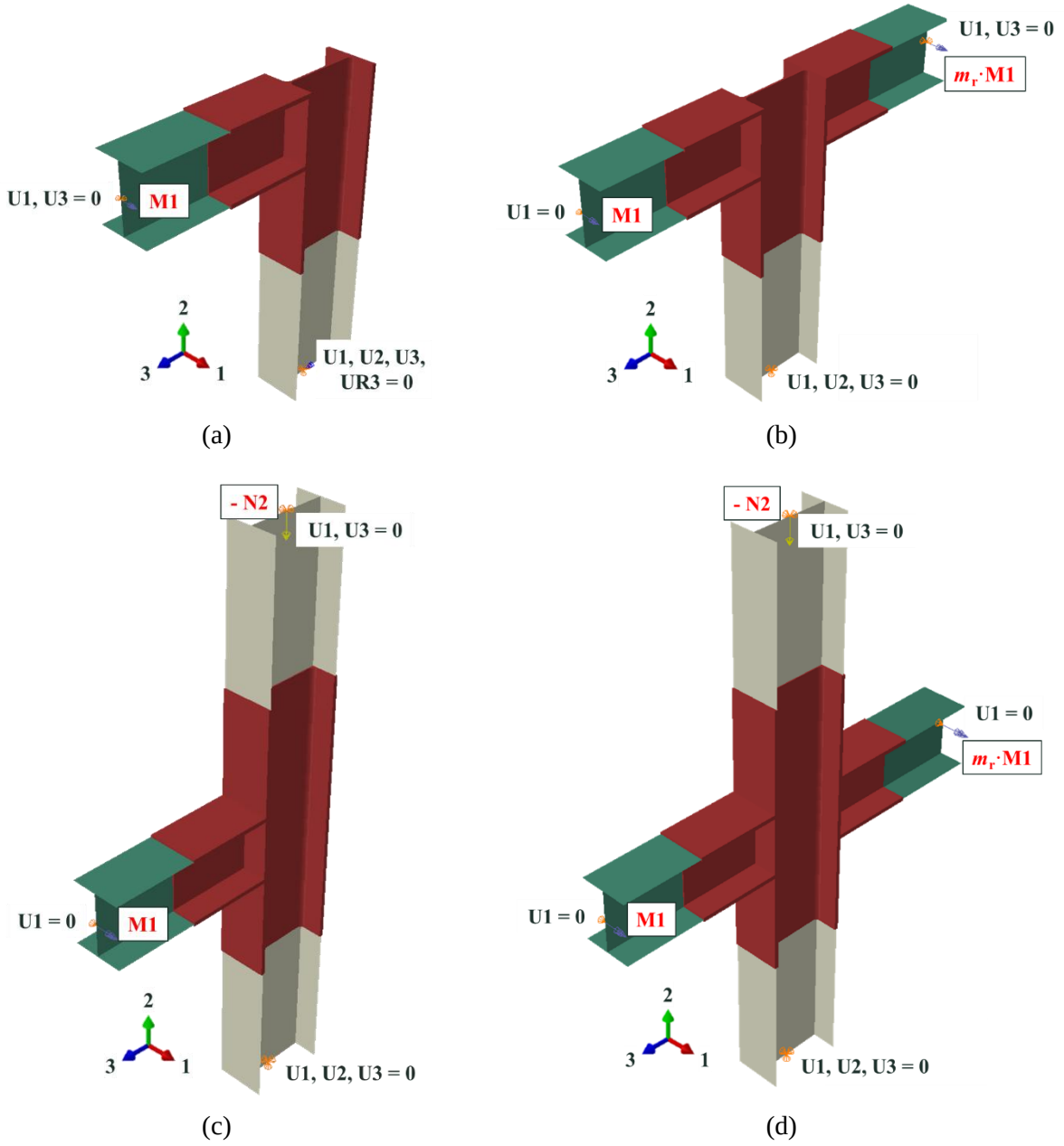

Fig. 2.7 – Boundary conditions and loads for the FE solid model.
(a) 1S-R; (b) 2S-R; (c) 1S-I; (d) 2S-I.

2.2.1.g Meshing

To check the convergence of the results, a mesh sensitivity analysis was carried out considering different mesh sizes, ranging from 250,000 up to 2,000,000 nodes. Additionally, different element types were analyzed, namely quadratic, full integration, and hybrid formulation elements. **Fig. 2.8**

presents the moment-rotation curves for this analysis, including the critical point in which the maximum equivalent plastic strain $\varepsilon_{pl,eq,max}$ reaches 5% in every curve.

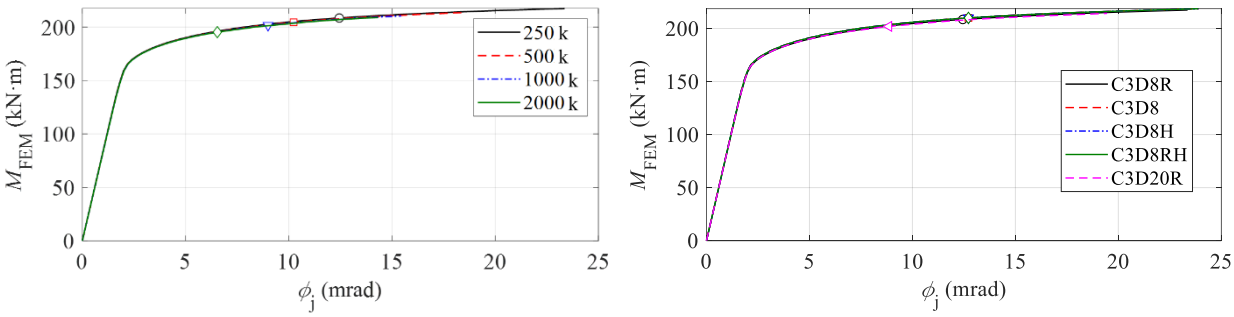

(a) (b)

Fig. 2.8 – Mesh sensitivity analysis for FE solid models.
(a) Mesh size; (b) Element type.

According to the results above, it can be observed that the initial stiffness and the overall moment-rotation curve do not vary significantly either for the mesh size or the element type. The moment resistance is mesh-dependent, but the range of variation is very small. However, the rotation is highly dependent on the mesh size, i.e., the finer the mesh, the smaller the rotation corresponding to the 5% point. Therefore, considering the computational time and storage required per model, the eight-node linear brick element with reduced integration (C3D8R) was selected to model the solid core. Likewise, the shell parts were modeled using four-node linear shell elements with reduced integration (S4R).

The FE model was meshed through an optimization process, where the approximate global size was reduced iteratively until the mesh reached nearly 250,000 nodes. This limit has been selected to allow the model to run efficiently on conventional computers. In the solid core, at least four elements were placed across the thickness of all plates. For fillet welds, at least six elements were placed across its legs for beam-column welds (geometry FR), and three elements for column welds (geometry BF). The region with greater stresses, i.e., the intersection between the beam and the column was kept with a finer mesh. This region, named "refined region", extended up to $0.3 \cdot h_b$ in the beam and $0.6 \cdot h_c$ in the column, see **Fig. 2.9**. The mesh was also optimized at the cross-section level, where regions with stress concentrations were more refined, e.g., close to the intersection between the column flange and web.

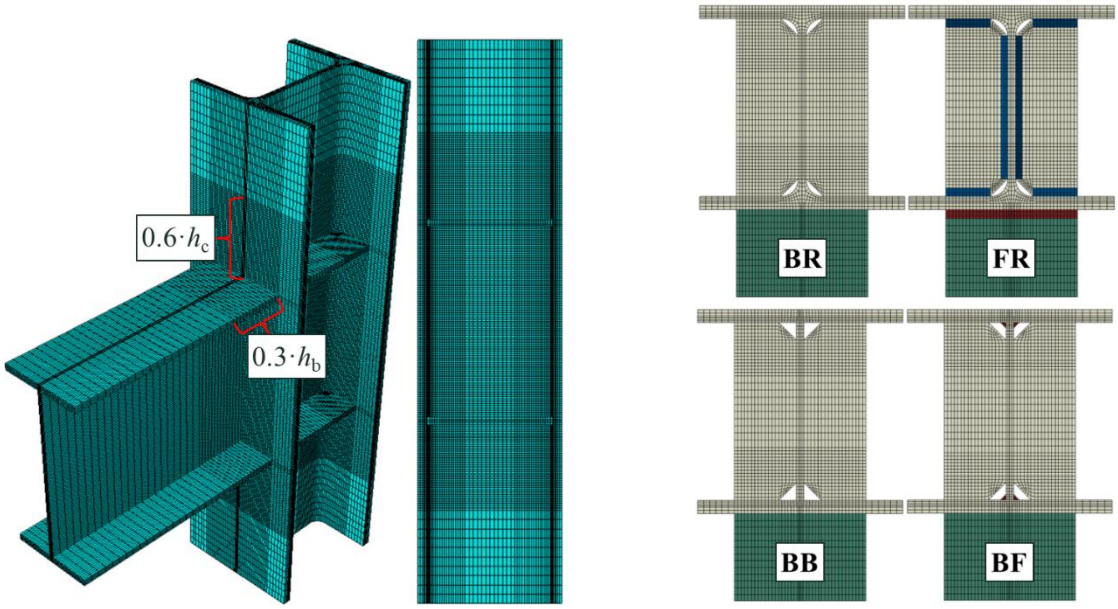

(a) (b)

Fig. 2.9 – FE mesh for the solid core – stiffened joint.
(a) Refined region; (b) Column cross section for different geometries.

The mesh quality was evaluated in terms of the worst (AR_w) and average (AR_a) aspect ratio with respect to the refined region. **Table 2.3** shows the worst factors for every joint layout comprised in the study, for unstiffened (U) and stiffened (T) joints.

Table 2.3. Worst and average aspect ratio for every joint layout (worst case).

Joint layout	$AR_{w,U}$	$AR_{w,T}$	$AR_{a,U}$	$AR_{a,T}$
1S-R	4.1	5.4	2.2	2.1
2S-R	5.2	5.9	2.7	2.6
1S-I	5.3	5.4	2.3	2.3
2S-I	5.4	5.4	2.5	2.5

2.2.1.h Imperfections and residual stresses

Initial geometric imperfections were introduced in the FE solid models by considering the first buckling mode from a linear buckling analysis (LBA), with an amplitude of d_c/200. This imperfection accounts indirectly for the effect of residual stresses, that were not explicitly modelled. For the LBA, only the web panel is free to move in the out-of-plane direction and no axial force is applied to the column. **Fig. 2.10** depicts examples of initial imperfections for different joint layouts.

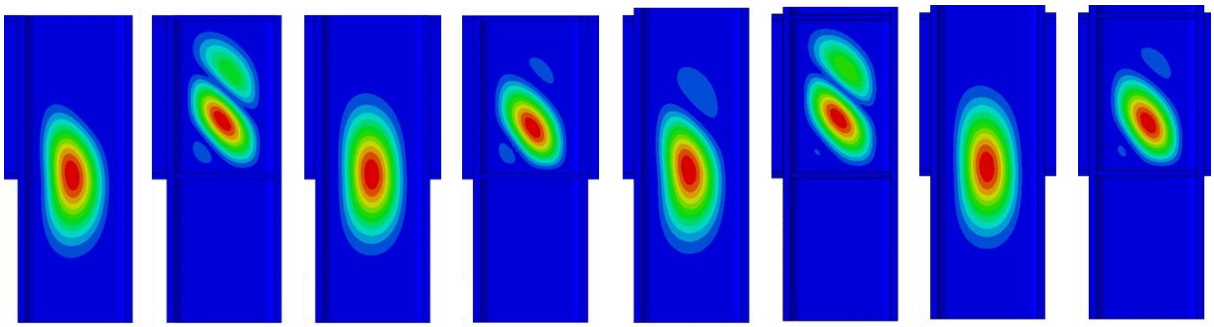

Fig. 2.10 – Initial geometric imperfections for FE solid models.

It is worth mentioning that the numerical models were generated automatically through Python scripts by reading an input file from Excel. In addition, auxiliary scripts were developed for:

a) Running and monitoring the analysis simultaneously: the analysis is terminated when a certain level of plastic strain is reached on the web panel.

b) Automatic extraction of results, including moment-rotation curves; stress, strain, and displacement components from the web panel; reactions, and rotations.

2.2.2 Model validation and verification

The FE solid model was validated against the experimental results of two welded joints from (Klein, 1985) and three welded joints from (Jordão, 2008). The joints were subjected to negative bending moments, with no axial load in the column. **Table 2.4** presents the geometric properties of the selected joints for validation.

Table 2.4. Geometry of the selected welded joints for validation.

Author	Test	Member	h (mm)	b (mm)	t_w (mm)	t_f (mm)	r (mm)	L (mm)	a_f (mm)	a_w (mm)
(Klein, 1985)	NR4	Col HEB160	159.0	160.0	8.0	12.2	15	1350	7.1	-
		Beam IPE330	329.0	162.0	8.0	11.4	18	698		
	NR16	Col HEB300	298.0	300.0	10.6	18.0	27	1600	12.7	-
		Beam HEB500	500.0	301.0	14.7	27.6	27	580		
(Jordão, 2008)	S355 E1.1	Col HEB240	245.4	242.3	10.4	16.5	21	3000	-	-
		Beam IPE400	404.3	179.5	8.8	12.8	21	1300	16.0	-
	S355 E1.2	Col HEB240	246.0	241.4	10.6	16.8	21	3000	-	-
		Beam IPE400	406.8	179.1	9.1	13.1	21	1300	16.0	5.0
	S355 E2	Col HEB240	245.6	241.3	10.3	16.5	21	3000	-	-
		Beam1 IPE400	402.7	178.8	8.9	12.9	21	1300	16.0	5.0
		Beam2 HEB200	199.0	201.0	9.0	14.4	18	700	13.0	6.0

For tests NR4 and NR16, only the yield f_y and ultimate f_u strength were made available in (Klein, 1985). In this regard, the quad-linear material model from prEN 1993-1-14 (CEN, 2022) was employed to build the stress-strain curves for each plate. The measured material properties for tests

S355 E1.1, S355 E1.2, and S355 E2 are reported in (Jordão, 2008). **Fig. 2.11** and **Fig. 2.12** present the true properties of the above-mentioned experimental tests.

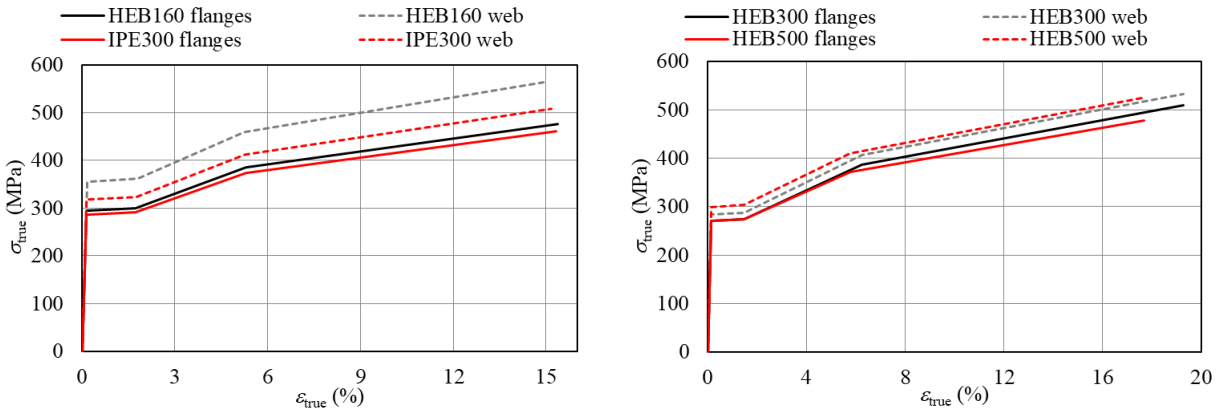

Fig. 2.11 – Material properties for tests from (Klein, 1985).

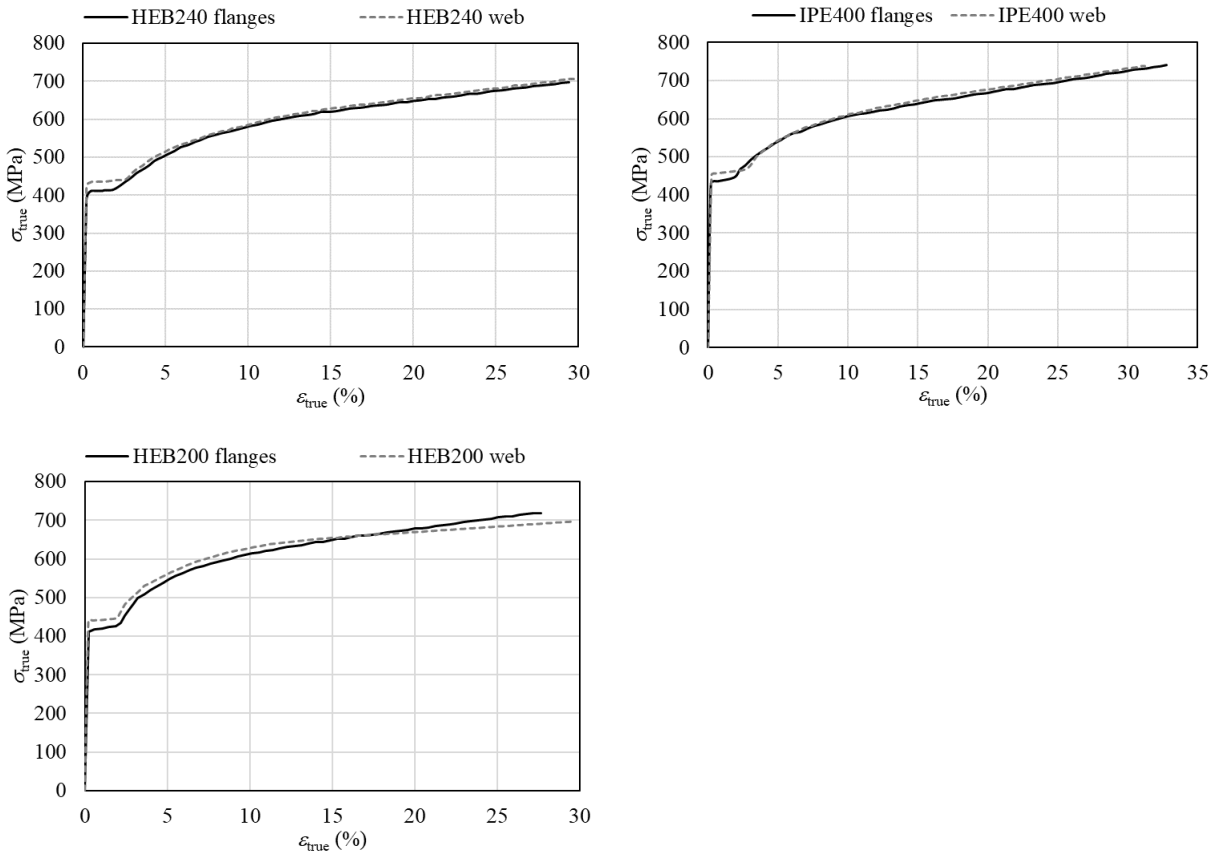

Fig. 2.12 – Material properties for tests from (Jordão, 2008).

Pinned boundary conditions were applied to the column ends, and the out-of-plane displacement was restrained at the beam end. A vertical displacement was introduced at the tip of the beam to simulate the real loading conditions.

The initial imperfections were accounted for by considering the first buckling mode from an LBA, with an amplitude of $d_c/200$. **Fig. 2.13** depicts the geometric imperfections for all validation models.

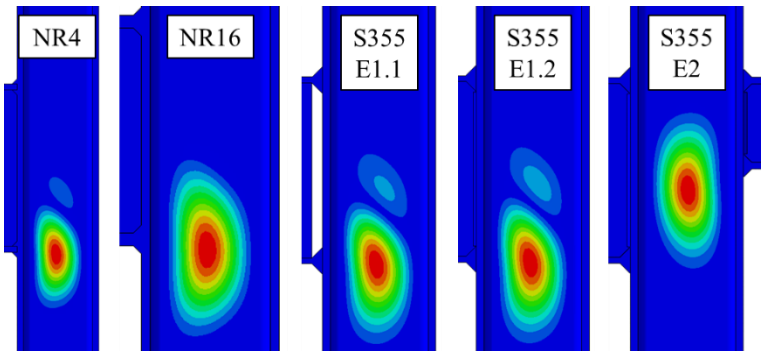

Fig. 2.13 – Geometric imperfections for validation models.

Fig. 2.14 presents a comparison between experimental (*"Exp"*) and numerical (*"Num"*) results for the tests from (Klein, 1985). The load-deflection curves correlate the displacement on the tip of the beam (δ) and the applied vertical force (F).

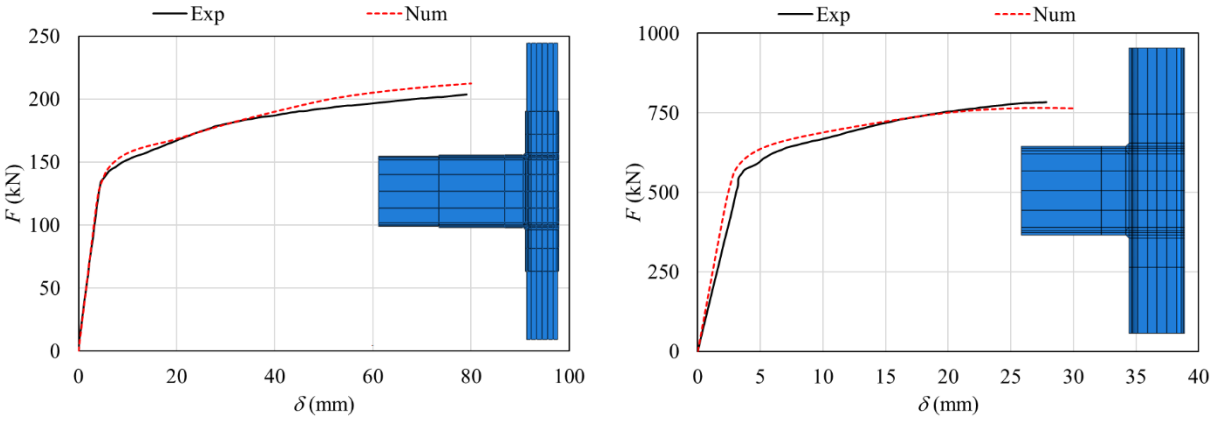

(a) (b)

Fig. 2.14 – Experimental vs numerical results for tests from (Klein, 1985).
(a) NR4; (b) NR16.

From the results above, it can be concluded that numerical and experimental results present a very good match. Consequently, the numerical model can reproduce the mechanical behavior of both joints with accuracy.

Regarding the tests from (Jordão, 2008), a comparison between experimental (*"Exp"*) and numerical (*"Num"*) results is given in **Fig. 2.15**. The displacement on the tip of the beam (δ) is plotted against the applied bending moment (M). For the double-sided joint S355 E2, the labels "SB" and "LB" refer to small beam and large beam, respectively. Lastly, the final deformed shape of each joint is also assessed.

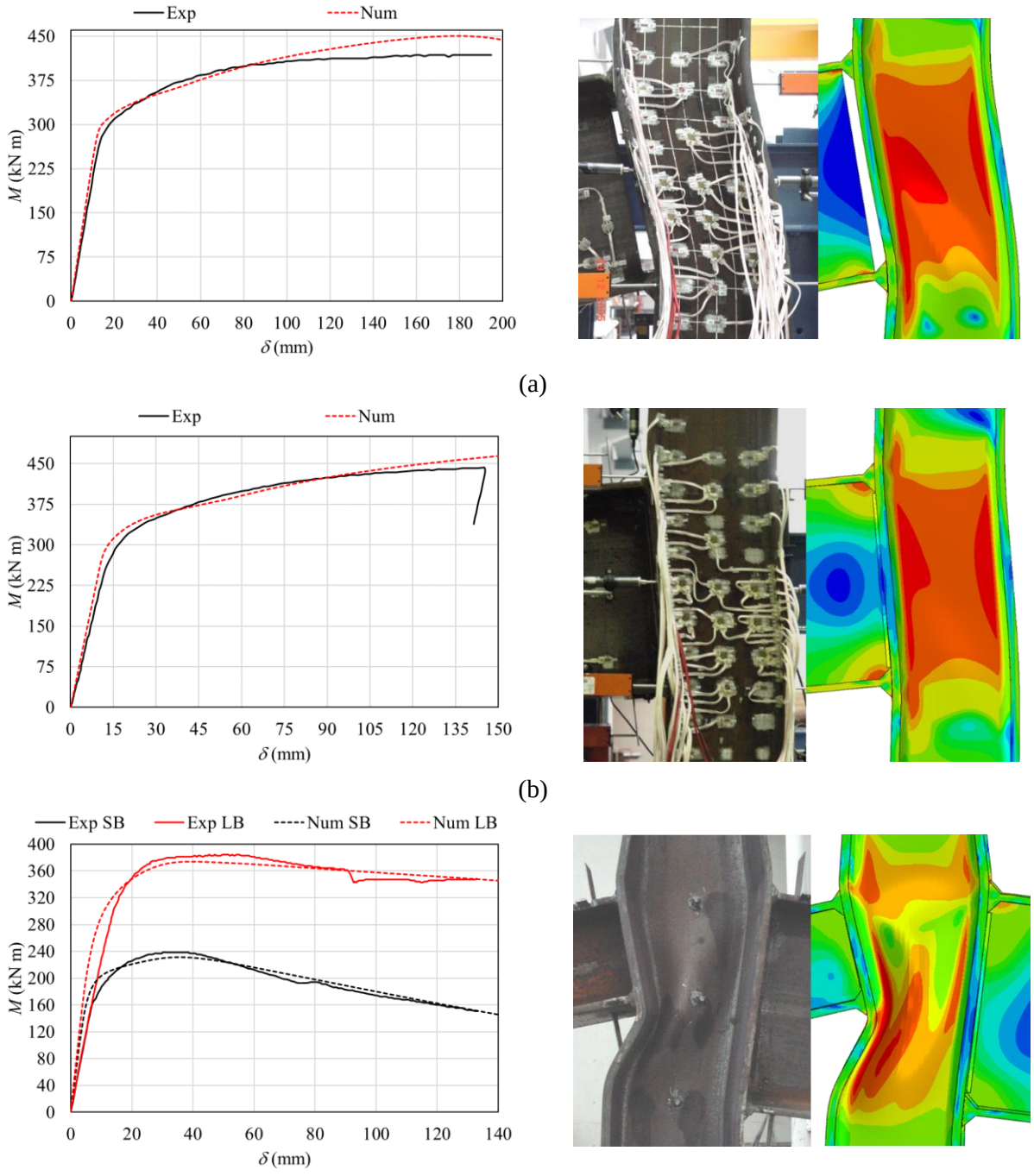

Fig. 2.15 – Experimental vs numerical results for tests from (Jordão, 2008).
(a) S355 E1.1; (b) S355 E1.2; (c) S355 E2.

The comparisons show that there is a good agreement between experimental and numerical results in terms of initial stiffness, resistance, and deformation. The largest differences in the M-δ curves were obtained for test S355 E2. However, it can be stated that the overall behavior of the joint is well captured, given the uncertainties from the experimental test.

Therefore, the FE solid model was successfully validated using experimental data available in the literature, meaning that the developed model provides a powerful tool for conducting extensive parametric studies.

2.3 CBFE MODELS

Besides the FE solid models, the steel connections are also modeled with the latest version (23.1.2 1027) of IDEA StatiCa software based on the so-called Component-Based Finite Element Method (CBFEM). This chapter describes the modeling assumptions, the main model properties (e.g., geometry, mesh, loading, boundary conditions, etc.), the type of analysis used, and the data extraction procedure.

2.3.1 Modeling and analysis using Python script

As the number of models and corresponding analyses for a statistically relevant amount of information is significant, in-house tailored Python scripts are developed for fast-track modeling, analysis, and result generation. Namely, a base model is manually created and subsequently, the parametric geometry, loading application, and model analysis are carried out using IDEA API. Finally, the changes and results are saved into a new connection model.

2.3.2 Model definition

The Python script used to change the geometry and introduce the loading uses the IDEA API and extracts all the geometrical and material information from an Excel file, as schematically shown in **Fig. 2.16**. Geometry is defined using the member and operation tools, setting the column as a bearing member, and concretizing the joint between the beam and the column with a "cut of member" operation. For all the models, full-penetration butt welds or fillet welds are considered. Once the geometry and loading are established, the IDEA API built-in calculator is called to run the analysis and generate an IDEA Connection file, **Fig. 2.16**.

2.3.2.a Material properties

For both columns and beams, the material properties are selected from IDEA StatiCa libraries. The materials adopted are S275 for columns and S235, S275, S355, S460, and S690 for beams. The material model adopted is elastic-plastic (for engineering stress and strain) with a nominal yielding plateau slope $E/1000$; it is worth mentioning that EN 1993-1-5 (CEN, 2006) in its annex C contemplates this material model, indicating "$E/10000$ or a similarly small value" for the post-yield tangent stiffness.

2.3.2.b Load application

Similar to FEM models, the loads applied in IDEA are obtained from equilibrium equations using the option 'Loads in Equilibrium', leading to single support at the bottom of the column. This is achieved using IDEA API, as presented in **Fig. 2.16**. The applied bending moment and the shear forces are adapted to be equal to the corresponding joint resistance values, calculated from EN 1993-1-8:2010.

2.3.2.c Mesh

Two different meshes are considered:

- i) 'default': with 12 finite elements along the longest member plate (web or flange), with a minimal size of the element of 8 mm and a maximal size of 50 mm;

- ii) ‘refined’: with 24 FE along the longest cross-section plate, whereas the minimum and the maximum size are kept at 4 mm and 25 mm, respectively. The mesh is controlled using the setup options, as shown in **Fig. 2.17**.

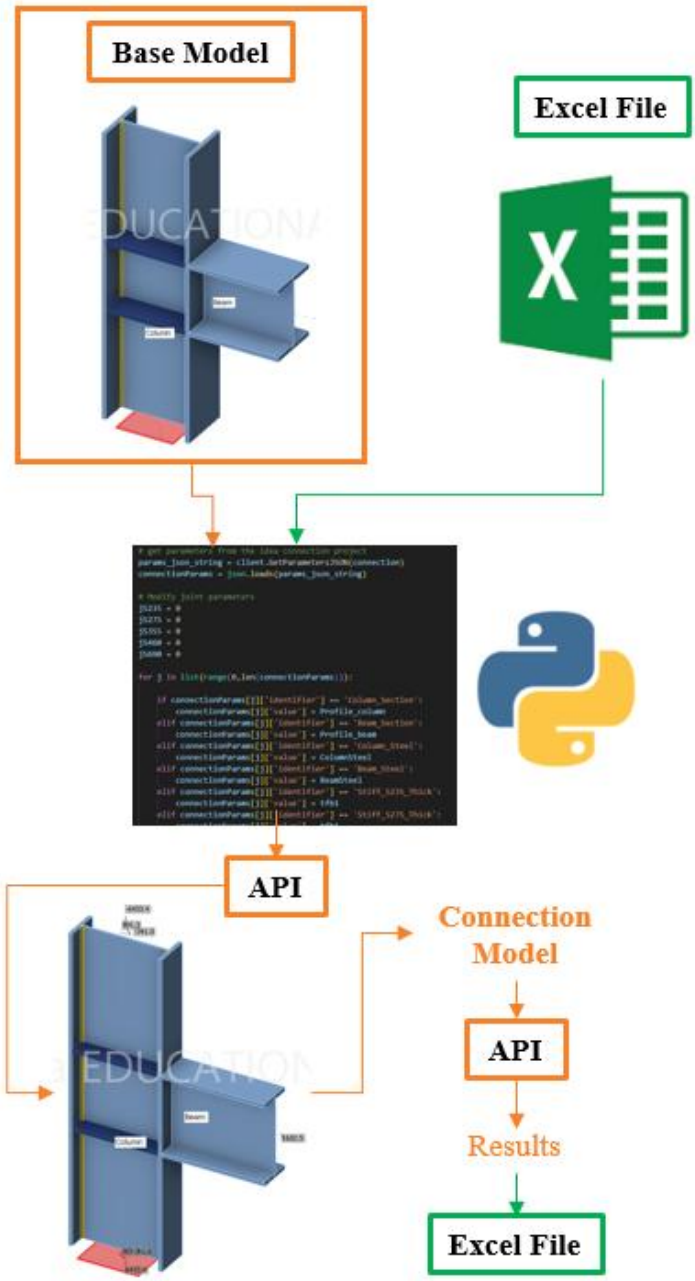

Fig. 2.16 – Python Scripting.
(a) IOM model; (b) API - Connection Model Generation.

2.3.2.d Fillet Welds

In the case of the fillet welds between the column and the beam, the material and thickness of the welds are defined as shown in **Fig. 2.18**(a). Similarly, in the case of welded column cross-section, the properties of the fillet welds between the adjacent plates can be directly defined in the software,

as shown in **Fig. 2.18**(b). It should be highlighted that in IDEA StatiCa 23.1 it is not possible to change the weld material or the throat thickness of the weld.

2.3.2.e Joint configurations

The joint configurations are those included in the numerical study, described in the following sections of this report. For every combination of column and beam, 8 different joint configurations are presented in **Fig. 2.19**.

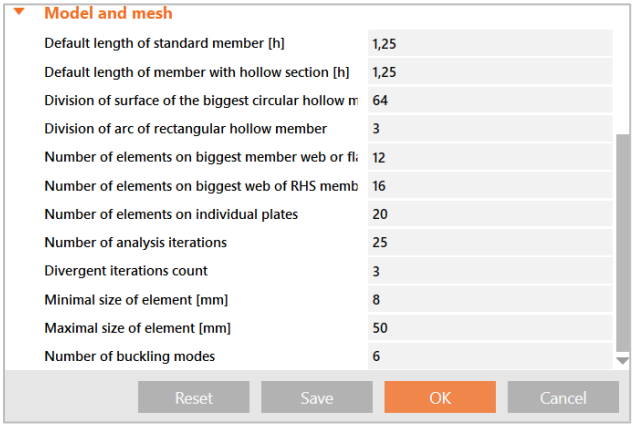

Fig. 2.17 – Mesh control in IDEA StatiCa.

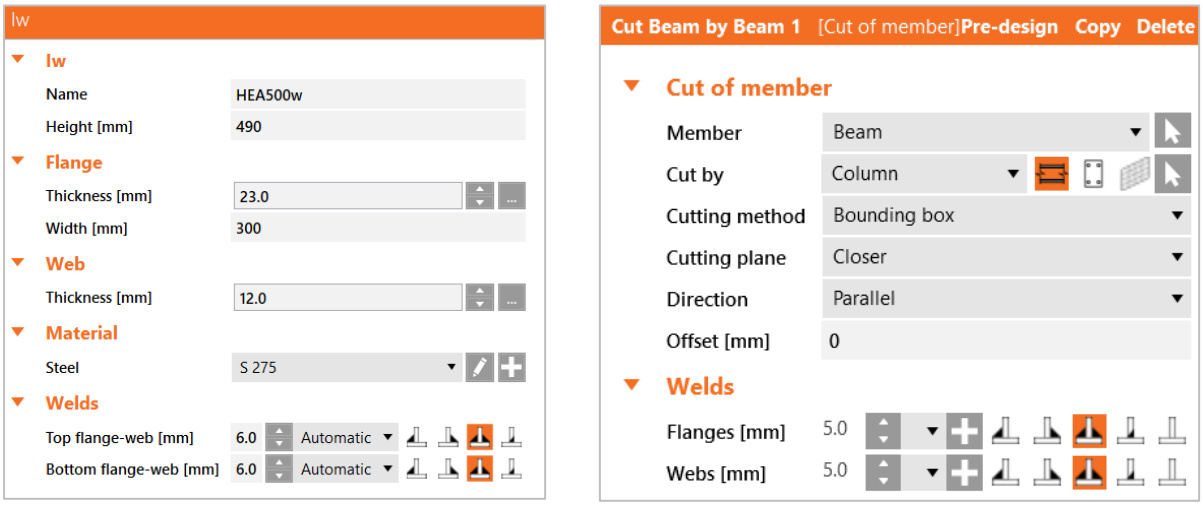

(a) (b)

Fig. 2.18 – Mesh control in IDEA StatiCa.

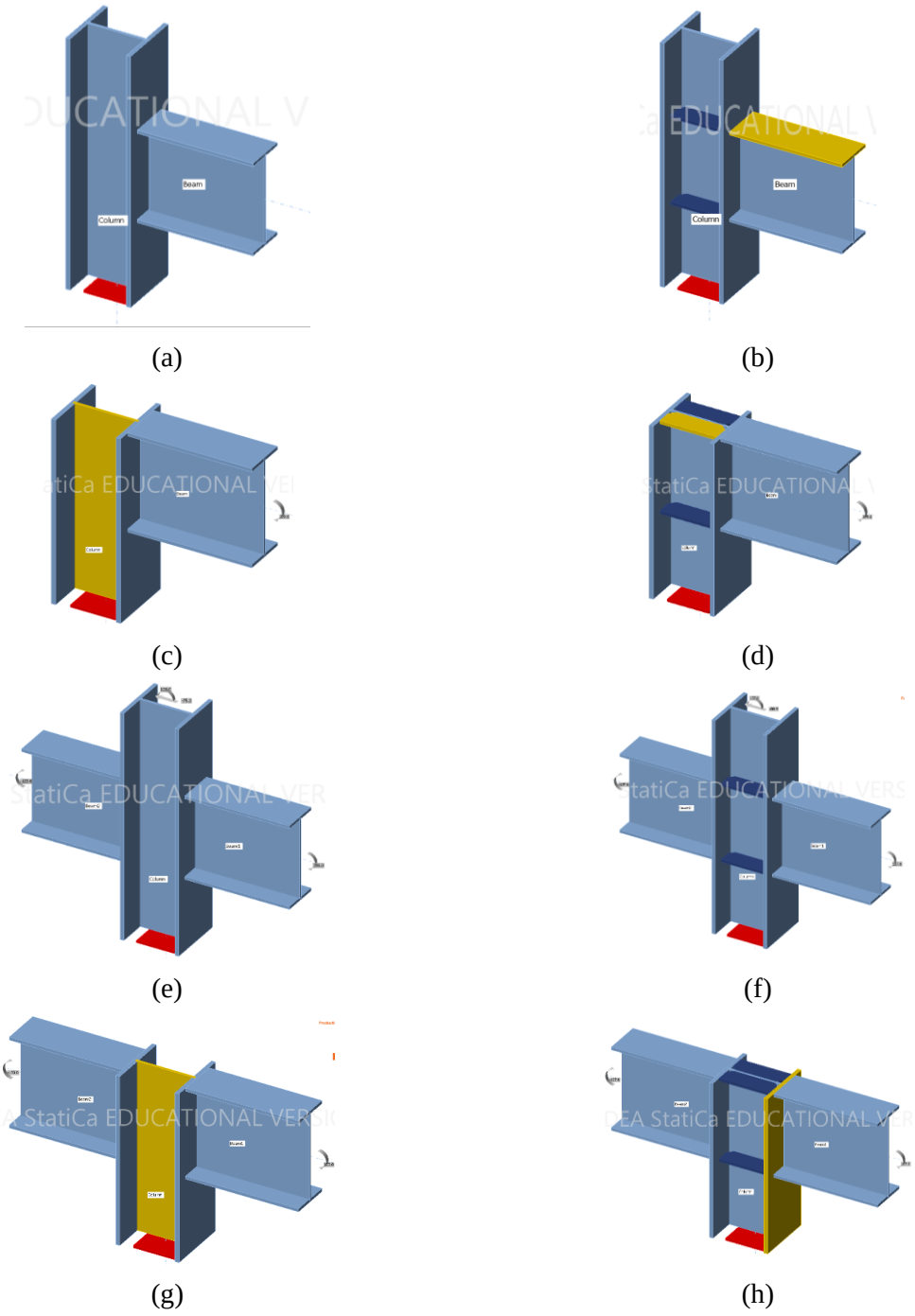

Fig. 2.19 – IDEA Connections.
a) one-sided unstiffened; b) one-sided stiffened; c) one-sided unstiffened top-floor; d) one-sided stiffened top-floor; e) two-sided unstiffened; f) two-sided stiffened; g) two-sided unstiffened top-floor; h) two-sided stiffened top-floor.

It is worth noting that the stiffener geometry consists of four plates in the same steel used for the beam, welded to the column web, and flanges with butt welds or fillet welds. The stiffeners are aligned with the beam flanges and have the same thickness as the beam flange, as presented in **Fig.**

2.20. The plates are chamfered at two corners with an angle of 45º measured from the edge point of the column section radius.

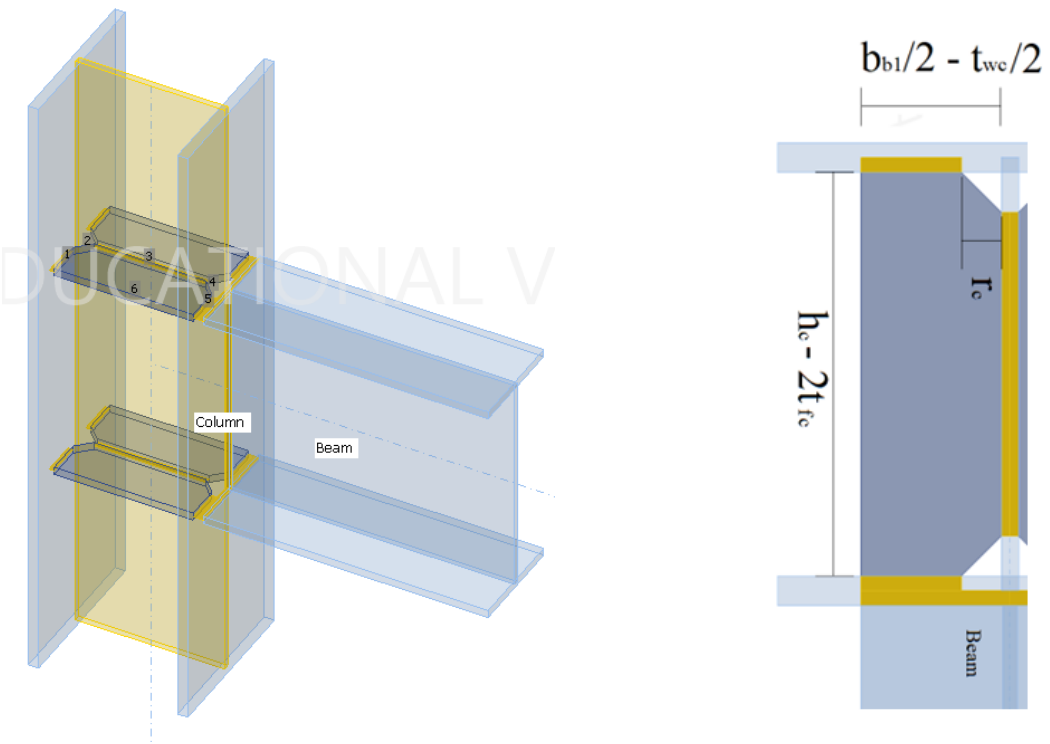

Fig. 2.20 – Horizontal stiffener plate geometry.

2.3.3 Type of analysis

For all models, the design resistance (DR) was carried out. Also, for some sets, other types of analyses available in the software were considered:

- i) Stiffness analysis (ST),
- ii) Linear buckling analysis (LBA).

The Design Resistance analysis returns the so-called *Applied Load Factor* (*ALF*) which represents the factor by which the applied load must be multiplied to obtain the joint design resistance. In this case, the design resistance is equal to the characteristic value, as no safety factors are considered. Once the moment resistance is obtained for each model, Stress-Strain Analysis is carried out, which gives a graphical interpretation of the Von Mises stress distribution (i.e. equivalent stress). For all the analyses, the stopping criterion is defined by the program, corresponding to 5% of the maximum equivalent plastic strain achieved at any point of the connection. An example is shown in **Fig. 2.21**, where the stress distribution, the strain distribution, and the deformed shapes are presented for two different mesh sizes.

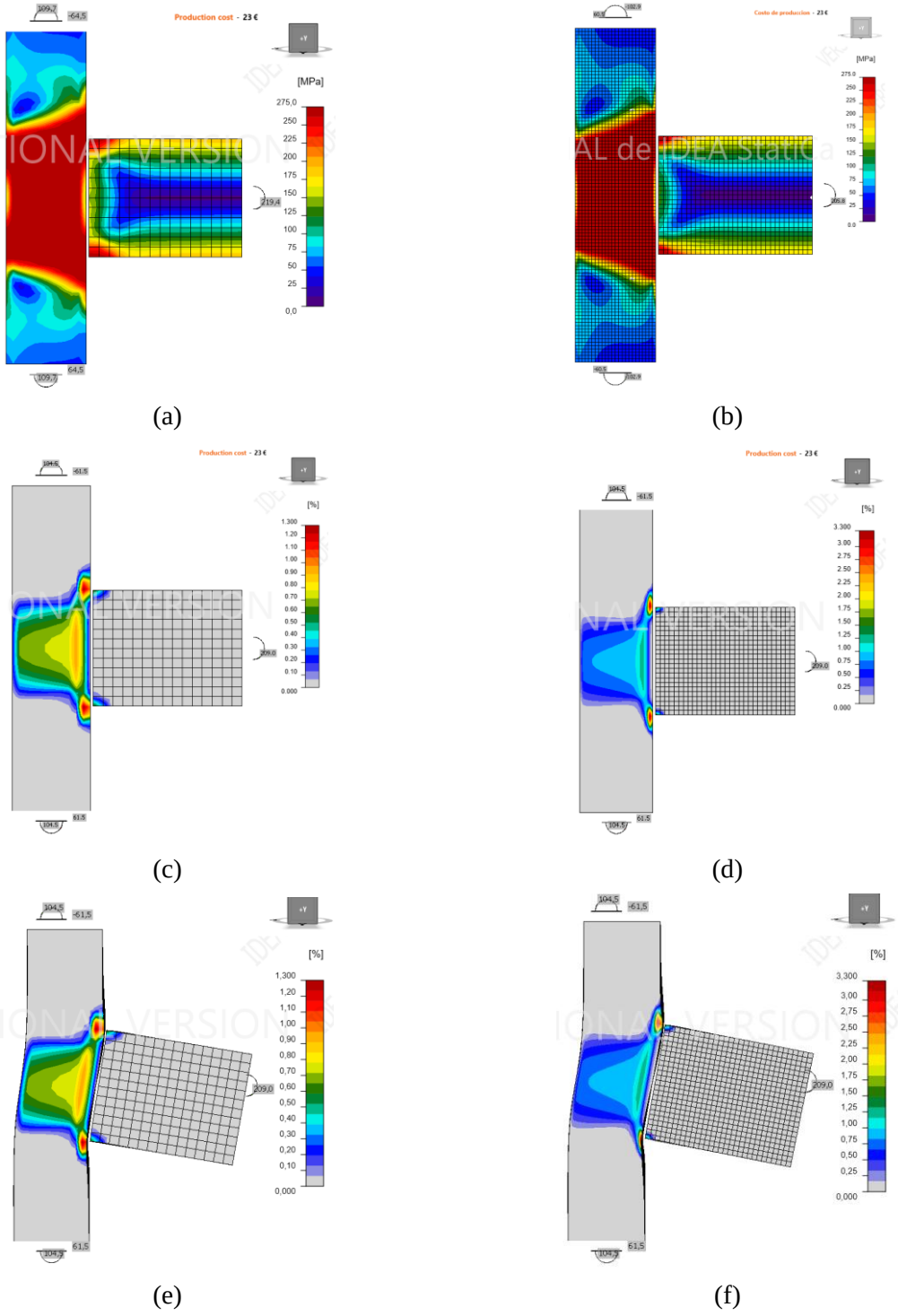

Fig. 2.21 – Von Mises Stress distribution.
a) 'default' mesh; b) 'refined' mesh; Plastic Stress distribution: c) 'default' mesh; d) 'refined' mesh; Deformed shape: e) 'default' mesh; f) 'refined' mesh.

The linear buckling analysis (LBA) is used to compute the buckling load factor (α_{cr}), as shown in **Fig. 2.22**(a). LBA is implemented by default in IDEA StatiCa 23.1 and can be accessed through

the check tab on the Stress-Strain analysis (SS) as shown in **Fig. 2.22**(b) or through IDEA API and Python scripts.

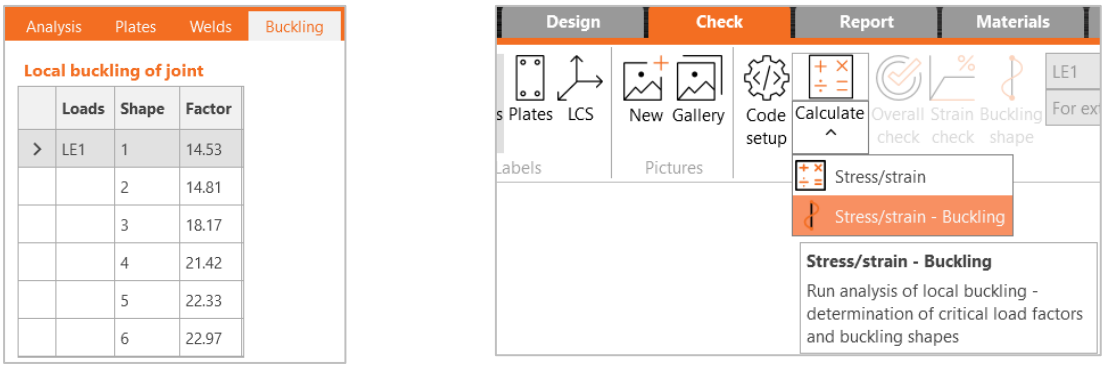

a) b)

Fig. 2.22 – LBA analysis in IDEA StatiCa 23.1.

Finally, the stiffness analysis (ST) is also implemented by default on IDEA StatiCa 23.1 and can be accessed both through the software user interface and the API. Among others, the following outputs can be computed using ST analysis:

- Initial Stiffness ($S_{j,ini}$)
- Secant Rotational Stiffness ($S_{j,sec}$)
- Rotational capacity (ϕ_j)
- Joint classification (Class)
- Moment-rotation curve, see **Fig. 2.23**.

It should be highlighted that the stiffness analysis implies a change in boundary conditions, fixing all members but the one that may be analyzed, as shown in **Fig. 2.24.**

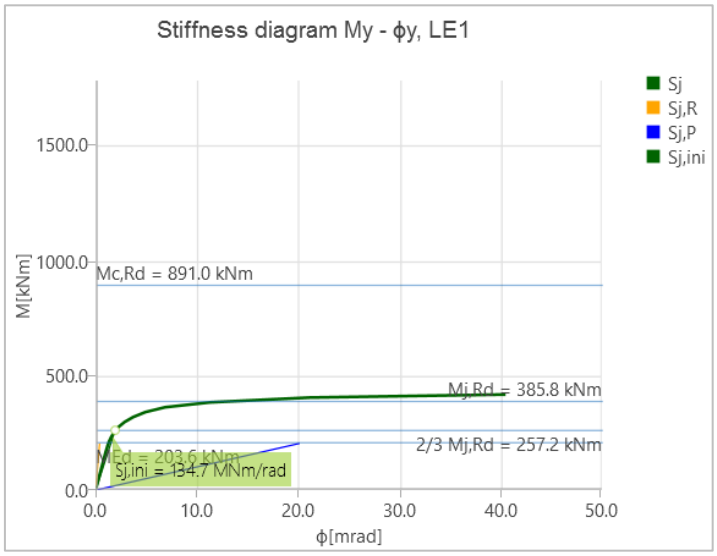

Fig. 2.23 – IDEA StatiCa 23.1 Moment-rotation curve.

ACIV - Associação para o Desenvolvimento da Engenharia Civil - **UNIVERSIDADE DE COIMBRA** – NIF 505448173
Departament of Civil Engineering - FCTUC * Rua Luís Reis Santos | Pólo II da Univ. Coimbra | 3030-788 COIMBRA
ISISE UC – Institute for Sustainability and Innovation in Structural Engineering

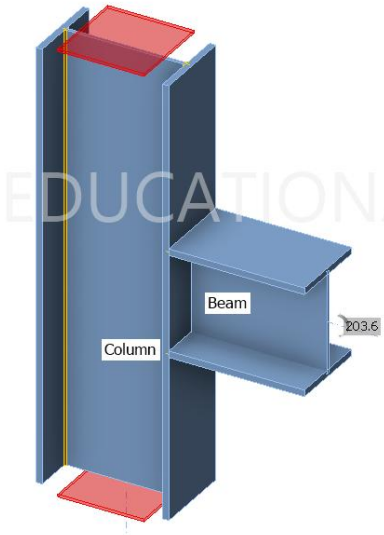

Fig. 2.24 – IDEA StatiCa 23.1 Stiffness analysis boundary conditions.

2.3.4 Geometrically non-linear analysis (GMNA)

For open sections, geometrically non-linear analysis (GMNA) is not implemented by default in IDEA StatiCa version 23.1, however, this option can be activated through the API Python scripts, as shown in **Fig. 2.25**.

Also, it is possible to perform the GMNA analysis by adding the line <add key="UserMode" value="16" /> to the file "IdeaConnection.exe.config", as shown in **Fig. 2.26**, and selecting the option "GMNA for each connection" in Code setup, as shown in **Fig. 2.27**.

```
codeSetup['analysisAllGNL'] = True
codeSetup['numElement'] = 12*Refinement_factor
codeSetup['minSize'] = 0.008/Refinement_factor
codeSetup['maxSize'] = 0.05/Refinement_factor
updated_codeSetup_json_string = json.dumps(codeSetup)
```

Fig. 2.25 – GMNA activation in IDEA StatiCa 23.1 API.

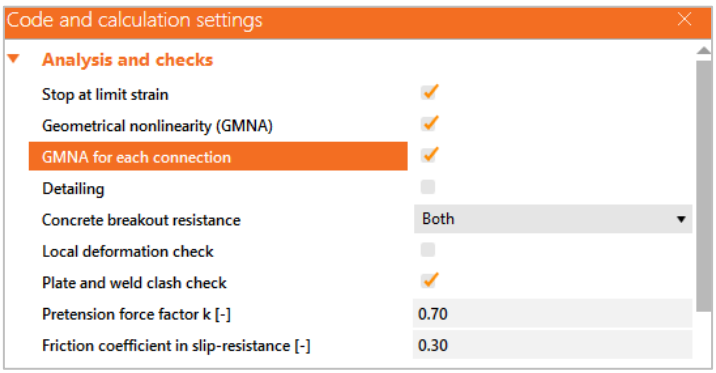

Fig. 2.26 – GMNA activation in IDEA StatiCa 23.1.

```
<?xml version="1.0" encoding="utf-8"?>
<configuration>
  <appSettings>
  <add key="UserMode" value="16" />
  </appSettings>
  <startup>
    <supportedRuntime version="v4.0" sku=".NETFramework,Version=v4.8" />
  </startup>
  <runtime>
    <assemblyBinding xmlns="urn:schemas-microsoft-com:asm.v1">
      <dependentAssembly>
        <assemblyIdentity name="CommonServiceLocator" publicKeyToken="489b6accfaf20ef0" culture="neutral" />
        <bindingRedirect oldVersion="0.0.0.0-2.0.5.0" newVersion="2.0.5.0" />
```

Fig. 2.27 – Developer version activation.

2.3.5 Results extraction in case of axially loaded columns

In those cases where, besides bending moment, an additional axial force is applied at the column, it is important to highlight that in the Design Resistance analysis, the obtained Applied Load Factor ALF (i.e., load multiplier) corresponds to all applied loads in the connection (and not only bending moment). The consequence is that the final level of axial force cannot be controlled. Therefore, another approach to obtain the moment resistance was used, namely, for a given axial force acting on the column, the objective is to maintain the force constant while increasing only the applied bending moment. To do so, in the Python script, an iterative procedure is introduced with the steps illustrated in **Fig. 2.28**, as follows:

1. Analyze the connection to obtain the first ALF.
2. Multiply only the moment acting on the connection by ALF and maintain the same axial force.
3. Analyze again the connection to obtain a new ALF and store the product of the old and the new ALF as Load Factor (LF).
4. Repeat 2 to 3 until the new ALF is not equal to 1.0.

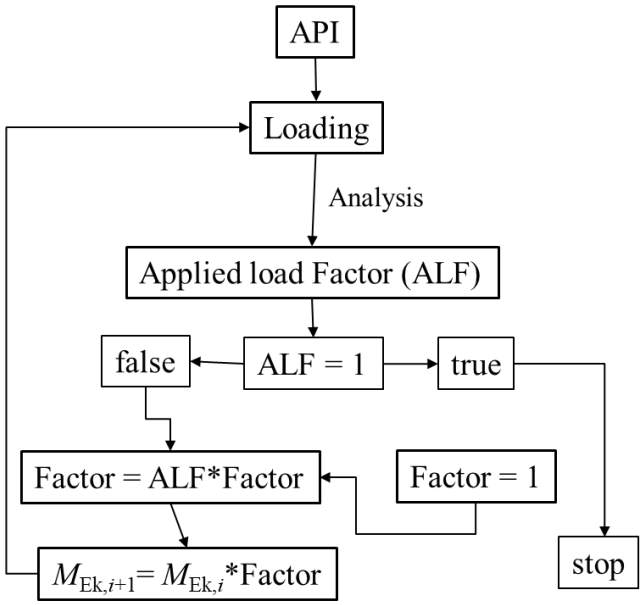

Fig. 2.28 – Algorithm implemented to obtain the real moment resistance.

ACIV - Associação para o Desenvolvimento da Engenharia Civil - **UNIVERSIDADE DE COIMBRA** – NIF 505448173
Departament of Civil Engineering - FCTUC * Rua Luís Reis Santos | Pólo II da Univ. Coimbra | 3030-788 COIMBRA
ISISE UC – Institute for Sustainability and Innovation in Structural Engineering

2.3.6 Mesh size and Richardson extrapolation

FEM results are dependent on the mesh size. Generally, a coarser mesh has a spurious stiffening effect, which results in higher values of moment resistance and stiffness. Therefore, the mesh size is a variable of interest in the predicted response. In this study, two meshes are considered for each model:

i) the default IDEA StatiCa (v23.1) mesh, referred to as ISdef,

ii) a refined mesh, half the size of the former, therefore with 4 times the number of planar elements, referred to as ISref.

Values of moment resistance are obtained with both meshes. In addition, a third value is obtained using the Richardson extrapolation (Oñate, 2009). A brief explanation follows (for simplicity, this is given for a unidimensional case, but the concept is directly applicable to multidimensional cases).

In the FE method, the displacement u is approximated by shape functions which are polynomials of order n. The n^{th}–degree Taylor approximation $u_{\text{approx},n}$ to the displacement u at a point of coordinate x is given by:

$$u_{\text{approx},n}(x) = u(x_i) + \frac{u'(x_i)}{1!}(x-x_i) + \ldots + \frac{u^{n)}(x_i)}{n!}(x-x_i)^n, \tag{2.5}$$

where $x_i \le x$. The exact value of displacement can be expressed as:

$$\begin{aligned} u(x) &= u(x_i) + \frac{u'(x_i)}{1!}(x-x_i) + \ldots + \frac{u^{n)}(x_i)}{n!}(x-x_i)^n + \frac{u^{n+1)}(x_0)}{(n+1)!}(x-x_i)^{n+1} = \\ &= u_{\text{approx},n}(x) + \frac{u^{n+1)}(x_0)}{(n+1)!}(x-x_i)^{n+1}, \end{aligned} \tag{2.6}$$

where $x_0 \le x_i \le x$. Therefore, the error e is:

$$e = u(x) - u_{\text{approx},n}(x) = \frac{u^{n+1)}(x_0)}{(n+1)!}(x-x_i)^{n+1} \approx \lambda (x-x_i)^{n+1}, \tag{2.7}$$

If a FEM mesh 1 of size s is used, the error e_1 for that mesh is of the order:

$$e_1 \approx \lambda (s)^{n+1}, \tag{2.8}$$

If a second mesh 2 is used, in which the size of the elements is s/d, the error is:

$$e_2 \approx \lambda (s/d)^{n+1}, \tag{2.9}$$

Therefore:

$$u - u_{approx}^{(1)} \approx \lambda (s)^{n+1}, \tag{2.10}$$

$$u - u_{approx}^{(2)} \approx \lambda (s/d)^{n+1}, \tag{2.11}$$

where u is the exact value of displacement, $u_{approx}^{(1)}$ is the approximation obtained with mesh 1, $u_{approx}^{(2)}$ and is the approximation obtained with mesh 2. Dividing both expressions:

$$\frac{u - u_{approx}^{(1)}}{u - u_{approx}^{(2)}} \approx \frac{\approx \lambda (s)^{n+1}}{\lambda (s/d)^{n+1}} = d^{n+1}, \tag{2.12}$$

whereupon:

$$u \approx \frac{u_{approx}^{(1)} - u_{approx}^{(2)} d^{n+1}}{1 - d^{n+1}}. \tag{2.13}$$

The previous expression allows for an estimate of any variable from the values obtained using two meshes. For this study, mesh 1 is the default IDEA StatiCa mesh (ISdef), and mesh 2 is the refined mesh (ISref), with halved element size, therefore $d = 2$. Eq. (2.13) can be rewritten in the following form:

$$M_{\mathrm{R,ISrich}} = \frac{4M^{(2)}_{\mathrm{R,ISref}} - M^{(1)}_{\mathrm{R,ISdef}}}{3}, \tag{2.14}$$

where $M_{\mathrm{R,ISdef}}$ is the moment resistance obtained with IDEA StatiCa using the default mesh, $M_{\mathrm{R,ISref}}$ is the moment resistance obtained with the refined mesh, and $M_{\mathrm{R,ISrich}}$ is the moment resistance estimated with the Richardson extrapolation.

2.4 NUMERICAL STUDY

2.4.1 Scope of study and case selection

The objective of the study is to compare the FEM solution (3D Abaqus model) with the predictions of CBFEM (IDEA StatiCa), EC3-1-8, and FprEC3-1-8 for a large and representative sample of beam-column joints, to provide an assessment of the accuracy of the code expressions. **Fig. 1.1** introduces the four different joint layouts treated: single-sided for an internal story (1S-I) or roof (1S-R), and double-sided for an internal story (2S-I) or roof (2S-R). Stiffened configurations for all layouts were considered and referred to with the tag 'T'. The study was limited to welded, strong-axis joints for hot-rolled and welded columns but considered several levels of axial load for the column. The steel grades assumed for the column were S235, S275, and S355, but a larger emphasis was placed on S275. The influence of imperfections and second-order effects was also addressed. The welds were assumed either as full-penetration butt welds with no oversize (not modeled) or fillet welds (explicitly modeled). In the first case (butt welds), total continuity was assumed between the welded parts.

The features of the FE models used in the study and their validation have already been discussed in Section 2.2. The layout for the different models (1S-I, 1S-R, 2S-I, 2S-R) is presented in **Fig. 2.29**. The moment M_1 was always the largest (in absolute terms) at the joint, that is, $-1 \leq m_r = M_2/M_1 < 1$. As discussed, the models presented a 'solid core' which was the focus of the study.

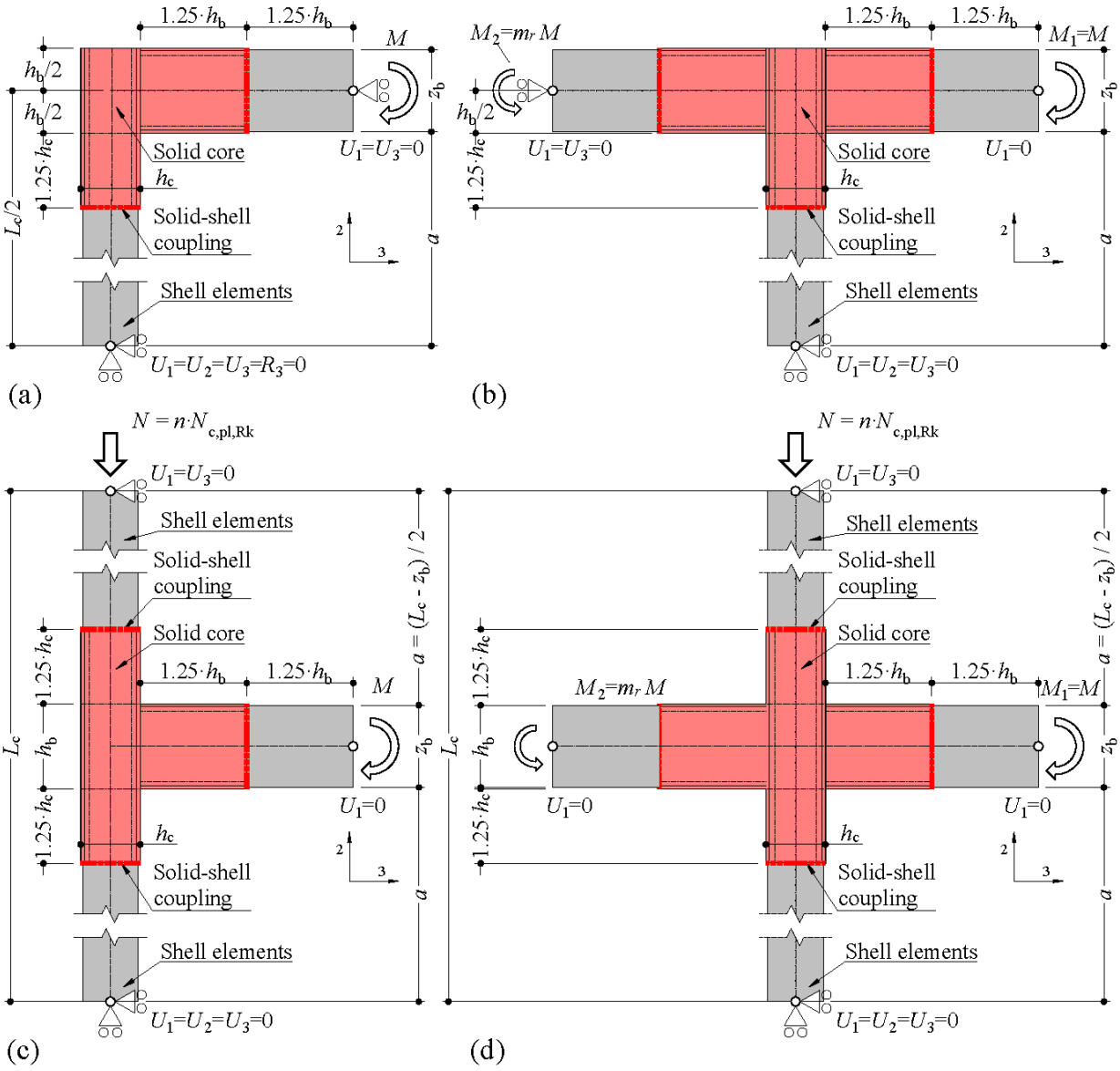

Fig. 2.29 – Layout for FE models.
(a) 1S-R; (b) 2S-R; (c) 1S-I; (d) 2S-I.

The response of the joint is strongly dependent on the column web panel slenderness d_c/t_{wc}, the column shear area A_{vc}, and the aspect ratio of the joint h_b/d_c. The selection of 20 cases (defined as combinations of a column and a beam) in this study was based on these parameters. Different sets were then defined, each containing the 20 cases, but with different configurations: one-sided (1S), two-sided (2S), roof (R), internal story (I), unstiffened, stiffened (T), with different levels of axial load, and different ratios of applied moment. The case and set selection are described next.

2.4.1.a Definition of cases

To select columns corresponding to the usual European engineering practice, the complete database of rolled sections typically used for columns in Europe (HE and UC) was adopted, excluding initially large columns ($h_c \geq 600$mm). The profiles were represented as points in the

(A_{vc}) – (d_c/t_{wc}) space, which was then divided into 5 parts by 4 horizontal lines located at chosen values of d_c/t_{wc} so that each part contained 1/5 of the total number of columns. The process was repeated for the vertical, thus dividing the space into 25 quadrants. 5 columns were then selected from 5 different quadrants following the Latin hypercube methodology, whereupon each column belonged to a different vertical and horizontal partition than the rest. To expand the sample, 2 large columns ($h_c \geq 600$mm) were then added with the same philosophy. In the selection of the 7 columns, care was taken to choose a variety of cross-section types, including HEA, HEB, HEM, and UC profiles. The points defining the final column selection in the (A_{vc}) – (d_c/t_{wc}) space are displayed in **Fig. 2.30**.

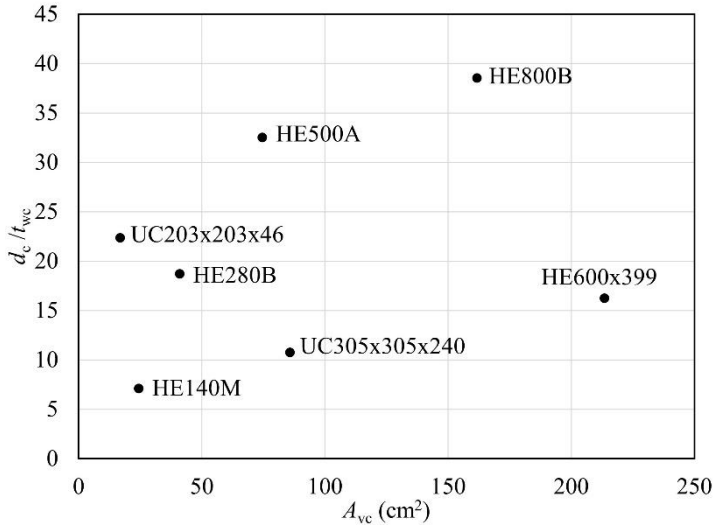

Fig. 2.30 – Selection of columns in the (A_{vc}) – (d_c/t_{wc}) space.

To complete the definition of the parametric study, 3 European beams (belonging to IPE, HE, UC, or UB series) were individually selected for each column, providing aspect ratios h_b/d_c of approximately 1, 1.5, and 2. The aspect ratio of 2 was not possible for column HE800B, therefore a total of 20 cases (3×6 + 2×1) are defined and listed in **Table 2.5**. The beam profile and steel grade were selected to:

- i) avoid beam failure before the column failure, and;
- ii) fulfil the requirements of EC3-1-8 (see clause 4.10(3) in the code) for unstiffened joints. This was only not possible for some two-sided joints with a moment ratio $m_r = 0.5$ (see below).

The table lists also the value of the web panel yield moment, $M_{y,wp}$, used as a normalization value for moment resistance, as is discussed in the following sub-sections.

Table 2.5. Selection of cases.

n	Column	Beam	d_c/t_{wc}	h_b/d_c	L_c (mm)	$M_{y,wp}$ (kNm)		
						S235	S275	S355
01	HE500A	HE400B	32.50	1.03	3400	300.0	351.0	453.1
02	HE500A	HE600A	32.50	1.51	3590	450.7	527.5	680.9
03	HE500A	HE800B	32.50	2.05	3800	611.9	716.1	924.4
04	UC203x203x46	HE160A	22.39	0.94	3152	28.4	33.2	42.9
05	UC203x203x46	IPE240	22.39	1.49	3240	45.7	53.5	69.0
06	UC203x203x46	IPE330	22.39	2.05	3330	63.2	74.0	95.5
07	HE280B	HE200B	18.67	1.02	3200	73.8	86.4	111.5
08	HE280B	IPE300	18.67	1.53	3300	115.4	135.0	174.3
09	HE280B	IPE400	18.67	2.04	3400	154.2	180.4	232.9
10	HE140M	HE100B	7.08	1.09	3100	25.4	29.7	38.4
11	HE140M	HE140B	7.08	1.52	3140	36.1	42.3	54.6
12	HE140M	IPE200	7.08	2.17	3200	54.0	63.2	81.6
13	UC305x305x240	HE260B	10.31	1.10	3260	266.8	312.2	403.0
14	UC305x305x240	HE360B	10.31	1.52	3360	371.3	434.4	560.8
15	UC305x305x240	IPE500	10.31	2.11	3500	532.4	623.0	804.3
16	HE600x399	HE450M	16.20	0.98	4478	1155.3	1351.9	1745.2
17	HE600x399	HE700M	16.20	1.47	4716	1783.0	2086.5	2693.5
18	HE600x399	HE1000M	16.20	2.07	5008	2553.2	2987.7	3856.9
19	HE800B	HE700B	38.51	1.04	4700	1268.9	1484.8	1916.8
20	HE800B	HE1000B	38.51	1.48	5000	1831.1	2142.8	2766.1

To keep consistency, the same geometrical properties (width h_c, depth h_c, flange thickness t_{fc}, web thickness t_{wc}) have been assumed for the welded columns. Slightly larger web panel slenderness is then obtained for the same cases.

2.4.1.b Definition of sets

The study was divided into sets. Every set comprised the 20 cases defined in **Table 2.5**, but with differences in:

- i) sides (one-sided ‘1S’, two-sided ‘2S’);
- ii) joint location (internal story ‘I’, roof ‘R’);
- iii) stiffened (‘T’) or unstiffened (‘U’ or blank);
- iv) level of applied axial force as a ratio of the column resistance (n = 0%, 30%, 50% or 70%, $n = N_E / N_{pl,Rk}$, where N_E is the applied axial load, and $N_{pl,Rk}$ is the characteristic column axial load resistance obtained as $A_c \cdot f_{yc}$; A_c is the total column cross-section area, and f_{yc} the column yield strength);
- v) for two-sided joints only, the moment ratio between both sides ($m_r = M_1/M_2$ = 0.50, –0.50, –1.00).

The 40 resulting sets are defined in **Table 2.6**, comprising 800 models in total.

Table 2.6. Definition of sets.

Set	Sides	Location	n	Stiffened	$m_r = M_2/M_1$	Model number
Set 01	1S	I	0%		-	0001-0020
Set 02_N30	1S	I	30%		-	0101-0120
Set 02_N50	1S	I	50%		-	0201-0220
Set 02_N70	1S	I	70%		-	0301-0320
Set 03	1S	I	0%	T	-	0401-0420
Set 04_N30	1S	I	30%	T	-	0501-0520
Set 04_N50	1S	I	50%	T	-	0601-0620
Set 04_N70	1S	I	70%	T	-	0701-0720
Set 05_MR-100	2S	I	0%		-1	0801-0820
Set 05_MR-050	2S	I	0%		-0.50	0901-0920
Set 05_MR050	2S	I	0%		0.50	1001-1020
Set 06_N30_MR-100	2S	I	30%		-1	2101-2120
Set 06_N30_MR-050	2S	I	30%		-0.50	2201-2220
Set 06_N30_MR050	2S	I	30%		0.50	2301-2320
Set 06_N50_MR-100	2S	I	50%		-1	1101-1120
Set 06_N50_MR-050	2S	I	50%		-0.50	1201-1220
Set 06_N50_MR050	2S	I	50%		0.50	1301-1320
Set 06_N70_MR-100	2S	I	70%		-1	2501-2520
Set 06_N70_MR-050	2S	I	70%		-0.50	2601-2620
Set 06_N70_MR050	2S	I	70%		0.50	2701-2720
Set 07_MR-100	2S	I	0%	T	-1	1401-1420
Set 07_MR-050	2S	I	0%	T	-0.50	1501-1520
Set 07_MR050	2S	I	0%	T	0.50	1601-1620
Set 08_N30_MR-100	2S	I	30%	T	-1	3101-3120
Set 08_N30_MR-050	2S	I	30%	T	-0.50	3201-3220
Set 08_N30_MR050	2S	I	30%	T	0.50	3301-3320
Set 08_N50_MR-100	2S	I	50%	T	-1	1701-1720
Set 08_ N50_MR-050	2S	I	50%	T	-0.50	1801-1820
Set 08_ N50_MR050	2S	I	50%	T	0.50	1901-1920
Set 08_ N70_MR-100	2S	I	70%	T	-1	3701-3720
Set 08_ N70_MR-050	2S	I	70%	T	-0.50	3801-3820
Set 08_ N70_MR050	2S	I	70%	T	0.50	3901-3920
Set 09	1S	R	0%		-	2001-2020
Set 11	1S	R	0%	T	-	2401-2420
Set 13_MR-100	2S	R	0%		-1	2801-2820
Set 13_MR-050	2S	R	0%		-0.50	2901-2920
Set 13_MR050	2S	R	0%		0.50	3001-3020
Set 15_MR-100	2S	R	0%	T	-1	3401-3420
Set 15_MR-050	2S	R	0%	T	-0.50	3501-3520
Set 15_MR050	2S	R	0%	T	0.50	3601-3620

ACIV - Associação para o Desenvolvimento da Engenharia Civil - **UNIVERSIDADE DE COIMBRA** – NIF 505448173
Departament of Civil Engineering - FCTUC * Rua Luís Reis Santos | Pólo II da Univ. Coimbra | 3030-788 COIMBRA
ISISE UC – Institute for Sustainability and Innovation in Structural Engineering

2.4.1.c Definition of clusters

A cluster is formed by a subset of the 40 sets listed in **Table 2.6**, with the following specifications (added to the 'case' and 'set' labels):

- i) Column steel grade (S275, S235, S355). If no indication is given, S275 is assumed.
- ii) Type of column (Rolled, Welded). If no indication is given, a rolled column is assumed.
- iii) Type of weld between beam and column (butt weld, fillet weld) or, only for welded columns, between column web and column flange (butt weld, fillet weld). If no indication is given, butt welds are assumed.

The clusters are listed in **Table 2.7**. Due to the large size of the study, for some clusters only some sets are included. Namely, in clusters FR-S275 and BW-S275, only 1S-I joints are considered.

Table 2.7. Definition of clusters.

Cluster	Steel grade	Beam-column weld	Column type	Column web to flange weld	Sets	Model number
BR-S275	S275	Butt	Rolled	-	All	+0
BR-S355	S355	Butt	Rolled	-	All	+5000
BR-S235	S235	Butt	Rolled	-	All	+10000
BB-S275	S275	Butt	Welded	Butt	All	+20000
FR-S275	S275	Fillet	Rolled	-	01 to 04	+30000
BF-S275	S275	Butt	Welded	Fillet	01 to 04	+40000

2.4.1.d Fillet welds

In the study, two types of fillet welds are considered: between the beam and the column (BCW) and between the column flange and the column web (CCW). The two types have not been mixed in any cluster. The weld throat is always adopted as a multiple of 0.5mm. It was defined in the following way:

- CCW: the throat a_c between column flange and column web was taken as $0.5 \cdot \min\{t_{fc}, t_{wc}\}$. Using the directional design method for welds, it can be easily verified that, for steel grades up to S355, full resistance is thus obtained. Therefore, the only influence of the fillet weld is on the dispersion of the forces in the column.
- BCW: the throats a_{bf} (beam flange) and a_{bw} (beam web), see **Fig. 2.2**, were predesigned as $0.6 \cdot t_{min}$, where t_{min} is the smallest plate (beam flange vs column flange, beam web vs column flange) joined in each case. Then the throats were increased by 0.5mm (if necessary) to reach a BCW resistance larger than the joint's moment resistance, according to the expressions presented in **Table 2.1**. However, this was not possible in the following cases: for sets 01 and 02, case 10. For sets 03 and 04, cases 10, 12 and 13. This is due to the limitation imposed to the weld design by EN 1993-1-8 (and FprEN 1993-1-8), whereby the resistance of the weld should be based on the weakest plate joined, which largely penalizes the cases for which beam and column are of different steel grades.

2.4.1.e Variability due to material model

To assess the influence of the material model, the full cluster BR-S275 is analyzed with both the bilinear (EPPL) material model and the quad-linear (QUAD) material model. In addition, set 01 of this cluster was also analyzed with the E1000 material model (material model in IDEA StatiCa).

2.4.1.f Variability due to initial imperfections

To assess the influence of the initial imperfections, only some sets of cluster 1 are analyzed with a reduced imperfection of $d_c/420$, besides the assumed imperfection of $d_c/200$.

2.4.2 Materials

The steel grade of the column was taken as S275 (f_{yc} = 275 MPa), S235 (f_{yc} = 235 MPa) or S355 (f_{yc} = 355 MPa). Nominal values are adopted, as per EN-1993-1-1. The steel grade of the beam was varied to ensure that only column components were critical in the behavior of the joint. This aspect is further described below. The modulus of elasticity of steel was adopted as E = 210 GPa and its Poisson's ratio as $\nu = 0.3$.

For the elastic-perfectly plastic model (EPPL), the material engineering stress-strain curve disregards strain hardening. For numerical reasons, the material model used by IDEA StatiCa features a small strain hardening (post-yield tangent stiffness $E_{sh} = E/1000$). The influence of this small value on resistance has been analyzed and found to be about 3% on average.

For the quad-linear model (QUAD), strain hardening is considered, using the expressions developed by (Yun and Gardner, 2017). The values of f_u for every material are taken as nominal values from EN-1993-1-1.

2.4.3 Limitations and assumptions of the study

The study presents the following limitations:

1. Only open-sections are considered.
2. Only strong-axis joints, with no weak-axis interaction, are considered.
3. Only welded joints are considered.
4. No axial force is considered on the beam.
5. For stiffened joints, transverse stiffeners are placed in both tension and compression areas simultaneously.

The study is subjected to the following assumptions:

1. The length of the solid part, taken as $1.25 \cdot h$, is enough to avoid interference with the joint area behavior.
2. Butt welds can be properly modeled by kinematic constraints between the shared nodes of the welded parts.
3. The effect of fillet welds up to the loading step where resistance is assessed can be adequately represented avoiding metallurgical effects (Heat Affected Zone HAZ) and damage considerations.
4. The steel material is elastic and perfectly plastic with no post-yield stiffness and no strain hardening.
5. Strain hardening is only considered for the weld and can be properly represented by a quad-linear model.

6. The amplitude of the initial imperfections (d_c/200) covers adequately the combined effect of geometrical imperfections and the residual stresses, which are not explicitly modeled.

2.4.4 Analysis

The FE models were subjected to increasing moments with load-controlled GMNIA (geometrical and material non-linear analysis with initial imperfections). For two-sided joints, the proportion between the applied moments at both beams m_r was kept constant throughout the analysis. The analysis ended when the maximum plastic true equivalent strain $\varepsilon_{pl,eq,\,max}$ at the joint solid core (beam excluded) was larger than the limit $\varepsilon_{pl,eq,lim}$ = 10%, or when a numerical lack of convergence, indicative of physical instability, was reached.

2.4.5 Post-processing and data extraction

For this study, the relevant output variables of the FE model at each loading step are:

- i) the applied moment $M = M_1$ (for two-sided joints M_2 can be calculated as $m_r \cdot M_1$, where a positive value of m_r indicates tension at the beam top);
- ii) the displacements $d_{FEM,T1}$, $d_{FEM,T2}$ (top) and $d_{FEM,B1}$, $d_{FEM,B2}$ (bottom), measured as the average of the displacements of the footprint of the corresponding (1 or 2) beam top and bottom flange on its connected column face;
- iii) the maximum value of $\varepsilon_{pl,eq,max}$ in the central solid core.

For a better understanding of the joint behavior, $\varepsilon_{pl,eq,max}$ is obtained at each load step for different non-intersecting regions of the solid core, as shown in **Fig. 2.31** for the different situations corresponding to different clusters (BR, FR, BB, BF). $\varepsilon_{pl,eq,max}$ is always retrieved at the FE element integration points with no averaging.

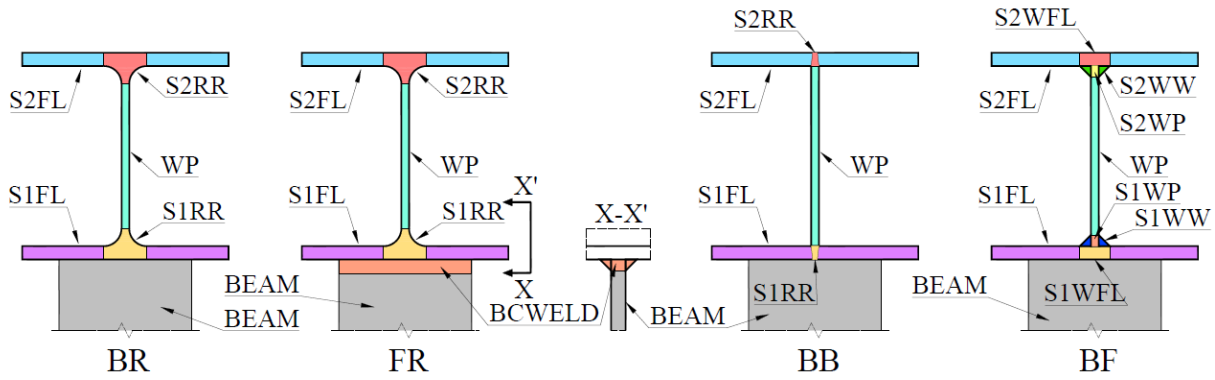

Fig. 2.31 – Joint output.

2.4.5.a Displacements and rotation

The FE model displacements ($d_{FEM,T1}$, $d_{FEM,T2}$, $d_{FEM,B1}$, $d_{FEM,B2}$) include components due to the column flexibility. To assess the joint stiffness, these components must be removed:

$$d_{T1} = d_{FEM,T1} - d_{RJ}, \tag{2.15}$$

$$d_{B1} = d_{FEM,B1} + d_{RJ}, \tag{2.16}$$

where d_{RJ} is the analytical displacement obtained assuming the column is infinitely rigid in the joint region. Similar equations can be written for d_{T2} and d_{B2}. d_{RJ} can be calculated with the expressions given in Section 1.4, repeated here for convenience:

$$d_{RJ,I} = M(1-m_r)\left(\frac{z_b\, a^3}{3L_c^2 EI_y} + \frac{z_b\, a}{L_c^2 GA_{vz}}\right), \tag{2.17}$$

$$d_{RJ,R} = 2d_{RJ,R}, \tag{2.18}$$

where $d_{RJ,I}$ is the correction term corresponding to the internal story configuration (I), $d_{RJ,R}$ is the correction term for the roof configuration (R), EI_y is the column bending stiffness, GA_{vz} is the column shear stiffness, E is the steel Young modulus, I_y is the column second moment of inertia for the strong axis, G is the steel shear modulus and A_{vz} is the column shear area coupled with I_y; all other variables in the expression are geometrically defined in **Fig. 1.3** to **Fig. 1.9**. For the one–sided joint, the expressions are valid, with $m_r = 0$.

As seen in **Fig. 2.32**, the corrected displacements obtained with the previous procedure define the apparent rotation $\phi_{j,ap}$ (measured from the horizontal), but the total joint rotation ϕ_j must be measured from the column axis, by adding the term $(d_{T1}+d_{B1})/(2a)$, or $(d_{T2}+d_{B2})/(2a)$, as applicable. The joint moment-rotation (M–ϕ_j) curve is built in this way, and its initial rotational stiffness is calculated as $S_{j,ini,FEM} = M/\phi_j$ at the first loading step.

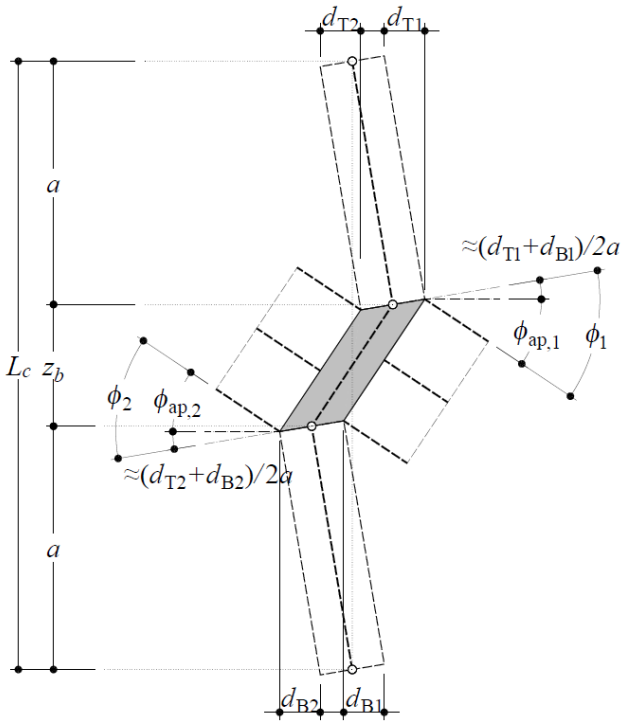

Fig. 2.32 – Joint output.

2.4.5.b Moment resistance and secant stiffness

Following the recommendations in prEN-1993-1-14 (CEN, 2022), the moment resistance $M_{R,FEM}$ is obtained as the minimum of:

- i) the maximum value reached during analysis;
- ii) the moment applied at the loading step where $\varepsilon_{pl,eq,max} \leq 5\%$ (in the solid core).

The joint rotation value at this step is $\phi_{j,R,FEM}$, and the secant stiffness $S_{j,sec,FEM}$ is defined as $M_{R,FEM}/\phi_{j,R,FEM}$. For brevity, the subscript 'FEM' is removed in successive equations, plots, and tables.

2.4.5.c Second-order effects

To assess the relevance of second-order effects, first- and second-order analyses for all sets and cases in cluster BR-S275 are compared using the following ratios: u_2 / u, $V_{max,2} / V_{max}$, $V_{min,2} / V_{min}$, $M_{max,2} / M_{max}$, $N_{min,2} / N_{min}$, where the subscript '2' indicates second-order analysis, no such subscript indicates first-order analysis, u is the in-plane displacement measured at the level of the centroid of the top beam flange, V_{max} and V_{min} are the maximum and minimum shear at the column, M_{max} is the maximum moment at the column, and N_{min} is the minimum axial force in the column (negative values indicate compression).

The results show a negligible influence (ratio < 1.05) of second-order effects for all variables in all cases, except for $V_{2,min}$ for which the ratio is 1.11. However, this is not a critical magnitude for the joint. The ratios for displacement are always below 1.04, with a mean value of 1.009 and a CoV of 0.85%.

The ratios for each variable are only dependent on the ratio of applied axial force n; for instance, for bending moment, all cases with n = 0.50 feature the same ratios. This is consistent with the general buckling theory, which predicts a dependency on the ratio N_E/N_{cr}. In addition, the results for N_{min} indicate that the axial force in the column can be taken as equal to the vertical force applied at the column end.

As a conclusion, for the selected joints, the second-order effects play a very small role in the horizontal displacements of the column at the beam flange levels, even for high values of axial load on the column (n = 0.7). Therefore, second-order effects are disregarded on the column flexibility used to correct the joint deformability, see Eq. (2.17).

2.4.5.d Beam yielding

As presented in **Fig. 2.33**, the total apparent rotation of the beam tip $\phi_{tot,ap,1}$ has two components, namely, joint rotation, $\phi_{j,ap,1}$ and the rotation of the beam segment between joint and tip $\phi_{b,1}$. That is,

$$\phi_{b,1} = \phi_{tot,ap,1} - \phi_{j,1}, \tag{2.19}$$

If these three values are plotted against the applied moment M_1, three M-ϕ curves are obtained. The tangent stiffness of each curve ($k_{t,tot,ap,1}$, $k_{t,j,ap,1}$, $k_{t,b,1}$) can easily be derived; for instance:

$$k_{t,tot,ap,1}^{(i)} = \frac{M_1^{(i+1)} - M_1^{(i)}}{\phi_{tot,ap,1}^{(i+1)} - \phi_{tot,ap,1}^{(i)}}, \tag{2.20}$$

where the superscript (i) indicates the loading step i. Similar equations can be written for $k_{t,j,ap,1}$ and $k_{t,b,1}$. Softening (that is, a value of tangent stiffness close to 0) of $k_{t,tot,ap,1}$ can be due to i) softening of $k_{t,j,ap,1}$; ii) softening of $k_{t,b,1}$; iii) softening of both. Only the first situation is desirable for the models included in the parametric study because the focus is on the column web components. Thus, the condition imposed is:

$$\frac{k_{t,j,ap,1}^{(i)}}{k_{t,b,1}^{(i)}} > \frac{k_{t,j,ap,1}^{(i-1)}}{k_{t,b,1}^{(i-1)}}, \tag{2.21}$$

If this condition occurs at step *i* before M_R is reached, the steel grade is increased. This is shown in **Fig. 2.34**(a), where M_R is marked with a dotted vertical line; it is not clear which element (beam or joint) governs the softening of the total rotation; contrarywise, in **Fig. 2.34**(b) this condition is never reached; it is apparent that the softening of total rotation is entirely due to the joint softening.

Choosing a beam with $M_{b,el,R}$ larger than $M_{j,R}$ is, not enough for two reasons: i) $M_{j,R}$ is not known a priori; only an approximate value can be obtained, which is sometimes smaller than the actual resistance; ii) the distribution of beam stresses in the vicinity of the joint does not follow the Navier assumption; on the contrary, stress concentrations appear, particularly in the central part of the flanges, so in this region the beam may yield locally even for levels of the applied moment below $M_{b,el,R}$, resulting in a large value of $\phi_{tot,ap,1}$, meaningless from the point of view of the study.

2.4.5.e Result normalization

To compare different cases, the FEM moment-rotation curves and the values of M_R and rotation $\phi_{j,R}$, are presented normalized to the panel zone yield moment $M_{y,wp}$ and yielding distortion $\phi_{y,wp}$:

$$M_{y,wp} = z_b\, d_c\, t_{wc}\, f_{yc} / \sqrt{3}, \tag{2.22}$$

$$\phi_{y,wp} = f_{yc} / (G\sqrt{3}). \tag{2.23}$$

The value of $M_{y,wp}$ is listed in **Table 2.5**. For S275, $\phi_{y,wp}$ = 0.197% ≈ 0.2%. An example of absolute and normalized moment-rotation plots is shown in **Fig. 2.35**. In the plots, the point where $\varepsilon_{pl,eq,max}$ = 5% is marked as ε_{lim}, and the column region where the limit is achieved is indicated (in this case, S1RR).

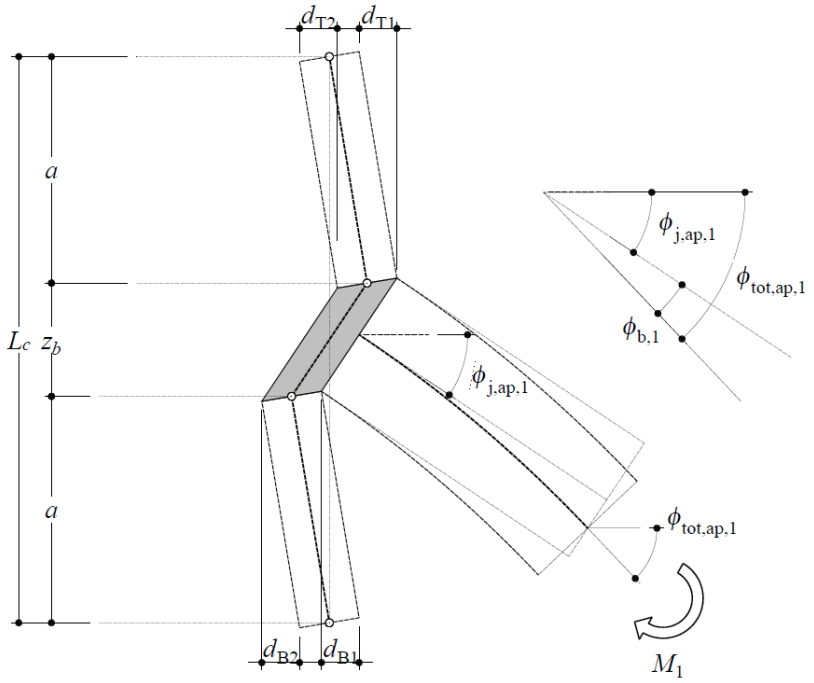

Fig. 2.33 – Rotation of beam tip.

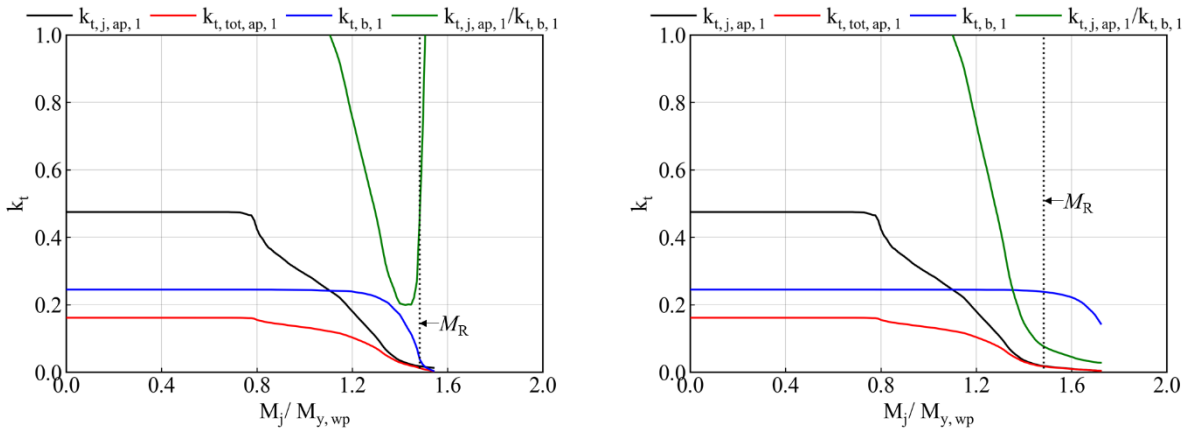

(a) (b)

Fig. 2.34 – Criterion to check beam yielding.
(a) beam governs; (b) joint governs.

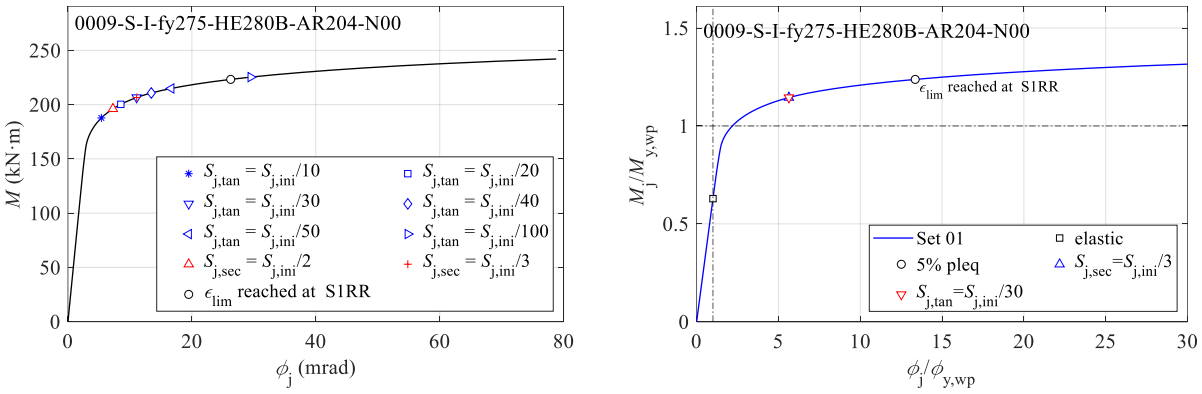

(a) (b)

Fig. 2.35 – Moment–rotation plots: (a) natural; (b) normalized.

2.4.5.f Other criteria to determine moment resistance

The absolute moment-rotation plot presented in **Fig. 2.35**(a) features different criteria to determine M_R. The 5% plastic strain criterion ($\varepsilon_{pl,eq,max} \leq 5\%$) already discussed is marked as 'ε_{lim}'. Two additional criteria are considered:

- 'Weynand' or 'secant stiffness' criterion, based on a softening of the secant stiffness with respect to the initial stiffness, $S_{j,sec} = S_{j,ini}/h$. Two different values of h (2, 3) are presented, but $h = 3$ is the most common in practice.
- 'Softening' or 'tangent stiffness' criterion, based on the softening of the tangent stiffness with respect to the initial stiffness, $S_{j,tan} = S_{j,ini}/h$. Six different values of h (10, 20, 30, 40, 50, 100) are presented.

For simplicity, in the normalized plot, **Fig. 2.35**(b), only three criteria are presented, namely, ε_{lim}, 'secant stiffness' with $h = 3$, and 'tangent stiffness' with $h = 30$.

2.4.5.g Failure of weld (BCW component) in butt welds

Further explanation is needed regarding the weld resistance. As mentioned, welds are not modeled in this study and are assumed to be full penetration butt welds, with no oversize. Hence, overmatching welds are assumed. The critical fusion face is assumed to be located at the interface of the beam in contact with the column. The moment resistance of the joint is limited by the moment resistance of the beam-column contact, calculated using the mechanical properties of the weakest material, either in the beam or the column. This failure mode is referred to as BCW (beam-column weld).

This failure mode would require a sophisticated FE model in the weld zone to be properly captured for the following reasons: First, from the point of view of material modeling, proper consideration of the material properties in the fusion zone and the heat-affected zone would have to be considered, with a much more refined mesh and fracture models such as, e.g., the Johnson-Cook model (Johnson & Cook, 1983). Second, from the point of view of numerical modeling, the following effect must be taken into account: consider a joint in which the column material is weaker than the beam material. In the corresponding FE model, focusing on a solid finite element that belongs to the column, and is located at the interface between the column and the beam, four nodes (A, B, C, D) define the outermost face of the element that is in contact with the beam, and four additional nodes (E, F, G, H) define the innermost face of the same element (not in contact with the beam). The integration point (I) is located at the Gauss point, within the boundaries of the surface defined by these eight nodes. Due to the large dispersion of stress across the thickness of the column flanges, the stresses at the innermost face will be much lower than those on the outermost face. However, the stress and strain values are unique for the element and are calculated at the integration point, which defines the stress-strain behavior of the whole element. Thus, the interface between the beam and the column might present very different values of normal stress, depending on which elements (beam or column) are selected. The models for which this phenomenon happens are easily detected, as those for which the FEM moment resistance is larger than the plastic moment resistance calculated by multiplying the strong-axis plastic section modulus of the beam $W_{pl,b}$ by the weakest of the yield strength of the beam or column $\min\{f_{yc}, f_{yb}\}$. The failure mode for these models is weld failure (BCW) and they are disregarded in the assessment. For this reason, the number of elements considered in the statistics does not always correspond to the total number of analyses performed.

2.4.5.h Fillet welds

Fillet welds are included in clusters FR-S275 (fillet welds between beam and hot-rolled column) and BF-S275 (fillet welds between column flange and column web of welded columns). The model adopted was described in Section 2.2.1.e. Thus, the fillet welds are a geometrical part of the joint core modeled with solid elements, and therefore, it is possible to evaluate their plastic equivalent strain.

This, however, presents some problems that might be illustrated using the simple model presented in **Fig. 2.36**(a). This model represents the connection of a plate in tension or compression (representing a beam flange) with a column, through the column flange, both in S355 steel. The column is formed by three plates, (flanges and web). The dimensions adopted are h_c = 200mm, b_c = b_b = 200mm, t_{fc} = 15mm, t_{wc} = 9mm, t_{fb} = 10mm, L_{fb} = 200mm, L_c = 800mm.

The model presents two connections, namely, the beam flange-to-column flange (connection 1) and the column flange-to-column web (connection 2). Connection 1 can be a full penetration weld with no oversize (P) or a fillet weld (F), which is designed using EN 1993-1-8 (directional

method) for full resistance, leading to a_b = 5.3mm. Connection 2 can be a transition radius r_c = 9mm (R) (rolled column), a butt weld with no oversize (P), or a fillet weld which is designed with a leg of 9mm, that is, a_c = 6.36mm (this weld size is chosen because, according to EN 1993-1-8, it should have the same geometrical effect on the distribution of load to the column web than the radius). For the fillet weld, E70 electrode is assumed, with mechanical properties above the base material S355.

The beam flange can be in compression (C) or tension (T). The following notation is established: the models are labeled with three letters, such as 'CPR'. The first letter refers to the axial load on the flange ('T' for tension, 'C' for compression). The second letter refers to connection 1 ('P' for full penetration butt weld, 'F' for fillet welds). The third letter refers to connection 2 ('R' for rolled, 'P' for full penetration butt weld, 'F' for fillet welds).

The FE model, **Fig. 2.36**(b), takes advantage of symmetry conditions, so only one quarter of the model is represented. The out-of-plane displacement (direction 1) is restrained in the column end and the beam flange end, as is the vertical displacement (direction 2) of the beam flange end. A displacement U_3 is applied, negative (C) or positive (T) according to the sign of the axial force on the beam flange. The material model is quad-linear, both for the plates and (for fillet welds) the welds. Butt welds are not modeled, instead a constraint is included in the model between the coincident nodes of the welded plates. The column web includes out-of-plane imperfections as described in Section 2.2.1.h. The fillet weld is modeled as explained in Section 2.2.1.e. Other features of the model are as described in Section 2.2.

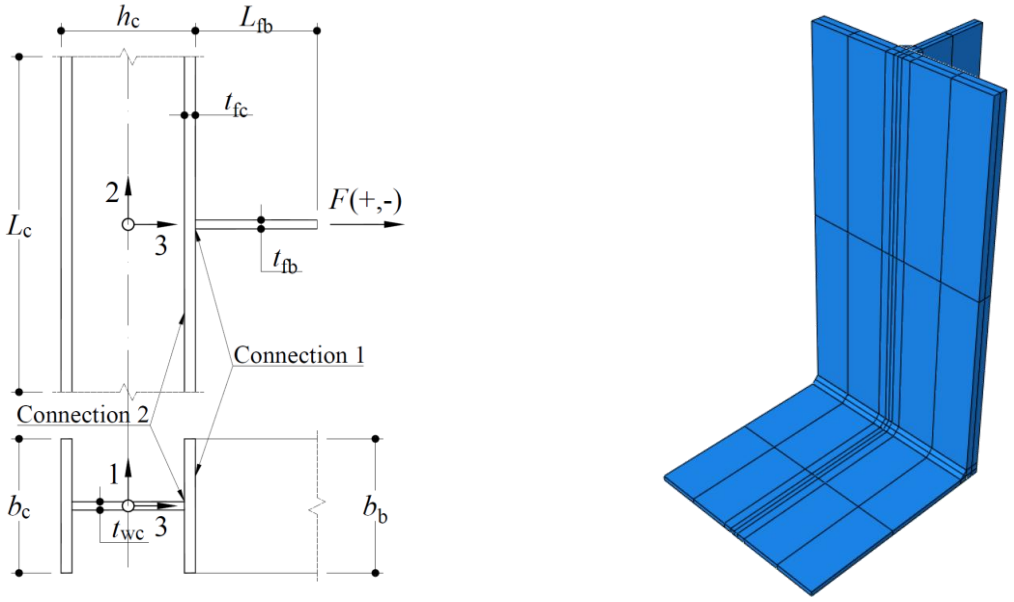

(a) (b)

Fig. 2.36 – Model for evaluation of fillet welds.
(a) problem; (b) MEF model.

The results of this simple analysis are shown in **Fig. 2.37**. Every sub-plot on the figure represents the force-displacement curve (*F-u*) for some specific case: (a) compression with fillet welds between beam flange and column CF*; (b) compression with butt welds between beam flange and column CP*; (c) tension with fillet welds between beam flange and column TF*; (d) tension with

butt welds between beam flange and column TP*. In every sub-plot, six main curves are shown with thick lines; solid curves are results of the FE analysis; dotted curves are results using EN 1993-1-8; the black curves correspond to fillet welds between web and flange (F); the red curves correspond to rolled column (R); the blue curves correspond to full penetration butt weld (P). The scale of force F is shown on the left of every sub-plot. Additional curves with thin lines on the bottom part show the evolution of the maximum plastic equivalent strain in the full model (including the welds) $\varepsilon_{pl,\,eq,max}$ (labeled on the figures as *MaxPEEQ*), with their scale on the right. The 5% limit is shown as a thin black horizontal line.

The values of resistance calculated from EN 1993-1-8 for the weld ($F_{w,Rd}$), for the CWC or CWT component ($F_{Rd,EC3}$), and obtained for the model at the last loading step where $\varepsilon_{pl,eq,max} \leq 5\%$ ($F_{R,FEM,5\%}$) are given on **Table 2.8**.

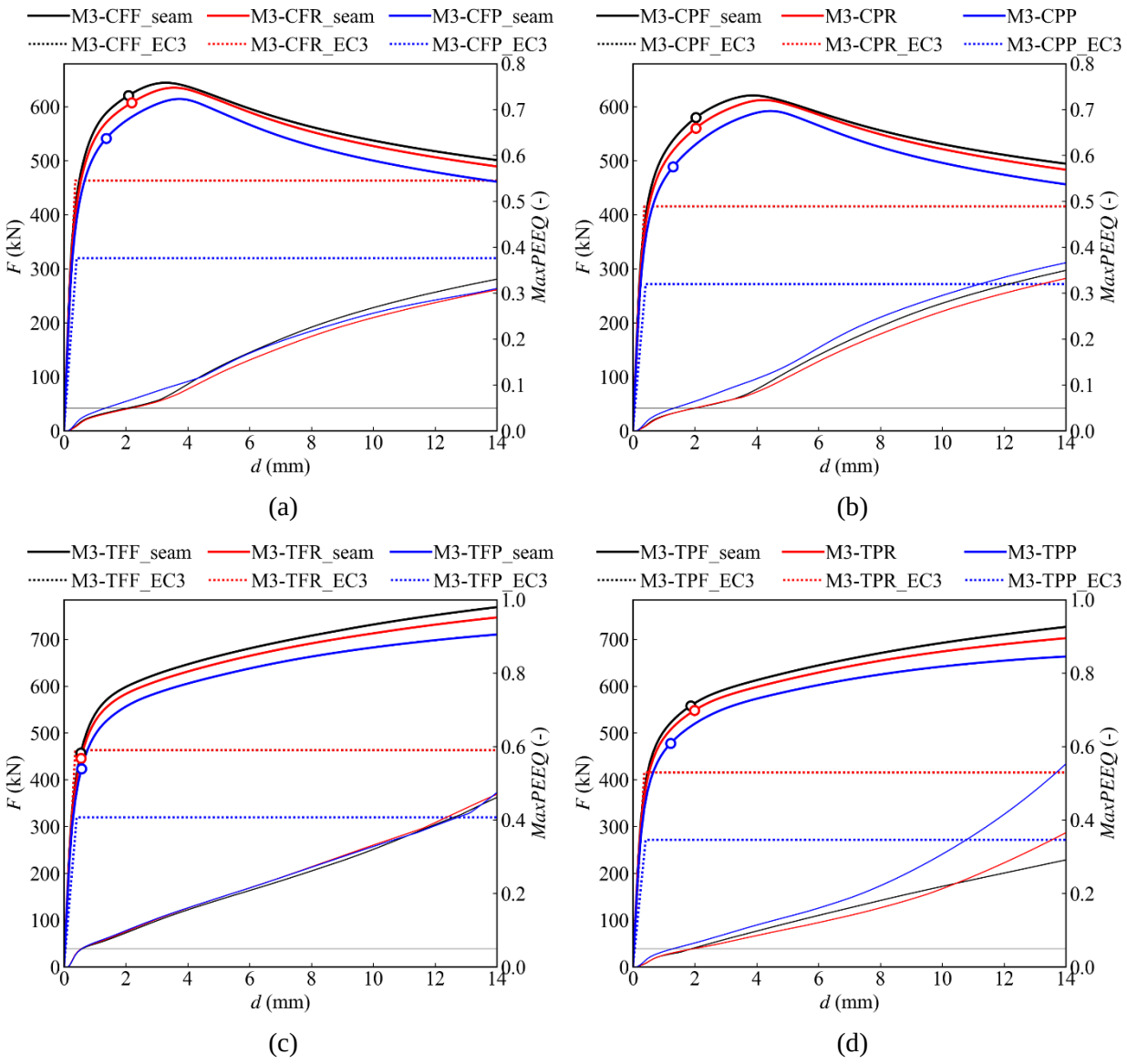

Fig. 2.37 – Results for evaluation of fillet welds.
(a) compression, beam-column fillet weld; (b) compression, beam-column butt weld; (c) tension, beam-column fillet weld; (d) tension, beam-column butt weld.

These results show that:

- In all plots the curves corresponding to models including fillet welds between column web and column flange (black solid curves) are above the others, but very close to the red curve (rolled columns). This is in line with the same effective width of the CWC/CWT in both cases predicted by the Eurocode.
- Likewise, the curves corresponding to models including root radius between column web and column flange (red solid curves) are above the models with butt weld between column web and column flange (blue solid curves). This is in line with a larger effective width of the CWC/CWT predicted on the latter.

- In models with butt weld between column web and column flange (blue solid curves) the 5% point happens at smaller values of displacement with respect to the other two curves, for which the 5% point occurs at very similar points.
- For models in compression, the resistance predicted by the FE model according to the 5% is superior to that predicted by the Eurocode.
- The same trend is observed for models in tension with butt welds.
- However, for models in tension with fillet welds, the resistance by the FE model according to the 5% is generally below the values predicted by the Eurocode, as the 5% points occur for very low levels of load. This is because, for fillet welds, the point of peak plastic equivalent strain occurs in the weld.

This is further explained by **Fig. 2.38**, which shows the plastic equivalent strain at the central cross-section cut of the joint TFF for a displacement of 1mm. The figure shows that high strain concentration occurs by shear in the interface between the weld and the welded plate. This is not in accordance with the Eurocode expression for weld resistance, that in this case predicts a resistance of 626.3 kN. The reason is the simplicity of the model used.

Therefore, the type of model chosen for this study, including the fillet welds on the region for evaluation of the maximum plastic equivalent strain results in incorrectly low values of resistance due to the strain concentration in the weld and adjacent zones. Further testing in the full joint models showed inconsistent values of resistance, for example, lower values of resistance with fillet welds than with butt welds, even with fillet welds designed for high overstrength.

As a conclusion, on the evaluation of resistance, the weld and adjacent plate regions are excluded from the evaluation of the 5% plastic equivalent strain.

Table 2.8. Resistance values for weld study.

			Case										
			CFF	**CFR**	**CFP**	**CPF**	**CPR**	**CPP**	**TFF**	**TFR**	**TFP**	**TPF**	**TPR**	**TPP**
[1]	$F_{w,Rd}$	kN	626.3	626.3	626.3	-	-	-	626.3	626.3	626.3	-	-	-
[2]	$F_{Rd,EC3}$	kN	463.2	463.2	319.5	415.3	415.3	271.6	463.2	463.2	319.5	415.3	415.3	271.6
[3]	$F_{R,FEM,5\%}$	kN	620.7	607.6	541.3	579.9	560.2	488.5	457.3	445.9	423.5	558.0	548.1	478.0
	[2]/[3]		0.75	0.76	0.59	0.72	0.74	0.56	1.01	1.04	0.75	0.74	0.76	0.57

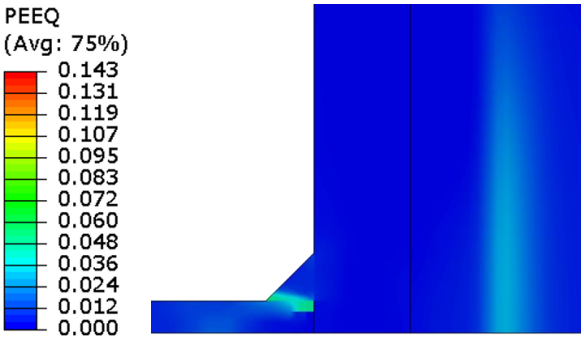

Fig. 2.38 – Plastic equivalent strain for simple weld model TFF.

3 Summary of Results

3.1 GENERALITIES

3.1.1 Assessment metrics

This Chapter presents results across selections of clusters, sets, or cases included in the study, using as metrics the following ratios:

$$r_{EN} = M_{R,EN} / M_{R,FEM,5\%}, \quad (3.1)$$

$$r_{prEN} = M_{R,prEN} / M_{R,FEM,5\%}, \quad (3.2)$$

$$r_{IS,MNA,def} = M_{R,IS,MNA,def} / M_{R,FEM,5\%}, \quad (3.3)$$

$$r_{IS,MNA,ref} = M_{R,IS,MNAref} / M_{R,FEM,5\%}, \quad (3.4)$$

$$r_{IS,MNA,rich} = M_{R,IS,MNA,rich} / M_{R,FEM,5\%}, \quad (3.5)$$

$$r_{IS,GMNA,def} = M_{R,IS,GMNA,def} / M_{R,FEM,5\%}, \quad (3.6)$$

$$r_{IS,GMNA,ref} = M_{R,IS,GMNA,ref} / M_{R,FEM,5\%}, \quad (3.7)$$

$$r_{IS,GMNA,rich} = M_{R,IS,GMNA,rich} / M_{R,FEM,5\%}, \quad (3.8)$$

$$r_{FEM,QUAD,5\%} = M_{R,FEM,QUAD,5\%} / M_{R,FEM,5\%}, \quad (3.9)$$

$$s_{EN} = S_{j,ini,EN} / S_{j,ini,FEM}, \quad (3.10)$$

$$s_{prEN} = S_{j,ini,prEN} / S_{j,ini,FEM}, \quad (3.11)$$

$$s_{j,sec,FEM,QUAD} = S_{j,sec,FEM,QUAD} / S_{j,sec,FEM}, \quad (3.12)$$

where

- $M_{R,FEM,5\%}$: is the moment resistance obtained from the FE analysis (Abaqus), with default options (EPPL material model, imperfection magnitude $d_c/200$), at the last step where the maximum equivalent plastic strain in the joint core is below or equal to 5%,
- $M_{R,EN}$ indicates the moment resistance estimated with EN 1993-1-8:2005 (EC3), assuming nominal properties and including no partial factors,
- $M_{R,prEN}$ is the moment resistance estimated with FprEN 1993-1-8:2023 (FprEC3), assuming nominal properties and including no partial factors,
- $M_{R,IS,MNA,def}$ is the moment resistance obtained from IDEA StatiCa (v23) with Materially Non-Linear Analysis (MNA) (that is, with no second-order effects) using the default mesh, assuming nominal properties and including no partial factors,
- $M_{R,IS,MNA,ref}$ is the moment resistance obtained from IDEA StatiCa (v23) with Materially Non-Linear Analysis (MNA) (that is, with no second-order effects) using a refined mesh, assuming nominal properties and including no partial factors,

- $M_{R,IS,MNA,rich}$ is the moment resistance obtained from $M_{R,IS,MNA,def,}$ and $M_{R,IS,MNA,ref}$ using the Richardson extrapolation, Eq. (2.14).
- $M_{R,IS,GMNA,def}$ is the moment resistance obtained from IDEA StatiCa (v23) with Geometrically and Materially Non-Linear Analysis (GMNA) (that is, with second-order effects) using the default mesh, assuming nominal properties and including no partial factors,
- $M_{R,IS,GMNA,ref}$ is the moment resistance obtained from IDEA StatiCa (v23) with Geometrically and Materially Non-Linear Analysis (GMNA) (that is, with second-order effects) using a refined mesh, assuming nominal properties and including no partial factors,
- $M_{R,IS,GMNA,rich}$ is the moment resistance obtained from $M_{R,IS,GMNA,def,}$ and $M_{R,IS,GMNA,ref}$ using the Richardson extrapolation, Eq. (2.14),
- $M_{R,FEM,QUAD,5\%}$: is the moment resistance obtained from the FE analysis (Abaqus), with QUAD material properties, at the last step where the maximum equivalent plastic strain in the joint core is below or equal to 5%,
- $S_{j,ini,FEM}$: is the initial stiffness obtained from the FE analysis (Abaqus) at the first loading step,
- $S_{j,ini,EN}$ is the initial stiffness estimated with EN 1993-1-8:2005 (EC3), assuming nominal properties,
- $S_{j,ini,prEN}$ is the initial stiffness estimated with FprEN 1993-1-8:2023 (FprEC3), assuming nominal properties,
- $S_{j,sec,FEM,5\%}$: is the secant stiffness obtained from the FE analysis (Abaqus), with default options (EPPL material model, magnitude of imperfection $d_c/200$), at the last step where the maximum equivalent plastic strain in the joint core is below or equal to 5%,
- $S_{j,sec,FEM,QUAD,5\%}$: is the secant stiffness obtained from the FE analysis (Abaqus), with QUAD material model, at the last step where the maximum equivalent plastic strain in the joint core is below or equal to 5%,

It is worth mentioning that IDEA StatiCa does not consider geometrical imperfections, therefore in the GMNA analysis with this software, the initial geometry is the undeformed shape.

3.1.2 Statistics

The ratios defined in the previous sub-section are calculated individually for each case within each set within each cluster. Then, statistics of the ratios across a sub-selection of cases can be performed, to capture trends. Relevant statistics of the ratios are:

- Mean,
- Coefficient of variation CoV,
- Extreme values maximum (max) and minimum (min),
- Number (>1) of unconservative cases.
- Percentage (>1)/*n* of unconservative cases relative to the number of cases considered (*n*).

3.1.3 Terminology and color code

Hereinafter, for discussion of results, the term '*conservative*' applied to a certain ratio *r* (or to its mean across selected cases), is used to indicate that the corresponding ratio is smaller than or equal to 1 (i.e., the method conveys a value of moment resistance smaller than, or equal to, the value obtained from the benchmark model). Conversely, the term '*unconservative*' is used to indicate

that the corresponding ratio is larger than 1 (i.e., the method conveys a value of moment resistance larger than the value obtained from the benchmark model). These terms should not be interpreted outside of this context.

In addition, **Table 3.1** shows other terms used for some thresholds applied to the statistics:

Table 3.1. Thresholds for statistics.

Statistic	Low deviation	Moderate deviation	High deviation
Mean	0.95 ≤ Mean ≤ 1.05	0.90 ≤ Mean < 0.95 1.05 < Mean ≤ 1.10	Mean < 0.90 Mean > 1.10
CoV	CoV < 7.5%	7.5% ≤ CoV < 15%	15% ≤ CoV

To improve clarity on tables, color codes have been used, as described:
For the ratios or the mean of ratios, the following color code is used:

- Exact ratios (r = 1) are presented in white cells, such as 1.00.
- Conservative ratios (r < 1) are presented in cells shaded in green, such as 0.95. The darker the shade, the lower the value, on the range from 1.00 - 0.90.
- Unconservative ratios (r > 1) are presented in cells shaded in red, such as 1.06. The darker the shade, the higher the value, on the range from 1 .00 - 1.10.
- For highly conservative ratios (r < 0.90), the cell font is marked with bold and green color, such as **0.86**.
- For highly unconservative ratios (r > 1.10), the cell font is marked with bold, italics and red color, such as ***1.54***.

This color code is summarized in **Table 3.2**.

Table 3.2. Color code for classification of ratios.

0.80	0.90	0.91	0.92	0.93	0.94	0.95	0.96	0.97	0.98	0.99	1.00	1.01	1.02	1.03	1.04	1.05	1.06	1.07	1.08	1.09	1.10	*1.20*

For the CoV, the following color code is used:

- Results below 7.5% (low deviation) are presented in cells shaded in green, such as 5.6%.
- Results between 7.5% and 15% (moderate deviation) are presented in cells shaded in orange, such as 9.5%.
- Results above 15% (high deviation) are presented in cells shaded in red, and marked with bold and italics, such as ***19.5%***.

For the max and min, values above 1 are shaded in red, such as 1.09.

3.1.4 Exclusions

3.1.4.a Butt welds

For those clusters in which beam-column butt welds are assumed, the cases with BCW (Beam-Column Weld) failure mode are excluded from resistance assessments (moment resistance and secant stiffness), because, as explained in Section 2.4.5.g, the Abaqus model cannot capture this

failure mode properly. The corresponding clusters are BR and BB. For these clusters, the total number of cases included in statistics does not match the total number of cases analyzed. For initial stiffness assessments, all cases are included.

This problem is not relevant for welded columns, because on the column-web-to-column-flange weld, it has been assumed that the steel grade is the same for web and flange.

3.2 RESULTS FOR ROLLED COLUMNS (CLUSTERS BR AND FR)

3.2.1 Influence of material model

Table 3.3 compares the results obtained for cluster BR-S275 (rolled columns, S275) using two different material models, namely QUAD and EPPL (see Section 2.4.1.e) on the moment resistance M_R, secant stiffness $S_{j,sec}$, and rotation $\phi_{j,R}$ (at M_R).

Overall, implementation of the QUAD material model compared to the EPPL model results in an average increase of 4% in resistance, and a maximum of 15%. However, the rotation at the resistance point is largely affected, with an average of 1.44 and a maximum of 2.82. The CoV of results for resistance is low (2.9%), but for rotation is high (23.1%).

It is concluded that the impact of strain hardening on the resistance is relatively small (around 1.04 on average), but it has a large effect on the joint rotation at the resistance point (around 1.44 on average and up to a maximum of 2.82).

For subsequent analysis, the EPPL material model is the default option, as it gives a lower bound of resistance that can be directly correlated to the Eurocode resistance and IDEA StatiCa (both based on yield strength).

3.2.2 Influence of imperfections

For one-sided joints with rolled columns in S275 (cluster BR-S275), the influence of the initial imperfection amplitude is assessed by examining the ratio $M_{R,420}$ / $M_{R,200}$, where $M_{R,420}$ is the moment resistance M_R obtained with an amplitude of d_c/420 and $M_{R,200}$ is the one obtained with an amplitude of d_c/200. The average of the ratio across all cases for every one of the eight sets studied is always 1.00, the CoV varies between 0.3% and 0.7%, the maximum is 1.03, and the minimum is 1.00, showing that the initial imperfection amplitude plays no significant role in the moment resistance of the joints examined.

Considering these results, the global assessment for the joints is carried out on the following sub-sections only for the models with no strain hardening and an imperfection amplitude of d_c/200.

Table 3.3. Rolled columns, S275 (cluster BR). Influence of material model QUAD vs EPPL.

Sets	Features					$M_{R,FEM,QUADL,5\%} / M_{R,FEM,EPPL,5\%}$					$S_{j,sec,FEM,QUAD,5\%} / S_{j,sec,FEM,EPPL,5\%}$				$\phi_{j,R,FEM,QUAD,5\%} / \phi_{j,R,FEM,EPPL,5\%}$			
	1S/2S	I/R	U/T	*n*	*mr*	*n*	Mean	CoV	Max	Min	Mean	CoV	Max	Min	Mean	CoV	Max	Min
set_01	1S	I	U	0	0	16	1.05	2.0%	1.10	1.01	0.73	*16.6%*	0.96	0.54	*1.47*	*19.1%*	2.04	1.04
set_02_N30	1S	I	U	0.3	0	16	1.03	1.5%	1.08	1.01	0.79	12.5%	0.93	0.58	*1.33*	15.0%	1.87	1.10
set_02_N50	1S	I	U	0.5	0	16	1.02	1.1%	1.04	1.01	0.83	10.0%	0.98	0.69	*1.24*	10.9%	1.49	1.02
set_02_N70	1S	I	U	0.7	0	16	1.01	1.0%	1.02	0.99	0.94	14.3%	1.34	0.73	1.10	13.4%	1.39	0.74
set_03	1S	I	T	0	0	14	1.08	3.7%	1.15	1.01	0.74	*20.0%*	1.10	0.53	*1.53*	*20.0%*	1.98	0.92
set_04_N30	1S	I	T	0.3	0	14	1.07	3.0%	1.12	1.00	0.65	*22.4%*	0.94	0.44	*1.73*	*25.4%*	2.54	1.06
set_04_N50	1S	I	T	0.5	0	14	1.03	2.6%	1.08	1.00	0.70	*23.6%*	1.03	0.47	*1.56*	*23.8%*	2.19	0.97
set_04_N70	1S	I	T	0.7	0	14	1.01	1.4%	1.03	1.00	0.89	*23.5%*	1.07	0.42	*1.23*	*37.5%*	2.48	0.93
set_05_MR050	2S	I	U	0	0.5	14	1.05	2.5%	1.09	1.01	0.79	*16.9%*	0.97	0.55	*1.36*	*20.7%*	1.95	1.05
set_05_MR-050	2S	I	U	0	-0.5	20	1.04	1.7%	1.07	1.01	0.82	7.8%	0.91	0.67	*1.27*	9.0%	1.55	1.12
set_05_MR-100	2S	I	U	0	-1	20	1.07	2.8%	1.11	1.02	0.78	15.0%	0.96	0.57	*1.40*	*18.3%*	1.94	1.08
set_06_N30_MR050	2S	I	U	0.3	0.5	14	1.03	1.6%	1.07	1.00	0.83	12.0%	0.96	0.64	*1.26*	14.3%	1.63	1.05
set_06_N30_MR-050	2S	I	U	0.3	-0.5	20	1.02	1.4%	1.05	1.00	0.80	10.5%	0.98	0.64	*1.30*	11.5%	1.62	1.04
set_06_N30_MR-100	2S	I	U	0.3	-1	20	1.05	2.4%	1.09	1.00	0.69	*15.0%*	0.87	0.45	*1.55*	*18.6%*	2.41	1.18
set_06_MR050	2S	I	U	0.5	0.5	14	1.03	1.4%	1.05	1.00	0.84	10.9%	0.96	0.64	*1.24*	13.1%	1.62	1.05
set_06_MR-050	2S	I	U	0.5	-0.5	20	1.01	1.0%	1.03	1.00	0.82	12.7%	0.97	0.59	*1.25*	14.5%	1.69	1.03
set_06_MR-100	2S	I	U	0.5	-1	20	1.03	2.5%	1.09	1.00	0.69	*23.9%*	1.05	0.47	*1.58*	*24.0%*	2.31	0.95
set_06_N70_MR050	2S	I	U	0.7	0.5	14	1.02	1.3%	1.04	1.00	0.85	12.8%	1.03	0.67	*1.22*	14.0%	1.53	0.97
set_06_N70_MR-050	2S	I	U	0.7	-0.5	20	1.00	0.9%	1.03	0.99	0.89	*18.4%*	1.27	0.50	*1.17*	*23.4%*	2.04	0.78
set_06_N70_MR-100	2S	I	U	0.7	-1	20	1.01	2.3%	1.08	1.00	0.78	*30.9%*	1.02	0.37	*1.47*	*42.0%*	2.80	0.98
set_07_MR050	2S	I	T	0	0.5	2	1.04	2.0%	1.05	1.02	0.82	2.2%	0.83	0.81	*1.26*	0.2%	1.27	1.26
set_07_MR-050	2S	I	T	0	-0.5	19	1.07	2.3%	1.11	1.03	0.79	11.3%	0.91	0.57	*1.36*	14.8%	1.95	1.14
set_07_MR-100	2S	I	T	0	-1	20	1.08	2.4%	1.13	1.04	0.76	13.4%	0.95	0.61	*1.44*	*15.8%*	1.85	1.10
set_08_N30_MR050	2S	I	T	0.3	0.5	2	1.03	1.3%	1.04	1.02	0.82	14.1%	0.90	0.74	*1.27*	12.8%	1.38	1.15
set_08_N30_MR-050	2S	I	T	0.3	-0.5	19	1.05	2.3%	1.09	1.02	0.74	*16.6%*	0.93	0.53	*1.47*	*18.8%*	2.06	1.10
set_08_N30_MR-100	2S	I	T	0.3	-1	20	1.06	2.1%	1.09	1.02	0.71	14.5%	0.93	0.54	*1.51*	14.3%	1.89	1.10
set_08_MR050	2S	I	T	0.5	0.5	2	1.02	1.5%	1.03	1.01	0.75	*16.4%*	0.84	0.66	*1.38*	*17.9%*	1.56	1.21
set_08_MR-050	2S	I	T	0.5	-0.5	19	1.04	2.0%	1.07	1.00	0.71	*17.8%*	0.95	0.45	*1.51*	*19.6%*	2.25	1.05
set_08_MR-100	2S	I	T	0.5	-1	20	1.05	2.3%	1.09	1.00	0.69	*19.5%*	0.98	0.42	*1.57*	*20.9%*	2.43	1.02
set_08_N70_MR050	2S	I	T	0.7	0.5	2	1.03	0.8%	1.04	1.03	0.69	7.5%	0.73	0.66	*1.50*	8.3%	1.58	1.41
set_08_N70_MR-050	2S	I	T	0.7	-0.5	19	1.02	1.8%	1.05	1.00	0.71	*30.8%*	1.06	0.39	*1.59*	*33.7%*	2.59	0.94
set_08_N70_MR-100	2S	I	T	0.7	-1	20	1.03	2.0%	1.07	1.00	0.65	*31.9%*	1.05	0.36	*1.75*	*32.7%*	2.82	0.95
set_09	1S	R	U	0	0	20	1.07	2.9%	1.13	1.00	0.67	*15.9%*	0.99	0.58	*1.63*	13.9%	1.85	1.01
set_11	1S	R	T	0	0	15	1.05	2.8%	1.09	1.00	0.77	14.5%	1.03	0.66	*1.38*	13.8%	1.63	0.97
set_13_MR050	2S	R	U	0	0.5	18	1.08	2.2%	1.12	1.02	0.64	7.0%	0.75	0.59	*1.71*	7.2%	1.84	1.36
set_13_MR-050	2S	R	U	0	-0.5	20	1.06	2.0%	1.11	1.03	0.63	7.3%	0.73	0.57	*1.70*	7.0%	1.85	1.46
set_13_MR-100	2S	R	U	0	-1	20	1.05	1.5%	1.08	1.02	0.62	5.6%	0.70	0.56	*1.68*	6.0%	1.87	1.49
set_15_MR050	2S	R	T	0	0.5	3	1.01	0.6%	1.02	1.01	0.87	4.6%	0.90	0.83	*1.16*	5.3%	1.23	1.11
set_15_MR-050	2S	R	T	0	-0.5	19	1.06	2.7%	1.10	1.02	0.84	6.3%	0.92	0.74	*1.27*	8.0%	1.49	1.12
set_15_MR-100	2S	R	T	0	-1	20	1.06	2.5%	1.10	1.02	0.83	7.4%	0.93	0.67	*1.29*	8.9%	1.59	1.10
All						635	1.04	2.9%	1.15	0.99	0.76	*19.4%*	1.34	0.36	*1.44*	*23.1%*	2.82	0.74

3.2.3 Influence of steel grade

Table 3.4 shows the statistics of ratios (including all methods on the study) for rolled columns with EPPL material properties (cluster BR), and three different steel grades, namely S235, S275, S355. The variability across steel grades is very small, showing that the influence of this parameter is negligible. For further analysis, steel grade S275 is selected, as it represents an intermediate case between the three steel grades included in the study.

Table 3.4. Rolled columns, EPPL (cluster BR). Influence of steel grade.

Method	Grade	CWC				CWT				CWS				ALL (EXCEPT BCW)			
		n	Mean	CoV	(>1)/*n*	*n*	Mean	CoV	(>1)/*n*	*n*	Mean	CoV	(>1)/*n*	*tot*	Mean	CoV	(>1)/tot
r_{EN}	S235	156	0.90	*16.8%*	24%	78	0.70	*16.8%*	4%	401	1.00	*15.5%*	47%	635	0.94	*19.0%*	36%
	S275	156	0.89	*18.3%*	23%	78	0.71	*17.1%*	4%	401	1.00	*15.7%*	48%	635	0.94	*19.5%*	36%
	S355	152	0.86	*21.0%*	23%	78	0.74	*17.5%*	4%	392	1.01	*16.2%*	51%	626	0.94	*20.4%*	38%
r_{FprEN}	S235	156	0.88	*16.8%*	18%	78	0.66	*18.1%*	4%	401	0.97	11.6%	35%	635	0.91	*17.6%*	27%
	S275	156	0.87	*18.2%*	18%	78	0.67	*18.4%*	4%	401	0.98	11.9%	36%	635	0.91	*18.0%*	28%
	S355	152	0.85	*20.5%*	18%	78	0.69	*18.8%*	4%	392	0.98	12.5%	39%	626	0.91	*18.8%*	30%
$r_{IS,MNA,def}$	S235	156	1.06	3.9%	96%	78	0.96	6.7%	31%	401	1.08	7.5%	87%	635	1.06	7.6%	82%
	S275	156	1.06	4.3%	95%	78	0.96	6.7%	31%	401	1.07	7.7%	86%	635	1.06	7.8%	82%
	S355	152	1.06	5.4%	93%	78	0.96	6.7%	31%	392	1.06	8.0%	82%	626	1.05	7.9%	78%
$r_{IS,MNA,ref}$	S235	156	1.00	4.3%	47%	78	0.90	5.4%	0%	401	1.04	7.1%	79%	635	1.01	7.8%	61%
	S275	156	1.00	4.9%	44%	78	0.89	5.4%	0%	401	1.04	7.4%	77%	635	1.01	8.2%	59%
	S355	152	0.99	6.3%	37%	78	0.88	5.4%	0%	392	1.02	7.8%	64%	626	0.99	8.5%	49%
$r_{IS,MNA,rich}$	S235	156	0.98	4.6%	28%	78	0.88	5.2%	0%	401	1.03	7.0%	73%	635	1.00	8.0%	53%
	S275	156	0.97	5.2%	27%	78	0.87	5.3%	0%	401	1.02	7.3%	71%	635	0.99	8.4%	51%
	S355	152	0.96	6.8%	22%	78	0.86	5.4%	0%	392	1.01	7.7%	59%	626	0.98	8.9%	42%
$r_{IS,GMNA,def}$	S235	156	1.02	3.5%	76%	78	0.96	6.6%	31%	401	1.01	4.9%	67%	635	1.01	5.2%	65%
	S275	156	1.02	3.7%	70%	78	0.96	6.6%	28%	401	1.00	4.9%	62%	635	1.00	5.2%	60%
	S355	152	1.02	4.6%	63%	78	0.96	6.6%	31%	392	0.98	5.0%	32%	626	0.99	5.4%	39%
$r_{IS,GMNA,ref}$	S235	156	0.98	3.7%	19%	78	0.89	5.3%	0%	401	0.98	4.8%	31%	635	0.97	5.4%	24%
	S275	156	0.97	4.1%	17%	78	0.89	5.3%	0%	401	0.97	5.1%	26%	635	0.96	5.6%	20%
	S355	152	0.96	5.4%	13%	78	0.88	5.3%	0%	392	0.95	5.8%	8%	626	0.94	6.1%	8%
$r_{IS,GMNA,rich}$	S235	156	0.96	4.0%	13%	78	0.87	5.2%	0%	401	0.97	4.8%	22%	635	0.96	5.7%	17%
	S275	156	0.95	4.5%	10%	78	0.87	5.3%	0%	401	0.96	5.3%	16%	635	0.95	6.0%	13%
	S355	152	0.94	6.0%	5%	78	0.86	5.3%	0%	392	0.94	6.3%	5%	626	0.93	6.8%	4%

3.2.4 Influence of joint configuration

This section discusses the influence of joint configuration on resistance, focusing on cluster BR in S275 steel grade and EPPL material model. The failure modes for all cases included in the cluster are shown in **Table 3.5**. As mentioned, BCW failure cases are excluded from the statistics. The following trends are visible:

- CWS and BCW are the only failure modes for stiffened cases.
- CWT only happens on the roof joints.
- CWC is dominant on one-sided unstiffened joints. CWS and BCW only happen in cases 10 to 15 that correspond to stocky columns.
- CWC and BCW are the only failure modes on two-sided unstiffened joints with $m_r = 0.5$.
- Two-sided unstiffened joints with negative m_r present a mixture of CWC, CWS, and BCW, but CWS is predominant.

3.2.4.a Unstiffened columns with no axial load

The results for unstiffened columns with no axial load are summarized in **Table 3.6**. These results indicate that:
For EN end FprEN:

- The current and forthcoming versions of Eurocode 3 are highly conservative, with mean ratios systematically below 0.85.
- The scatter of both code versions is high (about 17% when all cases are included).

- A small proportion of individual results are unconservative.
- The differences in both versions of the code are negligible, except for 2S joints with CWS failure, where the new version improves the scatter.

For IDEA StatiCa:

- With the default program options (default mesh and MNA), the ratios are moderately unconservative (> 1), and a large proportion of cases present ratios above 1.
- When the mesh is refined, the mean ratios are moderately conservative (< 1) and the number of individual unconservative cases reduces dramatically.
- Use of GMNA for this group of joints does not improve the results.
- The CoV of results is moderate (in all cases CoV is below 7.5%).

3.2.4.b Stiffened columns with no axial load

The results for stiffened columns with no axial load are summarized in **Table 3.7**. All stiffened columns fail by CWS, and for this reason the table does not contain CWC or CWT cases. These results indicate that:

For EN end FprEN:

- The mean of ratios for EN is moderately conservative for one-sided joints and highly conservative for two-sided joints.
- The mean of ratios for FprEN is highly conservative for all joints. Thus, the new FprEN is more conservative than the previous EN.
- With EN, a small proportion of individual cases is unconservative, about 20%, except for 1S-I, for which the percentage of individual unconservative cases is about 57%.
- FprEN reduces the proportion of individual unconservative cases. For 1S-I and 2S-I joints, no individual cases are unconservative.
- The scatter is low to moderate. FprEN improves slightly the scatter with respect to EN. For 1S-I and 2S-I joints, the CoV with FprEN falls below 3%.

For IDEA StatiCa:

- With the default program options (default mesh and MNA), the mean ratios are moderately unconservative (> 1) for internal (I) joints, moderately conservative (< 1) for roof (R) joints. For internal joints, a large proportion of cases presents ratios above 1. For roof joints, the proportion of cases with ratios above 1 is very small.
- Refining the mesh improves the mean results, but a large proportion of individual cases for internal (I) joints is still unconservative.
- GMNA analysis does not improve significantly the results.
- The scatter of results is low.

3.2.5 Influence of axial load

Results including the influence of axial load are shown in **Table 3.8** (for methods EN and FprEN), **Table 3.9** (for methods IS,MNA,def, IS,MNA,ref and IS,MNA,rich), and **Table 3.10** (for methods IS,GMNA,def, IS,GMNA,ref and IS,GMNA,rich). All the joints with axial load are internal (I), and none of them fail by CWT, so this column is suppressed in the tables. The results lead to the following conclusions

For EN end FprEN:

- For EN and FprEN, the increase of axial load results in an increase of the mean ratio.
- Using EN, for all the joint configurations, unconservative mean ratios (> 1) are obtained for large values of axial load n = 0.7. For stiffened joints, the mean ratios are highly unconservative. For 1S stiffened joints, ratios larger than 1 are obtained even for low values of axial load, n = 0.3. For 2S stiffened joints, ratios larger than 1 are already obtained for n = 0.5.
- Using FprEN, for all the joint configurations, average ratios larger than 1 are obtained for large values of axial load n = 0.7 except for 1S-I-U in cases failing by CWC or CWS. For stiffened joints, ratios larger than 1 are obtained for values of axial load, n = 0.5.
- For both methods, increasing axial load results in an increasing percentage of individual unconservative cases, regardless of failure mode.
- For EN, the CoV is generally moderate. For one-sided unstiffened failing by CWC, it is high. For two-sided unstiffened joints, failing by CWC or CWS, the CoV is high.
- For FprEN, the CoV is high for 2S-U-I joints with CWC failure mode. The CoV is low for all cases with CWS failure mode, except for n = 0.7, where the scatter is moderate but with a large proportion of unconservative results.
- The increase of axial load does not affect significantly the scatter of results. For the same joint configuration, the CoV remains approximately constant across the different values of n.

For IDEA StatiCa:

- The default options (MNA, default mesh) in all configurations and failure modes generally result in moderately to highly unconservative mean ratios, with 100% of unconservative individual results, regardless of the level of axial load. Increasing values of axial load result in increased unconservativeness.
- Reducing the mesh with MNA improves the ratios and the percentage of unconservative individual cases, but only for CWC failure mode.
- GMNA with a default mesh, results in moderately unconservative ratios (> 1), which are stable across the different values of axial force, but with a large proportion of unconservative values.
- GMNA with a refined mesh results in moderately conservative mean of ratios for all cases, with a large to moderate proportion of unconservative individual cases, for any failure mode.
- The CoV of the different options is low and quite stable regardless of mesh size, analysis option, and level of axial load.
- It is thus concluded that, for models with axial load, GMNA with a refined mesh should be used but, still so, a proportion of individual cases will be moderately unconservative.

Table 3.5. Rolled columns, S275 (cluster BR-S275), EPPL material model. Failure modes.

S275						Case																		
	1S/2S	I/R	U/T	*n*	*mr*	1	2	3	4	5	6	7	8	9	10	11	12	13	14	15	16	17	18	19	20
set_01	1S	I	U	0	0	CWC	CWC	CWC	CWC	CWC	CWC	CWC	CWC	CWC	BCW	CWS	BCW	BCW	CWS	BCW	CWC	CWC	CWC	CWC	CWC
set_02_N30	1S	I	U	0.3	0	CWC	CWC	CWC	CWC	CWC	CWC	CWC	CWC	CWC	BCW	CWS	BCW	BCW	CWS	BCW	CWC	CWC	CWC	CWC	CWC
set_02_N50	1S	I	U	0.5	0	CWC	CWC	CWC	CWC	CWC	CWC	CWC	CWC	CWC	BCW	CWS	BCW	BCW	CWS	BCW	CWC	CWC	CWC	CWC	CWC
set_02_N70	1S	I	U	0.7	0	CWC	CWC	CWC	CWC	CWC	CWC	CWC	CWC	CWC	BCW	CWS	BCW	BCW	CWS	BCW	CWC	CWC	CWC	CWC	CWC
set_03	1S	I	T	0	0	CWS	CWS	CWS	CWS	CWS	CWS	CWS	BCW	CWS	BCW	CWS	BCW	BCW	CWS	BCW	BCW	CWS	CWS	CWS	CWS
set_04_N30	1S	I	T	0.3	0	CWS	CWS	CWS	CWS	CWS	CWS	CWS	BCW	CWS	BCW	CWS	BCW	BCW	CWS	BCW	BCW	CWS	CWS	CWS	CWS
set_04_N50	1S	I	T	0.5	0	CWS	CWS	CWS	CWS	CWS	CWS	CWS	BCW	CWS	BCW	CWS	BCW	BCW	CWS	BCW	BCW	CWS	CWS	CWS	CWS
set_04_N70	1S	I	T	0.7	0	CWS	CWS	CWS	CWS	CWS	CWS	CWS	BCW	CWS	BCW	CWS	BCW	BCW	CWS	BCW	BCW	CWS	CWS	CWS	CWS
set_05_MR050	2S	I	U	0	0.5	CWC	CWC	CWC	CWC	CWC	CWC	CWC	BCW	CWC	BCW	BCW	BCW	BCW	CWC	BCW	CWC	CWC	CWC	CWC	CWC
set_05_MR-050	2S	I	U	0	-0.5	CWC	CWC	CWC	CWS	CWS	CWC	CWS	CWS	CWS	CWS	CWS	CWS	CWS	CWS	CWS	CWS	CWS	CWS	CWC	CWC
set_05_MR-100	2S	I	U	0	-1	CWC	CWC	CWC	CWS	CWS	CWS	CWS	CWS	CWS	CWS	CWS	CWS	CWS	CWS	CWS	CWS	CWS	CWS	CWC	CWC
set_06_N30_MR050	2S	I	U	0.3	0.5	CWC	CWC	CWC	CWC	CWC	CWC	CWC	BCW	CWC	BCW	BCW	BCW	BCW	CWC	BCW	CWC	CWC	CWC	CWC	CWC
set_06_N30_MR-050	2S	I	U	0.3	-0.5	CWC	CWC	CWC	CWS	CWS	CWC	CWS	CWS	CWS	CWS	CWS	CWS	CWS	CWS	CWS	CWS	CWS	CWS	CWC	CWC
set_06_N30_MR-100	2S	I	U	0.3	-1	CWC	CWC	CWC	CWS	CWS	CWS	CWS	CWS	CWS	CWS	CWS	CWS	CWS	CWS	CWS	CWS	CWS	CWS	CWC	CWC
set_06_MR050	2S	I	U	0.5	0.5	CWC	CWC	CWC	CWC	CWC	CWC	CWC	BCW	CWC	BCW	BCW	BCW	BCW	CWC	BCW	CWC	CWC	CWC	CWC	CWC
set_06_MR-050	2S	I	U	0.5	-0.5	CWC	CWC	CWC	CWS	CWS	CWC	CWS	CWS	CWS	CWS	CWS	CWS	CWS	CWS	CWS	CWS	CWS	CWS	CWC	CWC
set_06_MR-100	2S	I	U	0.5	-1	CWC	CWC	CWC	CWS	CWS	CWS	CWS	CWS	CWS	CWS	CWS	CWS	CWS	CWS	CWS	CWS	CWS	CWS	CWC	CWC
set_06_N70_MR050	2S	I	U	0.7	0.5	CWC	CWC	CWC	CWC	CWC	CWC	CWC	BCW	CWC	BCW	BCW	BCW	BCW	CWC	BCW	CWC	CWC	CWC	CWC	CWC
set_06_N70_MR-050	2S	I	U	0.7	-0.5	CWC	CWC	CWC	CWS	CWS	CWC	CWS	CWS	CWS	CWS	CWS	CWS	CWS	CWS	CWS	CWS	CWS	CWS	CWC	CWC
set_06_N70_MR-100	2S	I	U	0.7	-1	CWC	CWC	CWC	CWS	CWS	CWS	CWS	CWS	CWS	CWS	CWS	CWS	CWS	CWS	CWS	CWS	CWS	CWS	CWC	CWC
set_07_MR050	2S	I	T	0	0.5	BCW	BCW	CWS	BCW	BCW	CWS	BCW	BCW	BCW	BCW	BCW	BCW	BCW	BCW	BCW	BCW	BCW	BCW	BCW	BCW
set_07_MR-050	2S	I	T	0	-0.5	CWS	CWS	CWS	CWS	CWS	CWS	CWS	CWS	CWS	BCW	CWS	CWS	CWS	CWS	CWS	CWS	CWS	CWS	CWS	CWS
set_07_MR-100	2S	I	T	0	-1	CWS	CWS	CWS	CWS	CWS	CWS	CWS	CWS	CWS	CWS	CWS	CWS	CWS	CWS	CWS	CWS	CWS	CWS	CWS	CWS
set_08_N30_MR050	2S	I	T	0.3	0.5	BCW	BCW	CWS	BCW	BCW	CWS	BCW	BCW	BCW	BCW	BCW	BCW	BCW	BCW	BCW	BCW	BCW	BCW	BCW	BCW
set_08_N30_MR-050	2S	I	T	0.3	-0.5	CWS	CWS	CWS	CWS	CWS	CWS	CWS	CWS	CWS	BCW	CWS	CWS	CWS	CWS	CWS	CWS	CWS	CWS	CWS	CWS
set_08_N30_MR-100	2S	I	T	0.3	-1	CWS	CWS	CWS	CWS	CWS	CWS	CWS	CWS	CWS	CWS	CWS	CWS	CWS	CWS	CWS	CWS	CWS	CWS	CWS	CWS
set_08_MR050	2S	I	T	0.5	0.5	BCW	BCW	CWS	BCW	BCW	CWS	BCW	BCW	BCW	BCW	BCW	BCW	BCW	BCW	BCW	BCW	BCW	BCW	BCW	BCW
set_08_MR-050	2S	I	T	0.5	-0.5	CWS	CWS	CWS	CWS	CWS	CWS	CWS	CWS	CWS	BCW	CWS	CWS	CWS	CWS	CWS	CWS	CWS	CWS	CWS	CWS
set_08_MR-100	2S	I	T	0.5	-1	CWS	CWS	CWS	CWS	CWS	CWS	CWS	CWS	CWS	CWS	CWS	CWS	CWS	CWS	CWS	CWS	CWS	CWS	CWS	CWS
set_08_N70_MR050	2S	I	T	0.7	0.5	BCW	BCW	CWS	BCW	BCW	CWS	BCW	BCW	BCW	BCW	BCW	BCW	BCW	BCW	BCW	BCW	BCW	BCW	BCW	BCW
set_08_N70_MR-050	2S	I	T	0.7	-0.5	CWS	CWS	CWS	CWS	CWS	CWS	CWS	CWS	CWS	BCW	CWS	CWS	CWS	CWS	CWS	CWS	CWS	CWS	CWS	CWS
set_08_N70_MR-100	2S	I	T	0.7	-1	CWS	CWS	CWS	CWS	CWS	CWS	CWS	CWS	CWS	CWS	CWS	CWS	CWS	CWS	CWS	CWS	CWS	CWS	CWS	CWS
set_09	1S	R	U	0	0	CWT	CWT	CWT	CWT	CWT	CWT	CWT	CWT	CWT	CWT	CWT	CWT	CWT	CWT	CWT	CWT	CWT	CWT	CWT	CWT
set_11	1S	R	T	0	0	CWS	CWS	CWS	CWS	CWS	CWS	CWS	BCW	CWS	BCW	CWS	BCW	BCW	CWS	BCW	CWS	CWS	CWS	CWS	CWS
set_13_MR050	2S	R	U	0	0.5	CWT	CWT	CWT	CWT	CWT	CWT	CWT	CWT	CWT	BCW	CWT	BCW	CWT	CWT	CWT	CWT	CWT	CWT	CWT	CWT
set_13_MR-050	2S	R	U	0	-0.5	CWT	CWT	CWT	CWT	CWT	CWT	CWT	CWT	CWT	CWT	CWT	CWT	CWT	CWT	CWT	CWT	CWT	CWT	CWT	CWT
set_13_MR-100	2S	R	U	0	-1	CWT	CWT	CWT	CWT	CWT	CWT	CWT	CWT	CWT	CWT	CWT	CWT	CWT	CWT	CWT	CWT	CWT	CWT	CWT	CWT
set_15_MR050	2S	R	T	0	0.5	BCW	CWS	CWS	BCW	BCW	CWS	BCW	BCW	BCW	BCW	BCW	BCW	BCW	BCW	BCW	BCW	BCW	BCW	BCW	BCW
set_15_MR-050	2S	R	T	0	-0.5	CWS	CWS	CWS	CWS	CWS	CWS	CWS	CWS	CWS	BCW	CWS	CWS	CWS	CWS	CWS	CWS	CWS	CWS	CWS	CWS
set_15_MR-100	2S	R	T	0	-1	CWS	CWS	CWS	CWS	CWS	CWS	CWS	CWS	CWS	CWS	CWS	CWS	CWS	CWS	CWS	CWS	CWS	CWS	CWS	CWS

Table 3.6. Ratios for unstiffened rolled columns, S275 (cluster BR-S275), EPPL.

Method	Cases	CWC				CWT				CWS				ALL (EXCEPT BCW)			
		n	Mean	CoV	(>1)/*n*	*n*	Mean	CoV	(>1)/*n*	*n*	Mean	CoV	(>1)/*n*	*tot*	Mean	CoV	(>1)/tot
r_{EN}	**1S-U, n = 0**	14	**0.79**	14.4%	0%	20	**0.69**	***15.7%***	0%	2	**0.80**	5.6%	0%	36	**0.73**	***16.0%***	0%
	2S-U, n = 0	25	**0.80**	***15.1%***	8%	58	**0.72**	***17.5%***	5%	29	**0.82**	***15.4%***	10%	112	**0.77**	***17.2%***	7%
	1S-U-I, n = 0	14	**0.79**	14.4%	0%					2	**0.80**	5.6%	0%	16	**0.79**	13.5%	0%
	2S-U-I, n = 0	25	**0.80**	***15.1%***	8%					29	**0.82**	***15.4%***	10%	54	**0.81**	***15.2%***	9%
	1S-U-R, n = 0					20	**0.69**	***15.7%***	0%					20	**0.69**	***15.7%***	0%
	2S-U-R, n = 0					58	**0.72**	***17.5%***	5%					58	**0.72**	***17.5%***	5%
r_{FprEN}	**1S-U, n = 0**	14	**0.75**	11.6%	0%	20	**0.65**	13.9%	0%	2	**0.81**	3.4%	0%	36	**0.70**	14.7%	0%
	2S-U, n = 0	25	**0.80**	***15.5%***	8%	58	**0.67**	***19.6%***	5%	29	**0.85**	5.3%	0%	112	**0.75**	***18.4%***	4%
	1S-U-I, n = 0	14	**0.75**	11.6%	0%					2	**0.81**	3.4%	0%	16	**0.76**	11.2%	0%
	2S-U-I, n = 0	25	**0.80**	***15.5%***	8%					29	**0.85**	5.3%	0%	54	**0.83**	11.3%	4%
	1S-U-R, n = 0					20	**0.65**	13.9%	0%					20	**0.65**	13.9%	0%
	2S-U-R, n = 0					58	**0.67**	***19.6%***	5%					58	**0.67**	***19.6%***	5%
$r_{IS,MNA,def}$	**1S-U, n = 0**	14	1.02	2.6%	79%	20	0.96	4.7%	20%	2	1.04	4.0%	100%	36	0.99	4.9%	47%
	2S-U, n = 0	25	1.04	2.6%	92%	58	0.96	7.3%	34%	29	1.03	1.8%	100%	112	0.99	6.5%	64%
	1S-U-I, n = 0	14	1.02	2.6%	79%					2	1.04	4.0%	100%	16	1.02	2.8%	81%
	2S-U-I, n = 0	25	1.04	2.6%	92%					29	1.03	1.8%	100%	54	1.03	2.2%	96%
	1S-U-R, n = 0					20	0.96	4.7%	20%					20	0.96	4.7%	20%
	2S-U-R, n = 0					58	0.96	7.3%	34%					58	0.96	7.3%	34%
$r_{IS,MNA,ref}$	**1S-U, n = 0**	14	0.96	2.9%	7%	20	**0.88**	4.6%	0%	2	0.98	4.6%	50%	36	0.92	5.8%	6%
	2S-U, n = 0	25	0.98	3.6%	36%	58	**0.90**	5.6%	0%	29	1.00	1.7%	45%	112	0.94	6.6%	20%
	1S-U-I, n = 0	14	0.96	2.9%	7%					2	0.98	4.6%	50%	16	0.96	3.0%	13%
	2S-U-I, n = 0	25	0.98	3.6%	36%					29	1.00	1.7%	45%	54	0.99	2.8%	41%
	1S-U-R, n = 0					20	**0.88**	4.6%	0%					20	**0.88**	4.6%	0%
	2S-U-R, n = 0					58	**0.90**	5.6%	0%					58	**0.90**	5.6%	0%
$r_{IS,MNA,rich}$	**1S-U, n = 0**	14	0.94	3.1%	7%	20	**0.86**	5.1%	0%	2	0.96	4.8%	0%	36	**0.90**	6.5%	3%
	2S-U, n = 0	25	0.96	4.1%	16%	58	**0.87**	5.3%	0%	29	0.99	1.8%	14%	112	0.92	7.0%	7%
	1S-U-I, n = 0	14	0.94	3.1%	7%					2	0.96	4.8%	0%	16	0.94	3.3%	6%
	2S-U-I, n = 0	25	0.96	4.1%	16%					29	0.99	1.8%	14%	54	0.97	3.3%	15%
	1S-U-R, n = 0					20	**0.86**	5.1%	0%					20	**0.86**	5.1%	0%
	2S-U-R, n = 0					58	**0.87**	5.3%	0%					58	**0.87**	5.3%	0%
$r_{IS,GMNA,def}$	**1S-U, n = 0**	14	1.02	2.7%	71%	20	0.96	4.7%	20%	2	1.04	3.7%	100%	36	0.99	4.9%	44%
	2S-U, n = 0	25	1.04	2.6%	92%	58	0.95	7.1%	31%	29	1.03	2.2%	90%	112	0.99	6.5%	60%
	1S-U-I, n = 0	14	1.02	2.7%	71%					2	1.04	3.7%	100%	16	1.02	2.8%	75%
	2S-U-I, n = 0	25	1.04	2.6%	92%					29	1.03	2.2%	90%	54	1.03	2.4%	91%
	1S-U-R, n = 0					20	0.96	4.7%	20%					20	0.96	4.7%	20%
	2S-U-R, n = 0					58	0.95	7.1%	31%					58	0.95	7.1%	31%
$r_{IS,GMNA,ref}$	**1S-U, n = 0**	14	0.96	2.9%	7%	20	**0.88**	4.6%	0%	2	0.98	4.6%	50%	36	0.92	5.9%	6%
	2S-U, n = 0	25	0.98	3.4%	24%	58	**0.89**	5.5%	0%	29	0.99	2.0%	34%	112	0.94	6.6%	14%
	1S-U-I, n = 0	14	0.96	2.9%	7%					2	0.98	4.6%	50%	16	0.96	3.0%	13%
	2S-U-I, n = 0	25	0.98	3.4%	24%					29	0.99	2.0%	34%	54	0.99	2.9%	30%
	1S-U-R, n = 0					20	**0.88**	4.6%	0%					20	**0.88**	4.6%	0%
	2S-U-R, n = 0					58	**0.89**	5.5%	0%					58	**0.89**	5.5%	0%
$r_{IS,GMNA,rich}$	**1S-U, n = 0**	14	0.94	3.1%	7%	20	**0.86**	5.1%	0%	2	0.96	4.9%	0%	36	**0.89**	6.5%	3%
	2S-U, n = 0	25	0.96	3.9%	4%	58	**0.87**	5.3%	0%	29	0.98	2.1%	10%	112	0.92	6.9%	4%
	1S-U-I, n = 0	14	0.94	3.1%	7%					2	0.96	4.9%	0%	16	0.94	3.2%	6%
	2S-U-I, n = 0	25	0.96	3.9%	4%					29	0.98	2.1%	10%	54	0.97	3.3%	7%
	1S-U-R, n = 0					20	**0.86**	5.1%	0%					20	**0.86**	5.1%	0%
	2S-U-R, n = 0					58	**0.87**	5.3%	0%					58	**0.87**	5.3%	0%

Table 3.7. Ratios for stiffened rolled columns, S275 (cluster BR-S275), EPPL.

Method	r_{EN}	CWS			
	Cases	*n*	Mean	CoV	(>1)/*n*
r_{EN}	**1S-T, n = 0**	29	0.99	7.3%	38%
	2S-T, n = 0	83	0.92	8.9%	20%
	1S-T-I, n = 0	14	1.00	7.6%	57%
	2S-T-I, n = 0	41	0.93	9.3%	20%
	1S-T-R, n = 0	15	0.98	7.0%	20%
	2S-T-R, n = 0	42	0.92	8.5%	21%
r_{FprEN}	**1S-T, n = 0**	29	0.91	6.4%	3%
	2S-T, n = 0	83	**0.89**	7.7%	6%
	1S-T-I, n = 0	14	0.91	3.0%	0%
	2S-T-I, n = 0	41	**0.89**	2.9%	0%
	1S-T-R, n = 0	15	0.90	8.5%	7%
	2S-T-R, n = 0	42	**0.89**	10.5%	12%
$r_{IS,MNA,def}$	**1S-T, n = 0**	29	0.98	6.3%	45%
	2S-T, n = 0	83	0.98	8.8%	53%
	1S-T-I, n = 0	14	1.02	2.2%	86%
	2S-T-I, n = 0	41	1.05	1.9%	100%
	1S-T-R, n = 0	15	0.93	5.9%	7%
	2S-T-R, n = 0	42	0.91	7.3%	7%
$r_{IS,MNA,ref}$	**1S-T, n = 0**	29	0.95	6.1%	17%
	2S-T, n = 0	83	0.95	8.1%	40%
	1S-T-I, n = 0	14	1.00	2.0%	29%
	2S-T-I, n = 0	41	1.01	1.8%	73%
	1S-T-R, n = 0	15	0.91	5.6%	7%
	2S-T-R, n = 0	42	**0.89**	7.2%	7%
$r_{IS,MNA,rich}$	**1S-T, n = 0**	29	0.94	6.1%	17%
	2S-T, n = 0	83	0.94	7.9%	27%
	1S-T-I, n = 0	14	0.99	2.1%	29%
	2S-T-I, n = 0	41	1.00	1.9%	51%
	1S-T-R, n = 0	15	0.90	5.6%	7%
	2S-T-R, n = 0	42	**0.88**	7.2%	2%
$r_{IS,GMNA,def}$	**1S-T, n = 0**	29	0.97	6.0%	41%
	2S-T, n = 0	83	0.98	8.4%	53%
	1S-T-I, n = 0	14	1.02	2.3%	79%
	2S-T-I, n = 0	41	1.05	2.0%	100%
	1S-T-R, n = 0	15	0.93	5.7%	7%
	2S-T-R, n = 0	42	0.91	7.0%	7%
$r_{IS,GMNA,ref}$	**1S-T, n = 0**	29	0.94	6.1%	17%
	2S-T, n = 0	83	0.94	8.3%	27%
	1S-T-I, n = 0	14	0.98	3.2%	29%
	2S-T-I, n = 0	41	1.00	3.2%	51%
	1S-T-R, n = 0	15	0.91	5.6%	7%
	2S-T-R, n = 0	42	**0.88**	7.1%	2%
$r_{IS,GMNA,rich}$	**1S-T, n = 0**	29	0.93	6.2%	17%
	2S-T, n = 0	83	0.92	8.4%	18%
	1S-T-I, n = 0	14	0.97	3.8%	29%
	2S-T-I, n = 0	41	0.98	3.8%	34%
	1S-T-R, n = 0	15	**0.90**	5.6%	7%
	2S-T-R, n = 0	42	**0.87**	7.3%	2%

Table 3.8. Ratios rolled columns, axial load, S275 (cluster BR-S275), EPPL. EN, FprEN.

Method	Cases	CWC				CWS				ALL (EXCEPT BCW)			
		n	Mean	CoV	(>1)/*n*	*n*	Mean	CoV	(>1)/*n*	*tot*	Mean	CoV	(>1)/tot
r_{EN}	**1S Interior Unstiffened**												
	1S-U-I, n = 0	14	**0.79**	14.4%	0%	2	**0.80**	5.6%	0%	16	**0.79**	13.5%	0%
	1S-U-I, n = 0.3	14	**0.83**	***15.1%***	14%	2	**0.84**	5.5%	0%	16	**0.83**	14.1%	13%
	1S-U-I, n = 0.5	14	**0.88**	***15.5%***	29%	2	0.91	5.5%	0%	16	**0.89**	14.4%	25%
	1S-U-I, n = 0.7	14	1.02	***15.8%***	50%	2	1.05	4.8%	100%	16	1.02	14.8%	56%
	1S Interior Stiffened												
	1S-T-I, n = 0					14	1.00	7.6%	57%	14	1.00	7.6%	57%
	1S-T-I, n = 0.3					14	1.06	7.5%	79%	14	1.06	7.5%	79%
	1S-T-I, n = 0.5					14	***1.14***	6.6%	100%	14	***1.14***	6.6%	100%
	1S-T-I, n = 0.7					14	***1.31***	8.1%	100%	14	***1.31***	8.1%	100%
	2S Interior Unstiffened												
	2S-U-I, n = 0	25	**0.80**	***15.1%***	8%	29	**0.82**	***15.4%***	10%	54	**0.81**	***15.2%***	9%
	2S-U-I, n = 0.3	25	**0.84**	***15.4%***	12%	29	**0.87**	***15.3%***	14%	54	**0.86**	***15.4%***	13%
	2S-U-I, n = 0.5	25	**0.90**	***15.8%***	20%	29	0.94	14.5%	31%	54	0.92	***15.1%***	26%
	2S-U-I, n = 0.7	25	1.04	***16.0%***	52%	29	1.08	14.5%	69%	54	1.06	***15.1%***	61%
	2S Interior Stiffened												
	2S-T-I, n = 0					41	0.93	9.3%	20%	41	0.93	9.3%	20%
	2S-T-I, n = 0.3					41	0.99	9.0%	37%	41	0.99	9.0%	37%
	2S-T-I, n = 0.5					41	1.06	8.3%	73%	41	1.06	8.3%	73%
	2S-T-I, n = 0.7					41	***1.20***	7.7%	100%	41	***1.20***	7.7%	100%
r_{FprEN}	**1S Interior Unstiffened**												
	1S-U-I, n = 0	14	**0.75**	11.6%	0%	2	**0.81**	3.4%	0%	16	**0.76**	11.2%	0%
	1S-U-I, n = 0.3	14	**0.78**	12.2%	0%	2	**0.86**	3.5%	0%	16	**0.79**	11.7%	0%
	1S-U-I, n = 0.5	14	**0.84**	12.7%	0%	2	0.93	3.5%	0%	16	**0.85**	12.3%	0%
	1S-U-I, n = 0.7	14	0.96	13.7%	43%	2	1.08	4.2%	100%	16	0.98	13.2%	50%
	1S Interior Stiffened												
	1S-T-I, n = 0					14	0.91	3.0%	0%	14	0.91	3.0%	0%
	1S-T-I, n = 0.3					14	0.97	2.5%	14%	14	0.97	2.5%	14%
	1S-T-I, n = 0.5					14	1.03	2.7%	79%	14	1.03	2.7%	79%
	1S-T-I, n = 0.7					14	***1.20***	7.9%	100%	14	***1.20***	7.9%	100%
	2S Interior Unstiffened												
	2S-U-I, n = 0	25	**0.80**	***15.5%***	8%	29	**0.85**	5.3%	0%	54	**0.83**	11.3%	4%
	2S-U-I, n = 0.3	25	**0.83**	***15.8%***	12%	29	0.91	5.1%	0%	54	**0.87**	11.7%	6%
	2S-U-I, n = 0.5	25	**0.89**	***16.2%***	16%	29	0.98	4.6%	24%	54	0.94	11.9%	20%
	2S-U-I, n = 0.7	25	1.03	***16.6%***	52%	29	***1.13***	7.1%	100%	54	1.09	12.8%	78%
	2S Interior Stiffened												
	2S-T-I, n = 0					41	**0.89**	2.9%	0%	41	**0.89**	2.9%	0%
	2S-T-I, n = 0.3					41	0.95	2.8%	7%	41	0.95	2.8%	7%
	2S-T-I, n = 0.5					41	1.02	2.8%	76%	41	1.02	2.8%	76%
	2S-T-I, n = 0.7					41	***1.15***	4.4%	100%	41	***1.15***	4.4%	100%

Table 3.9. Ratios, rolled columns, axial load, S275 (cluster BR-S275), EPPL. IS MNA.

Method	Cases	CWC				CWS				ALL (EXCEPT BCW)			
		n	Mean	CoV	(>1)/*n*	*n*	Mean	CoV	(>1)/*n*	*tot*	Mean	CoV	(>1)/tot
$r_{IS,MNA,def}$	**1S Interior Unstiffened**												
	1S-U-I, n = 0	14	1.02	2.6%	79%	2	1.04	4.0%	100%	16	1.02	2.8%	81%
	1S-U-I, n = 0.3	14	1.04	2.2%	100%	2	1.08	4.0%	100%	16	1.05	2.7%	100%
	1S-U-I, n = 0.5	14	1.05	2.3%	100%	2	***1.11***	3.2%	100%	16	1.06	2.9%	100%
	1S-U-I, n = 0.7	14	1.07	3.1%	100%	2	***1.13***	2.7%	100%	16	1.08	3.5%	100%
	1S Interior Stiffened												
	1S-T-I, n = 0					14	1.02	2.2%	86%	14	1.02	2.2%	86%
	1S-T-I, n = 0.3					14	1.07	2.6%	100%	14	1.07	2.6%	100%
	1S-T-I, n = 0.5					14	***1.11***	2.7%	100%	14	***1.11***	2.7%	100%
	1S-T-I, n = 0.7					14	***1.15***	2.6%	100%	14	***1.15***	2.6%	100%
	2S Interior Unstiffened												
	2S-U-I, n = 0	25	1.04	2.6%	92%	29	1.03	1.8%	100%	54	1.03	2.2%	96%
	2S-U-I, n = 0.3	25	1.06	3.1%	96%	29	1.08	1.8%	100%	54	1.07	2.6%	98%
	2S-U-I, n = 0.5	25	1.07	3.4%	96%	29	***1.10***	2.1%	100%	54	1.09	3.1%	98%
	2S-U-I, n = 0.7	25	***1.11***	5.7%	96%	29	***1.14***	2.0%	100%	54	***1.12***	4.2%	98%
	2S Interior Stiffened												
	2S-T-I, n = 0					41	1.05	1.9%	100%	41	1.05	1.9%	100%
	2S-T-I, n = 0.3					41	***1.10***	1.8%	100%	41	***1.10***	1.8%	100%
	2S-T-I, n = 0.5					41	***1.14***	2.4%	100%	41	***1.14***	2.4%	100%
	2S-T-I, n = 0.7					41	***1.17***	3.6%	100%	41	***1.17***	3.6%	100%
$r_{IS,MNA,ref}$	**1S Interior Unstiffened**												
	1S-U-I, n = 0	14	0.96	2.9%	7%	2	0.98	4.6%	50%	16	0.96	3.0%	13%
	1S-U-I, n = 0.3	14	0.98	2.4%	7%	2	1.02	4.5%	50%	16	0.98	3.0%	13%
	1S-U-I, n = 0.5	14	0.98	2.4%	21%	2	1.05	3.6%	100%	16	0.99	3.4%	31%
	1S-U-I, n = 0.7	14	1.00	3.6%	57%	2	1.09	3.5%	100%	16	1.02	4.5%	63%
	1S Interior Stiffened												
	1S-T-I, n = 0					14	1.00	2.0%	29%	14	1.00	2.0%	29%
	1S-T-I, n = 0.3					14	1.04	2.1%	86%	14	1.04	2.1%	86%
	1S-T-I, n = 0.5					14	1.07	2.4%	100%	14	1.07	2.4%	100%
	1S-T-I, n = 0.7					14	***1.11***	2.6%	100%	14	***1.11***	2.6%	100%
	2S Interior Unstiffened												
	2S-U-I, n = 0	25	0.98	3.6%	36%	29	1.00	1.7%	45%	54	0.99	2.8%	41%
	2S-U-I, n = 0.3	25	0.99	4.5%	52%	29	1.04	1.5%	100%	54	1.02	3.9%	78%
	2S-U-I, n = 0.5	25	1.00	4.6%	60%	29	1.07	1.9%	100%	54	1.04	4.6%	81%
	2S-U-I, n = 0.7	25	1.04	6.8%	72%	29	1.10	2.6%	100%	54	1.07	5.6%	87%
	2S Interior Stiffened												
	2S-T-I, n = 0					41	1.01	1.8%	73%	41	1.01	1.8%	73%
	2S-T-I, n = 0.3					41	1.06	1.9%	100%	41	1.06	1.9%	100%
	2S-T-I, n = 0.5					41	1.09	2.4%	100%	41	1.09	2.4%	100%
	2S-T-I, n = 0.7					41	***1.12***	4.1%	100%	41	***1.12***	4.1%	100%
$r_{IS,MNA,rich}$	**1S Interior Unstiffened**												
	1S-U-I, n = 0	14	0.94	3.1%	7%	2	0.96	4.8%	0%	16	0.94	3.3%	6%
	1S-U-I, n = 0.3	14	0.96	2.7%	7%	2	1.00	4.7%	50%	16	0.96	3.3%	13%
	1S-U-I, n = 0.5	14	0.96	2.8%	7%	2	1.03	3.7%	100%	16	0.97	3.7%	19%
	1S-U-I, n = 0.7	14	0.98	4.0%	36%	2	1.08	3.8%	100%	16	0.99	5.1%	44%
	1S Interior Stiffened												
	1S-T-I, n = 0					14	0.99	2.1%	29%	14	0.99	2.1%	29%
	1S-T-I, n = 0.3					14	1.03	2.0%	86%	14	1.03	2.0%	86%
	1S-T-I, n = 0.5					14	1.06	2.4%	100%	14	1.06	2.4%	100%
	1S-T-I, n = 0.7					14	***1.10***	2.7%	100%	14	***1.10***	2.7%	100%
	2S Interior Unstiffened												
	2S-U-I, n = 0	25	0.96	4.1%	16%	29	0.99	1.8%	14%	54	0.97	3.3%	15%
	2S-U-I, n = 0.3	25	0.97	5.1%	36%	29	1.03	1.6%	100%	54	1.00	4.6%	70%
	2S-U-I, n = 0.5	25	0.98	5.2%	36%	29	1.05	2.1%	100%	54	1.02	5.3%	70%
	2S-U-I, n = 0.7	25	1.01	7.3%	48%	29	1.08	2.9%	100%	54	1.05	6.3%	76%
	2S Interior Stiffened												
	2S-T-I, n = 0					41	1.00	1.9%	51%	41	1.00	1.9%	51%
	2S-T-I, n = 0.3					41	1.04	2.1%	98%	41	1.04	2.1%	98%
	2S-T-I, n = 0.5					41	1.08	2.5%	100%	41	1.08	2.5%	100%
	2S-T-I, n = 0.7					41	***1.11***	4.4%	95%	41	***1.11***	4.4%	95%

Table 3.10. Ratios rolled columns, axial load, S275 (cluster BR-S275), EPPL. IS GMNA.

Method	Cases	CWC				CWS				ALL (EXCEPT BCW)			
		n	Mean	CoV	(>1)/*n*	*n*	Mean	CoV	(>1)/*n*	*tot*	Mean	CoV	(>1)/tot
$r_{IS,GMNA,def}$	**1S Interior Unstiffened**												
	1S-U-I, n = 0	14	1.02	2.7%	71%	2	1.04	3.7%	100%	16	1.02	2.8%	75%
	1S-U-I, n = 0.3	14	1.01	2.8%	64%	2	1.02	3.0%	50%	16	1.01	2.7%	63%
	1S-U-I, n = 0.5	14	1.00	3.1%	36%	2	1.00	2.5%	50%	16	1.00	3.0%	38%
	1S-U-I, n = 0.7	14	0.99	4.5%	36%	2	1.01	1.6%	50%	16	0.99	4.2%	38%
	1S Interior Stiffened												
	1S-T-I, n = 0					14	1.02	2.3%	79%	14	1.02	2.3%	79%
	1S-T-I, n = 0.3					14	1.00	1.9%	57%	14	1.00	1.9%	57%
	1S-T-I, n = 0.5					14	1.00	2.1%	43%	14	1.00	2.1%	43%
	1S-T-I, n = 0.7					14	1.01	4.1%	50%	14	1.01	4.1%	50%
	2S Interior Unstiffened												
	2S-U-I, n = 0	25	1.04	2.6%	92%	29	1.03	2.2%	90%	54	1.03	2.4%	91%
	2S-U-I, n = 0.3	25	1.03	3.1%	88%	29	1.00	1.9%	55%	54	1.01	2.7%	70%
	2S-U-I, n = 0.5	25	1.02	3.1%	68%	29	1.00	1.9%	41%	54	1.01	2.8%	54%
	2S-U-I, n = 0.7	25	1.03	5.0%	72%	29	0.99	2.3%	48%	54	1.01	4.3%	59%
	2S Interior Stiffened												
	2S-T-I, n = 0					41	1.05	2.0%	100%	41	1.05	2.0%	100%
	2S-T-I, n = 0.3					41	1.02	2.2%	88%	41	1.02	2.2%	88%
	2S-T-I, n = 0.5					41	1.02	2.4%	83%	41	1.02	2.4%	83%
	2S-T-I, n = 0.7					41	1.01	4.1%	66%	41	1.01	4.1%	66%
$r_{IS,GMNA,ref}$	**1S Interior Unstiffened**												
	1S-U-I, n = 0	14	0.96	2.9%	7%	2	0.98	4.6%	50%	16	0.96	3.0%	13%
	1S-U-I, n = 0.3	14	0.96	2.8%	7%	2	0.99	4.3%	50%	16	0.96	3.0%	13%
	1S-U-I, n = 0.5	14	0.95	2.9%	7%	2	0.98	2.6%	50%	16	0.95	3.0%	13%
	1S-U-I, n = 0.7	14	0.95	4.4%	14%	2	0.98	2.4%	50%	16	0.96	4.3%	19%
	1S Interior Stiffened												
	1S-T-I, n = 0					14	0.98	3.2%	29%	14	0.98	3.2%	29%
	1S-T-I, n = 0.3					14	0.98	1.9%	7%	14	0.98	1.9%	7%
	1S-T-I, n = 0.5					14	0.98	2.2%	21%	14	0.98	2.2%	21%
	1S-T-I, n = 0.7					14	0.99	4.1%	43%	14	0.99	4.1%	43%
	2S Interior Unstiffened												
	2S-U-I, n = 0	25	0.98	3.4%	24%	29	0.99	2.0%	34%	54	0.99	2.9%	30%
	2S-U-I, n = 0.3	25	0.97	3.9%	20%	29	0.98	1.9%	21%	54	0.98	3.0%	20%
	2S-U-I, n = 0.5	25	0.97	3.6%	16%	29	0.98	2.0%	7%	54	0.97	2.8%	11%
	2S-U-I, n = 0.7	25	0.98	6.0%	24%	29	0.97	2.7%	3%	54	0.98	4.5%	13%
	2S Interior Stiffened												
	2S-T-I, n = 0					41	1.00	3.2%	51%	41	1.00	3.2%	51%
	2S-T-I, n = 0.3					41	0.99	2.2%	32%	41	0.99	2.2%	32%
	2S-T-I, n = 0.5					41	1.00	2.4%	34%	41	1.00	2.4%	34%
	2S-T-I, n = 0.7					41	0.99	4.0%	39%	41	0.99	4.0%	39%
$r_{IS,GMNA,rich}$	**1S Interior Unstiffened**												
	1S-U-I, n = 0	14	0.94	3.1%	7%	2	0.96	4.9%	0%	16	0.94	3.2%	6%
	1S-U-I, n = 0.3	14	0.94	3.0%	7%	2	0.98	4.7%	50%	16	0.95	3.4%	13%
	1S-U-I, n = 0.5	14	0.93	3.1%	0%	2	0.98	2.6%	0%	16	0.94	3.3%	0%
	1S-U-I, n = 0.7	14	0.94	4.5%	14%	2	0.98	2.7%	0%	16	0.94	4.5%	13%
	1S Interior Stiffened												
	1S-T-I, n = 0					14	0.97	3.8%	29%	14	0.97	3.8%	29%
	1S-T-I, n = 0.3					14	0.98	2.0%	7%	14	0.98	2.0%	7%
	1S-T-I, n = 0.5					14	0.98	2.3%	14%	14	0.98	2.3%	14%
	1S-T-I, n = 0.7					14	0.99	4.2%	29%	14	0.99	4.2%	29%
	2S Interior Unstiffened												
	2S-U-I, n = 0	25	0.96	3.9%	4%	29	0.98	2.1%	10%	54	0.97	3.3%	7%
	2S-U-I, n = 0.3	25	0.96	4.6%	8%	29	0.98	1.9%	14%	54	0.97	3.5%	11%
	2S-U-I, n = 0.5	25	0.95	4.2%	12%	29	0.97	2.0%	0%	54	0.96	3.3%	6%
	2S-U-I, n = 0.7	25	0.96	6.5%	24%	29	0.96	2.8%	3%	54	0.96	4.9%	13%
	2S Interior Stiffened												
	2S-T-I, n = 0					41	0.98	3.8%	34%	41	0.98	3.8%	34%
	2S-T-I, n = 0.3					41	0.98	2.3%	17%	41	0.98	2.3%	17%
	2S-T-I, n = 0.5					41	0.99	2.5%	24%	41	0.99	2.5%	24%
	2S-T-I, n = 0.7					41	0.98	4.0%	27%	41	0.98	4.0%	27%

3.2.6 Influence of fillet welds

The influence of fillet welds was studied only for I-1S joints. For these cases, the fillet welds were designed for full resistance, except for case 10 where this condition led to unrealistic weld throat size. **Table 3.11** presents the failure modes by case. Only case 10 in stiffened joints presents BCW failure. Consequently, this case has been excluded from the statistical evaluation for stiffened joints. The table shows that:

- For unstiffened joints, CWC failure is dominant, except for cases 10 to 15 which correspond to very stocky columns.
- For stiffened joints, CWS failure is dominant, except for case 10.

Statistics of the ratios are presented in **Table 3.12** (EN and FprEN), **Table 3.13** (IS, MNA), and **Table 3.14** (IS, GMNA). The following trends are observed:
For EN and FprEN:

- With no axial load (n = 0), the mean of ratios for EN and FprEN is highly conservative. For EN and stiffened joints (T), a considerable proportion of cases (26%) is unconservative. This is not so for FprEN, for which all cases are conservative.
- With moderate values of axial load (n = 0.30), the same trends are observed, except that the number of unconservative cases with EN increases up to 47%.
- As axial load increases, more unconservative results are obtained with both codes.
- With the limit value of axial load in this study, n = 0.70, both codes are highly unconservative. For stiffened joints (CWS failure mode), 100% of cases are unconservative.
- The scatter of results for EN is generally moderate. Only unstiffened joints with high axial load (n = 0.5, n = 0.7) present high CoV.
- The scatter of results for FprEN is generally moderate. For stiffened joints, the CoV is moderate in all cases except with high axial load (n = 0.7).
- FprEN improves slightly the results when compared to EN, but to the cost of higher conservativeness. Even so, for high values of axial load, the results are still unconservative.

For IDEA StatiCa:

- With no axial load (n = 0), and default options (MNA, default mesh), IDEA StatiCa mean ratios are moderately conservative, with a small proportion (about 5% - 10%) of unconservative cases.
- With axial load and default options, IDEA StatiCa mean ratios are generally moderately conservative for CWC and moderately unconservative for CWS. As axial load increases, the mean ratios increase beyond 1 (unconservative) and the proportion of unconservative cases increases, particularly so for stiffened joints.
- Reducing the mesh size without axial load results in highly conservative results for cases with CWC failure mode, and moderately conservative results for cases with CWS failure mode.
- For cases with axial load, a reduction of the mesh size improves the mean ratio and reduces the proportion of unconservative cases. However, for stiffened joints and n > 0.3, the mean ratios are above 1 and a large proportion of cases is unconservative.
- Using GMNA with the default mesh size results in mean ratios moderately conservative, although a moderate proportion of cases remains unconservative.

- Combining GMNA with a reduction of mesh size results in mean ratios moderately conservative and no unconservative results, except for a very small proportion of unconservative cases (5%) for high axial load (n = 0.7).
- With IDEA StatiCa, the CoV is consistently low (below 7.5%) and stable across all sets, regardless of the method or mesh.

Table 3.11. Rolled columns with fillet welds, S275 (cluster FR-S275), EPPL. Failure modes.

S275						Case																		
	1S/2S	I/R	U/T	*n*	*mr*	1	2	3	4	5	6	7	8	9	10	11	12	13	14	15	16	17	18	19	20
set_01	1S	I	U	0	0	CWC	CWC	CWC	CWC	CWC	CWC	CWC	CWC	CWC	CWS	CWS	CWS	CWS	CWS	CWS	CWC	CWC	CWC	CWC	CWC
set_02_N30	1S	I	U	0.3	0	CWC	CWC	CWC	CWC	CWC	CWC	CWC	CWC	CWC	CWS	CWS	CWS	CWS	CWS	CWS	CWC	CWC	CWC	CWC	CWC
set_02_N50	1S	I	U	0.5	0	CWC	CWC	CWC	CWC	CWC	CWC	CWC	CWC	CWC	CWS	CWS	CWS	CWS	CWS	CWS	CWC	CWC	CWC	CWC	CWC
set_02_N70	1S	I	U	0.7	0	CWC	CWC	CWC	CWC	CWC	CWC	CWC	CWC	CWC	CWS	CWS	CWS	CWS	CWS	CWS	CWC	CWC	CWC	CWC	CWC
set_03	1S	I	T	0	0	CWS	CWS	CWS	CWS	CWS	CWS	CWS	CWS	CWS	BCW	CWS	CWS	CWS	CWS	CWS	CWS	CWS	CWS	CWS	CWS
set_04_N30	1S	I	T	0.3	0	CWS	CWS	CWS	CWS	CWS	CWS	CWS	CWS	CWS	BCW	CWS	CWS	CWS	CWS	CWS	CWS	CWS	CWS	CWS	CWS
set_04_N50	1S	I	T	0.5	0	CWS	CWS	CWS	CWS	CWS	CWS	CWS	CWS	CWS	BCW	CWS	CWS	CWS	CWS	CWS	CWS	CWS	CWS	CWS	CWS
set_04_N70	1S	I	T	0.7	0	CWS	CWS	CWS	CWS	CWS	CWS	CWS	CWS	CWS	BCW	CWS	CWS	CWS	CWS	CWS	CWS	CWS	CWS	CWS	CWS

Table 3.12. Ratios rolled columns, fillet welds, S275 (cluster FR-S275), EPPL. EN, FprEN.

Method	Cases	CWC				CWS				ALL (EXCEPT BCW)			
		n	Mean	CoV	(>1)/*n*	*n*	Mean	CoV	(>1)/*n*	*tot*	Mean	CoV	(>1)/tot
r_{EN}	**1S-I**	56	**0.88**	***18.3%***	21%	100	1.00	***17.2%***	49%	156	0.96	***18.6%***	39%
	1S-I-U	56	**0.88**	***18.3%***	21%	24	**0.84**	***16.1%***	8%	80	**0.86**	***17.7%***	18%
	1S-I-T					76	1.06	14.2%	62%	76	1.06	14.2%	62%
	1S-U-I, n = 0	14	**0.78**	14.0%	0%	6	**0.74**	12.1%	0%	20	**0.77**	13.4%	0%
	1S-U-I, n = 0.3	14	**0.82**	14.9%	7%	6	**0.78**	12.4%	0%	20	**0.81**	14.1%	5%
	1S-U-I, n = 0.5	14	**0.88**	***15.5%***	14%	6	**0.85**	12.0%	0%	20	**0.87**	14.3%	10%
	1S-U-I, n = 0.7	14	1.02	***16.1%***	64%	6	0.99	11.3%	33%	20	1.01	14.7%	55%
	1S-T-I, n = 0					19	0.94	10.0%	26%	19	0.94	10.0%	26%
	1S-T-I, n = 0.3					19	0.99	9.9%	47%	19	0.99	9.9%	47%
	1S-T-I, n = 0.5					19	1.06	9.4%	74%	19	1.06	9.4%	74%
	1S-T-I, n = 0.7					19	***1.23***	10.4%	100%	19	***1.23***	10.4%	100%
r_{FprEN}	**1S-I**	56	**0.83**	***15.9%***	9%	100	0.95	13.1%	29%	156	0.91	***15.5%***	22%
	1S-I-U	56	**0.83**	***15.9%***	9%	24	**0.89**	14.1%	21%	80	**0.84**	***15.6%***	13%
	1S-I-T					76	0.98	12.0%	32%	76	0.98	12.0%	32%
	1S-U-I, n = 0	14	**0.73**	10.7%	0%	6	**0.78**	8.1%	0%	20	**0.75**	10.0%	0%
	1S-U-I, n = 0.3	14	**0.78**	11.5%	0%	6	**0.82**	8.7%	0%	20	**0.79**	10.8%	0%
	1S-U-I, n = 0.5	14	**0.83**	12.0%	0%	6	**0.90**	8.6%	17%	20	**0.85**	11.4%	5%
	1S-U-I, n = 0.7	14	0.96	13.6%	36%	6	1.04	8.5%	67%	20	0.99	12.5%	45%
	1S-T-I, n = 0					19	**0.87**	5.3%	0%	19	**0.87**	5.3%	0%
	1S-T-I, n = 0.3					19	0.92	5.1%	0%	19	0.92	5.1%	0%
	1S-T-I, n = 0.5					19	0.98	4.7%	26%	19	0.98	4.7%	26%
	1S-T-I, n = 0.7					19	***1.13***	8.3%	100%	19	***1.13***	8.3%	100%

Table 3.13. Ratios for rolled columns, fillet welds, S275 (cluster FR-S275), EPPL. IS, MNA.

Method	Cases	CWC				CWS				ALL (EXCEPT BCW)			
		n	Mean	CoV	(>1)/*n*	*n*	Mean	CoV	(>1)/*n*	*tot*	Mean	CoV	(>1)/tot
$r_{IS,MNA,def}$	**1S-I**	56	0.97	4.4%	21%	100	1.02	4.9%	63%	156	1.00	5.3%	48%
	1S-I-U	56	0.97	4.4%	21%	24	1.02	4.6%	71%	80	0.98	5.0%	36%
	1S-I-T					76	1.02	5.0%	61%	76	1.02	5.0%	61%
	1S-U-I, n = 0	14	0.93	3.7%	0%	6	0.97	4.4%	33%	20	0.94	4.3%	10%
	1S-U-I, n = 0.3	14	0.96	3.1%	14%	6	1.01	3.7%	67%	20	0.98	4.0%	30%
	1S-U-I, n = 0.5	14	0.98	3.0%	21%	6	1.03	2.7%	83%	20	0.99	3.8%	40%
	1S-U-I, n = 0.7	14	1.01	4.2%	50%	6	1.06	3.1%	100%	20	1.02	4.5%	65%
	1S-T-I, n = 0					19	0.96	2.4%	5%	19	0.96	2.4%	5%
	1S-T-I, n = 0.3					19	1.00	2.4%	58%	19	1.00	2.4%	58%
	1S-T-I, n = 0.5					19	1.03	3.0%	84%	19	1.03	3.0%	84%
	1S-T-I, n = 0.7					19	1.08	3.8%	95%	19	1.08	3.8%	95%
$r_{IS,MNA,ref}$	**1S-I**	56	0.91	4.6%	4%	100	0.99	5.1%	38%	156	0.96	6.3%	26%
	1S-I-U	56	0.91	4.6%	4%	24	0.97	5.2%	25%	80	0.93	5.6%	10%
	1S-I-T					76	0.99	5.0%	42%	76	0.99	5.0%	42%
	1S-U-I, n = 0	14	**0.88**	3.9%	0%	6	0.92	4.7%	0%	20	**0.89**	4.6%	0%
	1S-U-I, n = 0.3	14	0.90	3.2%	0%	6	0.96	4.0%	17%	20	0.92	4.4%	5%
	1S-U-I, n = 0.5	14	0.91	3.3%	0%	6	0.98	3.2%	33%	20	0.93	4.8%	10%
	1S-U-I, n = 0.7	14	0.94	5.4%	14%	6	1.02	3.5%	50%	20	0.96	6.1%	25%
	1S-T-I, n = 0					19	0.94	2.7%	0%	19	0.94	2.7%	0%
	1S-T-I, n = 0.3					19	0.98	2.8%	21%	19	0.98	2.8%	21%
	1S-T-I, n = 0.5					19	1.01	3.2%	58%	19	1.01	3.2%	58%
	1S-T-I, n = 0.7					19	1.05	3.8%	89%	19	1.05	3.8%	89%
$r_{IS,MNA,rich}$	**1S-I**	56	**0.89**	4.9%	2%	100	0.98	5.2%	31%	156	0.94	6.8%	21%
	1S-I-U	56	**0.89**	4.9%	2%	24	0.95	5.4%	13%	80	0.91	6.0%	5%
	1S-I-T					76	0.98	5.0%	37%	76	0.98	5.0%	37%
	1S-U-I, n = 0	14	**0.86**	4.4%	0%	6	0.90	4.9%	0%	20	**0.88**	4.9%	0%
	1S-U-I, n = 0.3	14	**0.88**	3.7%	0%	6	0.94	4.2%	0%	20	0.90	4.8%	0%
	1S-U-I, n = 0.5	14	**0.89**	3.8%	0%	6	0.97	3.3%	0%	20	0.91	5.3%	0%
	1S-U-I, n = 0.7	14	0.92	6.0%	7%	6	1.00	3.7%	50%	20	0.94	6.8%	20%
	1S-T-I, n = 0					19	0.93	2.9%	0%	19	0.93	2.9%	0%
	1S-T-I, n = 0.3					19	0.97	2.9%	16%	19	0.97	2.9%	16%
	1S-T-I, n = 0.5					19	1.00	3.3%	53%	19	1.00	3.3%	53%
	1S-T-I, n = 0.7					19	1.03	3.9%	79%	19	1.03	3.9%	79%

Table 3.14. Ratios rolled columns, fillet welds, S275 (cluster FR-S275), EPPL. IS, GMNA.

Method	Cases	CWC				CWS				ALL (EXCEPT BCW)			
		n	Mean	CoV	(>1)/*n*	*n*	Mean	CoV	(>1)/*n*	*tot*	Mean	CoV	(>1)/tot
$r_{IS,GMNA,def}$	**1S-I**	56	0.93	3.8%	2%	100	0.95	3.3%	6%	156	0.94	3.6%	4%
	1S-I-U	56	0.93	3.8%	2%	24	0.95	3.6%	13%	80	0.94	3.8%	5%
	1S-I-T					76	0.95	3.3%	4%	76	0.95	3.3%	4%
	1S-U-I, n = 0	14	0.93	3.8%	0%	6	0.97	4.4%	33%	20	0.94	4.2%	10%
	1S-U-I, n = 0.3	14	0.94	3.0%	0%	6	0.95	4.1%	17%	20	0.94	3.4%	5%
	1S-U-I, n = 0.5	14	0.93	3.0%	0%	6	0.94	3.0%	0%	20	0.93	3.0%	0%
	1S-U-I, n = 0.7	14	0.93	5.4%	7%	6	0.94	2.6%	0%	20	0.93	4.7%	5%
	1S-T-I, n = 0					19	0.96	2.1%	5%	19	0.96	2.1%	5%
	1S-T-I, n = 0.3					19	0.94	2.3%	0%	19	0.94	2.3%	0%
	1S-T-I, n = 0.5					19	0.94	2.8%	0%	19	0.94	2.8%	0%
	1S-T-I, n = 0.7					19	0.95	4.8%	11%	19	0.95	4.8%	11%
$r_{IS,GMNA,ref}$	**1S-I**	56	**0.88**	4.2%	0%	100	0.93	3.5%	2%	156	0.91	4.4%	1%
	1S-I-U	56	**0.88**	4.2%	0%	24	0.92	3.3%	0%	80	**0.89**	4.4%	0%
	1S-I-T					76	0.93	3.6%	3%	76	0.93	3.6%	3%
	1S-U-I, n = 0	14	**0.88**	3.9%	0%	6	0.92	4.7%	0%	20	**0.89**	4.6%	0%
	1S-U-I, n = 0.3	14	**0.89**	3.3%	0%	6	0.93	3.8%	0%	20	**0.90**	3.9%	0%
	1S-U-I, n = 0.5	14	**0.88**	3.5%	0%	6	0.92	2.7%	0%	20	**0.89**	3.8%	0%
	1S-U-I, n = 0.7	14	**0.89**	5.9%	0%	6	0.92	2.4%	0%	20	**0.90**	5.3%	0%
	1S-T-I, n = 0					19	0.93	3.1%	0%	19	0.93	3.1%	0%
	1S-T-I, n = 0.3					19	0.93	2.6%	0%	19	0.93	2.6%	0%
	1S-T-I, n = 0.5					19	0.92	3.2%	0%	19	0.92	3.2%	0%
	1S-T-I, n = 0.7					19	0.93	5.0%	11%	19	0.93	5.0%	11%
$r_{IS,GMNA,rich}$	**1S-I**	56	**0.87**	4.6%	0%	100	0.92	3.7%	1%	156	**0.90**	4.8%	1%
	1S-I-U	56	**0.87**	4.6%	0%	24	0.91	3.4%	0%	80	**0.88**	4.7%	0%
	1S-I-T					76	0.92	3.8%	1%	76	0.92	3.8%	1%
	1S-U-I, n = 0	14	**0.86**	4.4%	0%	6	0.90	4.9%	0%	20	**0.87**	4.9%	0%
	1S-U-I, n = 0.3	14	**0.87**	3.8%	0%	6	0.92	3.8%	0%	20	**0.88**	4.4%	0%
	1S-U-I, n = 0.5	14	**0.86**	3.9%	0%	6	0.91	2.7%	0%	20	**0.88**	4.3%	0%
	1S-U-I, n = 0.7	14	**0.87**	6.2%	0%	6	0.91	2.5%	0%	20	**0.88**	5.6%	0%
	1S-T-I, n = 0					19	0.92	3.6%	0%	19	0.92	3.6%	0%
	1S-T-I, n = 0.3					19	0.92	2.8%	0%	19	0.92	2.8%	0%
	1S-T-I, n = 0.5					19	0.92	3.4%	0%	19	0.92	3.4%	0%
	1S-T-I, n = 0.7					19	0.92	5.1%	5%	19	0.92	5.1%	5%

3.2.7 Stiffness

3.2.7.a Boundary conditions

The results for stiffness obtained using IDEA StatiCa are fundamentally different from those obtained from Abaqus and cannot be compared directly. The reason is that, for the stiffness analysis, the software imposes restraints in the free end of all members attached to the joint (located at a short distance from the connection), except the one for which the moment-rotation curve needs to be obtained, see **Fig. 2.24** and Section 2.3.3. This is not consistent with the Abaqus model developed for this study, in which the boundary conditions are constant, as described in Chapter 1. Thus, the results in this Section are presented independently using Abaqus and IDEA StatiCa as reference models.

3.2.7.b EN and FprEN vs Abaqus

Table 3.15 shows statistics of ratios for initial stiffness, for different joint configurations, only for EN and FprEN. As discussed in Section 2.3.3 the stiffness ratios are not meaningful for IDEA StatiCa. Considering all sets, the results show that:

- The trends for both EN and FprEN are very similar. FprEN results in a small improvement with respect to EN.
- Both EN and FprEN are highly unconservative, and present mean ratios of about 1.30 (for EN) or 1.13 (for FprEN).
- A large percentage of individual cases (67% for EN, 56% for FprEN) is unconservative (ratios above 1).
- Large max ratios are obtained, 3.16 (EN) and 2.69 (FprEN).
- Both methods present a high CoV of 36.8% (EN) and 33.0% (FprEN).

Focusing on the influence of joint typology, the following trends can be observed in both EN and FprEN:

- The mean ratios for unstiffened joints with no axial load are conservative (< 1), but with a large CoV and a large proportion of unconservative individual results.
- The mean ratios for stiffened joints with no axial load are highly unconservative (> 1.5).
- For one-sided stiffened joints with no axial load, all individual results are unconservative.
- For two-sided stiffened joints with no axial load, the scatter is high (about 25%), and very unconservative results (ratios up to 2.69) are obtained.
- The increase of axial load does not affect the results.

Additionally, **Table 3.16** shows the stiffness ratios for rolled columns with fillet welds in S275 (cluster FR-S275), with the EPPL material model. Comparing with the previous **Table 3.15**, the same trends are observed.

Table 3.15. Initial stiffness ratios, rolled columns, S275 (BR-S275), EPPL. EN, FprEN.

Cases	s_{EN}							s_{FprEN}						
	tot	Mean	CoV	Max	Min	(>1)	(>1)/tot	*tot*	Mean	CoV	Max	Min	(>1)	(>1)/tot
All	800	***1.30***	***36.8%***	3.16	0.60	533	67%	800	***1.13***	***33.0%***	2.69	0.59	450	56%
No axial force														
1S-U, n = 0	40	0.95	***20.4%***	1.42	0.61	16	40%	40	**0.89**	***19.2%***	1.30	0.59	9	23%
1S-T, n = 0	40	***1.81***	***16.2%***	2.42	1.43	40	100%	40	***1.52***	***16.3%***	2.20	1.20	40	100%
2S-U, n = 0	120	0.96	***21.5%***	1.46	0.60	48	40%	120	**0.89**	***20.7%***	1.37	0.59	26	22%
2S-T, n = 0	120	***1.82***	***25.4%***	3.16	1.14	120	100%	120	***1.52***	***25.6%***	2.69	0.97	119	99%
Stiffened														
All, T-I, n = 0	80	***1.57***	***19.3%***	2.43	1.14	80	100%	80	***1.32***	***18.9%***	2.02	0.97	79	99%
All, T-R, n = 0	80	***2.06***	***19.0%***	3.16	1.42	80	100%	80	***1.72***	***19.6%***	2.69	1.20	80	100%
All, T,(I+R), n = 0	160	***1.82***	***23.4%***	3.16	1.14	160	100%	160	***1.52***	***23.6%***	2.69	0.97	159	99%
1S Interior Unstiffened														
1S-U-I, n = 0	20	**0.89**	***16.4%***	1.15	0.61	5	25%	20	**0.82**	14.3%	1.03	0.59	1	5%
1S-U-I, n = 0.3	20	**0.90**	***16.7%***	1.17	0.62	5	25%	20	**0.82**	14.6%	1.05	0.59	1	5%
1S-U-I, n = 0.5	20	0.90	***16.9%***	1.19	0.62	5	25%	20	**0.83**	14.8%	1.07	0.59	1	5%
1S-U-I, n = 0.7	20	0.91	***17.1%***	1.21	0.62	5	25%	20	**0.84**	15.0%	1.09	0.60	1	5%
1S Interior Stiffened														
1S-T-I, n = 0	20	***1.57***	6.8%	1.85	1.43	20	100%	20	***1.31***	4.9%	1.41	1.20	20	100%
1S-T-I, n = 0.3	20	***1.58***	6.9%	1.87	1.44	20	100%	20	***1.32***	4.9%	1.42	1.21	20	100%
1S-T-I, n = 0.5	20	***1.59***	6.9%	1.88	1.44	20	100%	20	***1.33***	5.0%	1.43	1.21	20	100%
1S-T-I, n = 0.7	20	***1.60***	7.0%	1.89	1.45	20	100%	20	***1.34***	5.0%	1.44	1.22	20	100%
2S Interior Unstiffened														
2S-U-I, n = 0	60	**0.88**	***16.8%***	1.20	0.60	16	27%	60	**0.81**	***15.2%***	1.10	0.59	2	3%
2S-U-I, n = 0.3	60	**0.89**	***17.0%***	1.22	0.60	16	27%	60	**0.82**	***15.5%***	1.12	0.59	4	7%
2S-U-I, n = 0.5	60	**0.90**	***17.2%***	1.23	0.60	18	30%	60	**0.82**	***15.6%***	1.13	0.59	5	8%
2S-U-I, n = 0.7	60	0.90	***17.4%***	1.24	0.61	20	33%	60	**0.83**	***15.7%***	1.15	0.59	6	10%
2S Interior Stiffened														
2S-T-I, n = 0	60	***1.58***	***22.0%***	2.43	1.14	60	100%	60	***1.32***	***21.7%***	2.02	0.97	59	98%
2S-T-I, n = 0.3	60	***1.59***	***21.8%***	2.45	1.15	60	100%	60	***1.33***	***21.6%***	2.04	0.99	59	98%
2S-T-I, n = 0.5	60	***1.60***	***21.7%***	2.46	1.15	60	100%	60	***1.34***	***21.5%***	2.05	1.00	59	98%
2S-T-I, n = 0.7	60	***1.61***	***21.6%***	2.47	1.16	60	100%	60	***1.35***	***21.4%***	2.07	1.01	60	100%
Roof														
1S-U-R, n = 0	20	1.02	***21.3%***	1.42	0.64	11	55%	20	0.95	***19.9%***	1.30	0.62	8	40%
2S-U-R, n = 0	60	1.04	***22.0%***	1.46	0.65	32	53%	60	0.96	***20.8%***	1.37	0.64	24	40%
1S-T-R, n = 0	20	***2.06***	9.7%	2.42	1.80	20	100%	20	***1.72***	10.4%	2.20	1.44	20	100%
2S-T-R, n = 0	60	***2.06***	***21.3%***	3.16	1.42	60	100%	60	***1.72***	***21.8%***	2.69	1.20	60	100%
Steel grade dependency														
S235	800	***1.30***	***36.8%***	3.16	0.60	531	66%	800	***1.13***	***33.0%***	2.69	0.59	450	56%
S275	800	***1.30***	***36.8%***	3.16	0.60	533	67%	800	***1.13***	***33.0%***	2.69	0.59	450	56%
S355	800	***1.31***	***36.7%***	3.16	0.60	536	67%	800	***1.13***	***32.9%***	2.69	0.59	453	57%

Table 3.16. Initial stiffness ratios, rolled columns, fillet welds, S275 (FR-S275), EPPL. EN, FprEN.

Cases	S_{EN}							S_{FprEN}						
	tot	Mean	CoV	Max	Min	(>1)	(>1)/tot	*tot*	Mean	CoV	Max	Min	(>1)	(>1)/tot
1S-I	160	***1.21***	***27.1%***	1.84	0.63	103	64%	160	1.05	***22.4%***	1.39	0.61	85	53%
1S-I-U	80	0.91	***15.6%***	1.21	0.63	23	29%	80	**0.83**	13.5%	1.08	0.61	5	6%
1S-I-T	80	***1.51***	7.9%	1.84	1.27	80	100%	80	***1.26***	5.8%	1.39	1.08	80	100%
1S-U-I, n = 0	20	**0.89**	***15.5%***	1.14	0.63	5	25%	20	**0.82**	13.4%	1.02	0.61	1	5%
1S-U-I, n = 0.3	20	0.91	***15.8%***	1.17	0.64	5	25%	20	**0.84**	13.6%	1.05	0.61	1	5%
1S-U-I, n = 0.5	20	0.92	***16.0%***	1.19	0.64	6	30%	20	**0.84**	13.8%	1.07	0.62	1	5%
1S-U-I, n = 0.7	20	0.92	***16.2%***	1.21	0.65	7	35%	20	**0.85**	14.0%	1.08	0.62	2	10%
1S-T-I, n = 0	20	***1.48***	8.1%	1.78	1.27	20	100%	20	***1.24***	5.8%	1.36	1.08	20	100%
1S-T-I, n = 0.3	20	***1.51***	7.9%	1.82	1.32	20	100%	20	***1.26***	5.7%	1.38	1.12	20	100%
1S-T-I, n = 0.5	20	***1.52***	7.9%	1.83	1.33	20	100%	20	***1.27***	5.7%	1.38	1.14	20	100%
1S-T-I, n = 0.7	20	***1.53***	7.9%	1.84	1.34	20	100%	20	***1.28***	5.8%	1.39	1.15	20	100%

3.2.7.c EN and FprEN vs IDEA StatiCa

Table 3.17 shows statistics of ratios for initial stiffness, for one-sided joint configurations (internal and roof), for EN and FprEN. In these ratios, IDEA StatiCa is the reference value. The results show that considering all sets:

- IDEA StatiCa tends to overestimate the initial stiffness, with mean ratios of about 1.68 (for EN) or 1.93 (for FprEN).
- The trends for both EN and FprEN are very similar, with slightly higher deviation from IDEA StatiCa results in the case of FprEN.
- Very few cases (30% for EN, 5% for FprEN) provide stiffness lower than the respective codes (ratios above 1).
- Max ratios obtained are 1.32 (EN) and 1.04 (FprEN), both obtained for stiffened internal joints.
- Minimum ratios are significant, 0.09 (EN) and 0.08 (FprEN), whereas in 6 cases, IDEA StatiCa specifies indefinite stiffness.
- Both methods present a very high CoV of 51.8% (EN) and 47.9% (FprEN).

Focusing on the influence of joint typology, the following trends can be observed in both EN and FprEN:

- For stiffened internal joints, a particularly large scatter is noticed (CoV > 100%).

For roof joints, a smaller deviation in results is obtained, with mean values of 0.822 (roof EN), and 0.722 (roof FprEN), whereas for the internal joints, these values are 0.365 (EN) and 0.316 (FprEN).

Table 3.17. Initial stiffness ratios, rolled columns, S275 (FR-S275), EPPL. EN, FprEN vs IS.

Cases	S_{EN}							S_{FprEN}						
	tot	Mean	CoV	Max	Min	(>1)	(>1)/tot	*tot*	Mean	CoV	Max	Min	(>1)	(>1)/tot
1S-I	40	0.365	*78.5%*	1.32	0.00	2	5%	40	0.316	*73.9%*	1.04	0.00	1	3%
1S-I-U	20	0.374	*52.9%*	0.76	0.00	0	0%	20	0.343	*51.7%*	0.67	0.00	0	0%
1S-I-T	20	0.357	*100.8%*	1.32	0.00	2	10%	20	0.290	*97.3%*	1.04	0.00	1	5%
1S-R	40	0.822	*25.0%*	1.19	0.43	10	25%	40	0.722	*21.8%*	1.10	0.41	1	3%
1S-R-U	20	0.765	*28.7%*	1.19	0.43	4	20%	20	0.714	*27.7%*	1.10	0.41	1	5%
1S-R-T	20	0.879	*20.3%*	1.18	0.58	6	30%	20	0.730	14.9%	0.88	0.52	0	0%

3.2.8 LBA study

This section reports the results obtained with IDEA StatiCa for an independent study, whose objective is twofold:

- i) to compare the moment resistance results obtained using two types of analyses - GMNA and MNA for the entire scope of the study (in the previous study this was done only for some sets) and three different mesh sizes, using a 'reduction' coefficient χ defined as:

$$\chi = M_{R,IS,GMNA} / M_{R,IS,MNA}, \tag{3.13}$$

- ii) to carry out the linear buckling analysis (LBA) and calculate the critical buckling coefficient α_{cr} for all cases and assess whether there is a correlation between α_{cr} and χ.

The study covers the first cluster (see **Table 2.7**), comprising 800 models, all with steel S275. For each model, LBA, MNA, and GMNA are carried out, using three meshes (default, refined, and Richardson), resulting in four output values for each joint (α_{cr} ; χ_{def} ; χ_{ref} ; χ_{Rich})

$$\chi_{def} = M_{R,IS,GMNA,def} / M_{R,IS,MNA,def}, \tag{3.14}$$

$$\chi_{ref} = M_{R,IS,GMNA,ref} / M_{R,IS,MNA,ref}, \tag{3.15}$$

$$\chi_{rich} = M_{R,IS,GMNA,rich} / M_{R,IS,MNA,rich}, \tag{3.16}$$

In **Fig. 3.1**, α_{cr} is plotted against the reduction coefficient χ for each of the three meshes, whereas a more detailed statistical assessment is summarized in **Table 3.18**, **Table 3.19**, and **Table 3.20**. In these tables, *N* represents the number of cases that fall within a specific range of α_{cr}. In addition, the buckling shapes (1st Eigenmode) for the first four sets (SET01-SET04, see **Table 2.6**) are shown in **Fig. 3.2-Fig. 3.5**, grouped based on the column profile, for three aspect ratios each. Several observations may be stated:

- No correlation between α_{cr} and χ can be found. χ is almost constant across the entire range of α_{cr}, with a very low and stable CoV.
- Although the sample size with $\alpha_{cr} < 3$ is small (1% of all cases), against the expectations, the reduction factor χ is very high, with a mean value of around 0.97 across all three meshes.
- The minimum $\chi = 0.833$ is obtained for a double-sided stiffened joint from Set 05_MR050, with the axial force of $n = 70\%$, with the buckling factor of around $\alpha_{cr} = 9$.
- Between the three meshes, χ varies only marginally, i.e.: χ_{def} = [0.828-1.020]; χ_{ref} = [0.833-1.017] and χ_{rich} = [0.834-1.018], and almost uniform CoV = [4.3% – 5.2%].

- Although no clear trends in buckling patterns can be established, 1st Eigenmode is often associated with the beam buckling and/or parts of the column outside the studied web panel.
- Approximately, 33% and 70% of the cases attain such *non-web* buckling shape, for the unstiffened (SET01 and SET02) and stiffened joints (SET03 and SET04), respectively.

Finally, in **Table 3.21**, the computational times are compared between the two types of analysis (GMNA and MNA) for different joint configuration groups and two mesh densities (default and refined), whereas a similar comparison is made in **Table 3.22**, however, emphasizing the importance of the mesh size on the computational time.

These comparisons indicate that the computational time is affected mainly by the mesh size, rather than the choice of the analysis type. Therefore, given that the MNA analysis may lead to rather unsafe results (with a maximum of 17% resistance overestimation), GMNA analysis should always be employed, regardless of the critical buckling factor, whereas compromises could be made on the mesh density, for the sake of the computational time savings.

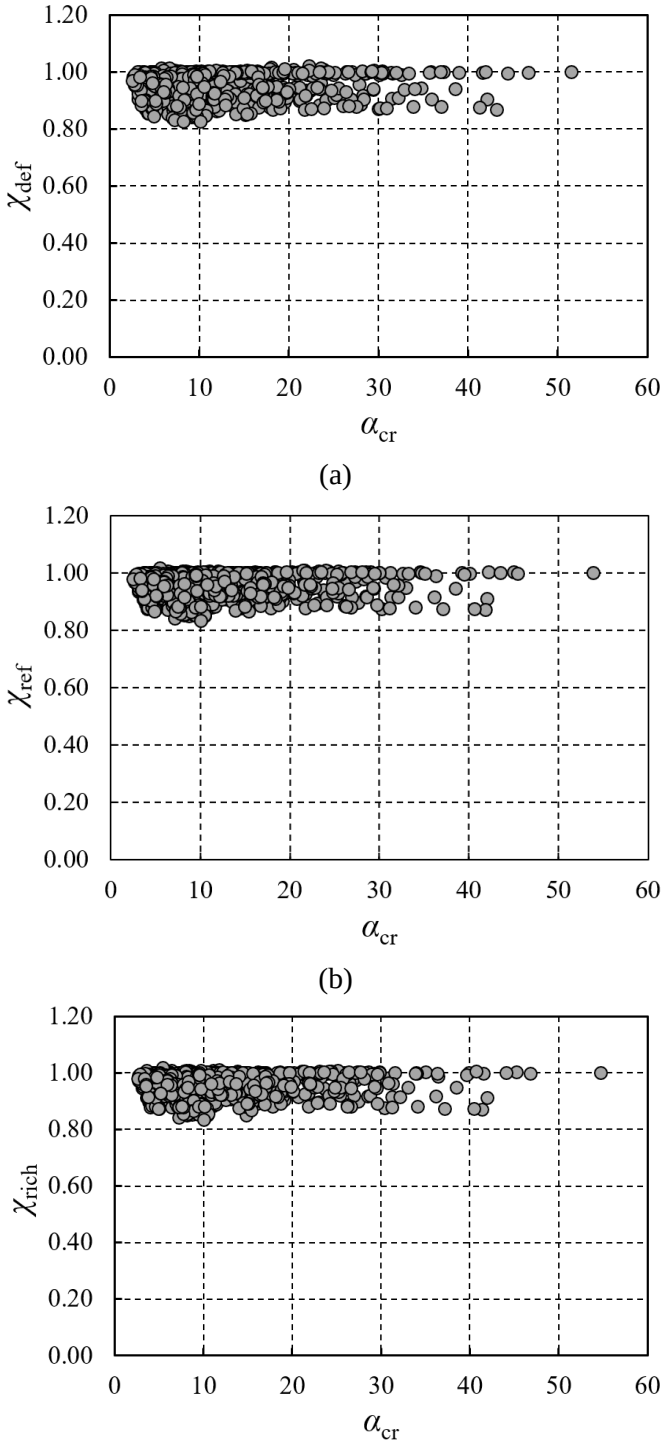

Fig. 3.1 – LBA analysis. α_{cr} vs χ.
(a) default mesh; (b) refined mesh; (c) Richardson extrapolation.

Table 3.18. Statistics of χ_{def} for different ranges of α_{cr}.

χ_{def}	$\alpha_{cr} \leq 3$	$\alpha_{cr} \leq 4$	$\alpha_{cr} \leq 5$	$\alpha_{cr} \leq 10$	$\alpha_{cr} \leq 60$
N	8	57	118	394	800
***N* (%)**	1.0	7.1	14.8	49.3	100.0
Mean	0.968	0.952	0.944	0.944	0.949
CoV	1.5%	3.8%	4.7%	5.3%	5.2%
Max	0.990	1.000	1.000	1.014	1.020
Min	0.949	0.884	0.845	0.828	0.828

Table 3.19. Statistics of χ_{ref} for different ranges of α_{cr}.

χ_{ref}	$\alpha_{cr} \leq 3$	$\alpha_{cr} \leq 4$	$\alpha_{cr} \leq 5$	$\alpha_{cr} \leq 10$	$\alpha_{cr} \leq 60$
N	9	61	120	398	800
***N* (%)**	1.1	7.6	15.0	49.8	100.0
Mean	0.977	0.962	0.957	0.953	0.956
CoV	1.1%	3.2%	3.9%	4.6%	4.5%
Max	0.994	1.000	1.000	1.017	1.017
Min	0.964	0.889	0.866	0.841	0.833

Table 3.20. Statistics of χ_{rich} for different ranges of α_{cr}.

χ_{rich}	$\alpha_{cr} \leq 3$	$\alpha_{cr} \leq 4$	$\alpha_{cr} \leq 5$	$\alpha_{cr} \leq 10$	$\alpha_{cr} \leq 60$
N	9	61	124	400	800
***N* (%)**	1.1	7.6	15.5	50.0	100.0
Mean	0.981	0.967	0.961	0.957	0.958
CoV	0.9%	2.9%	3.7%	4.4%	4.3%
Max	0.995	1.009	1.009	1.018	1.018
Min	0.970	0.897	0.873	0.842	0.834

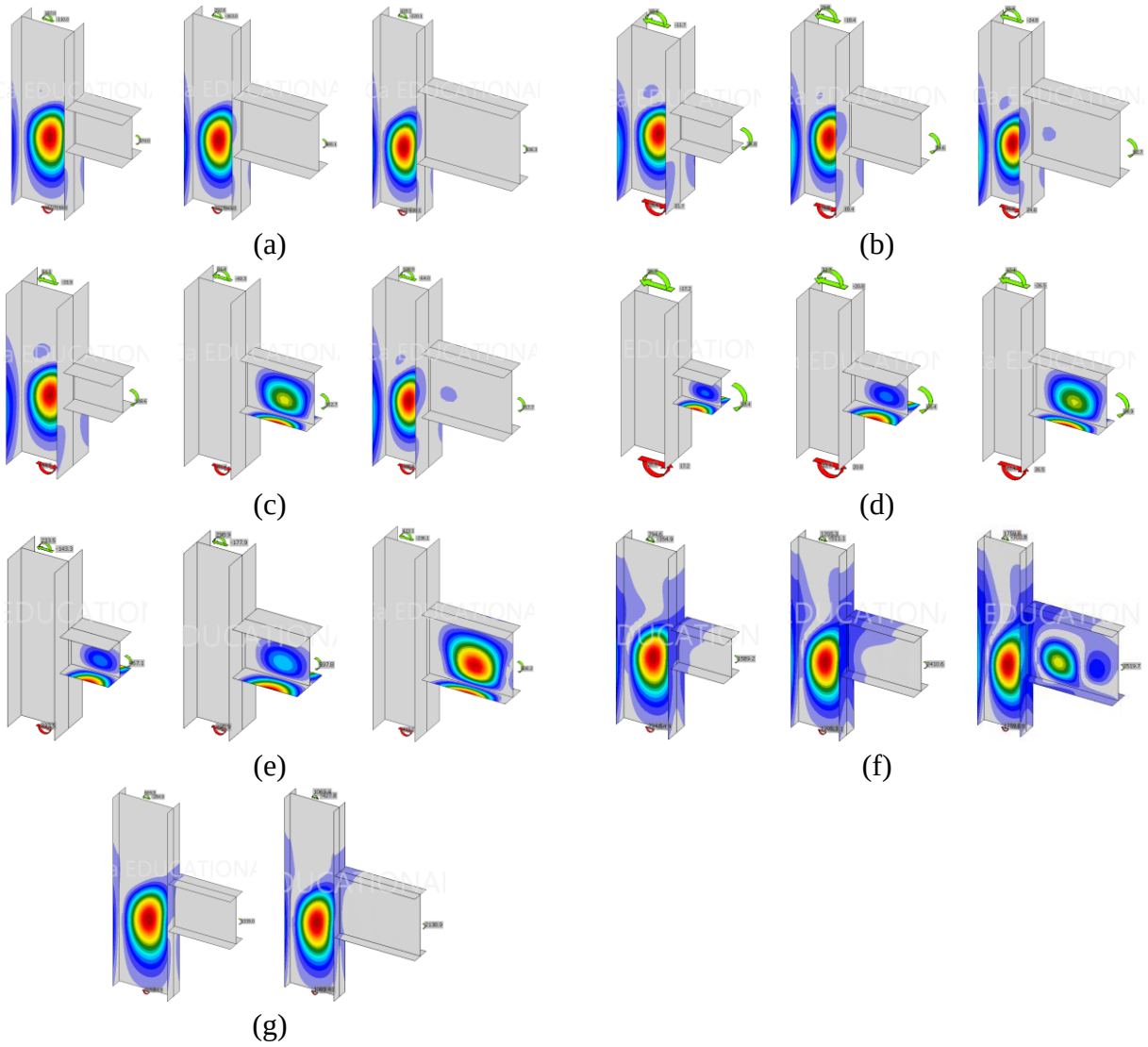

Fig. 3.2 – SET01 - buckling shapes.
(a) HEA500; (b) UC203x203x46; (c) HEB280; (d) HEM140; (e) UC305x305x240; (f) HE600x399; (g) HEB800.

ACIV - Associação para o Desenvolvimento da Engenharia Civil - **UNIVERSIDADE DE COIMBRA** – NIF 505448173
Departament of Civil Engineering - FCTUC * Rua Luís Reis Santos | Pólo II da Univ. Coimbra | 3030-788 COIMBRA
ISISE UC – Institute for Sustainability and Innovation in Structural Engineering

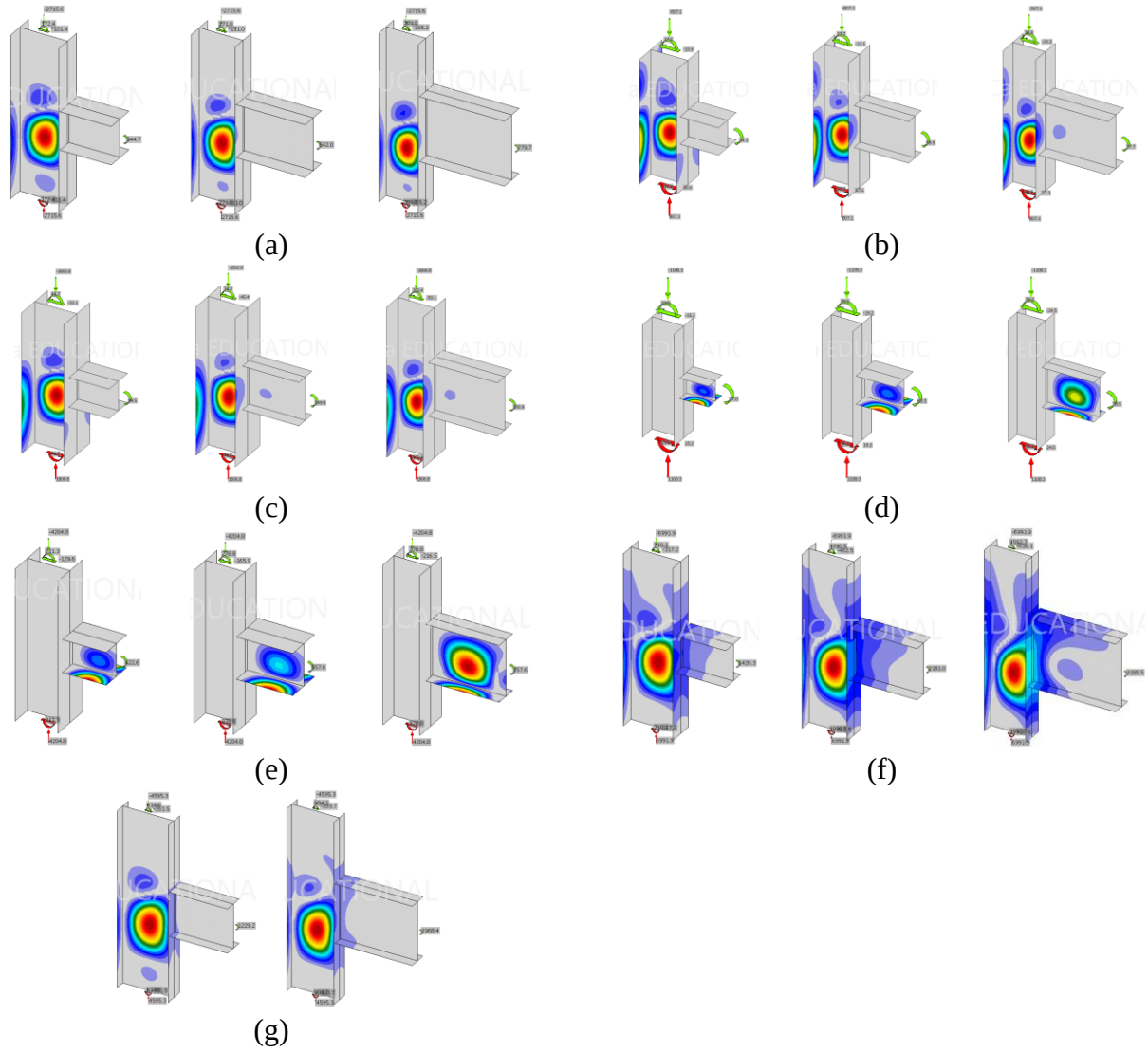

Fig. 3.3 – SET02 (n = 50%) - buckling shapes.
(a) HEA500; (b) UC203x203x46; (c) HEB280; (d) HEM140; (e) UC305x305x240; (f) HE600x399; (g) HEB800.

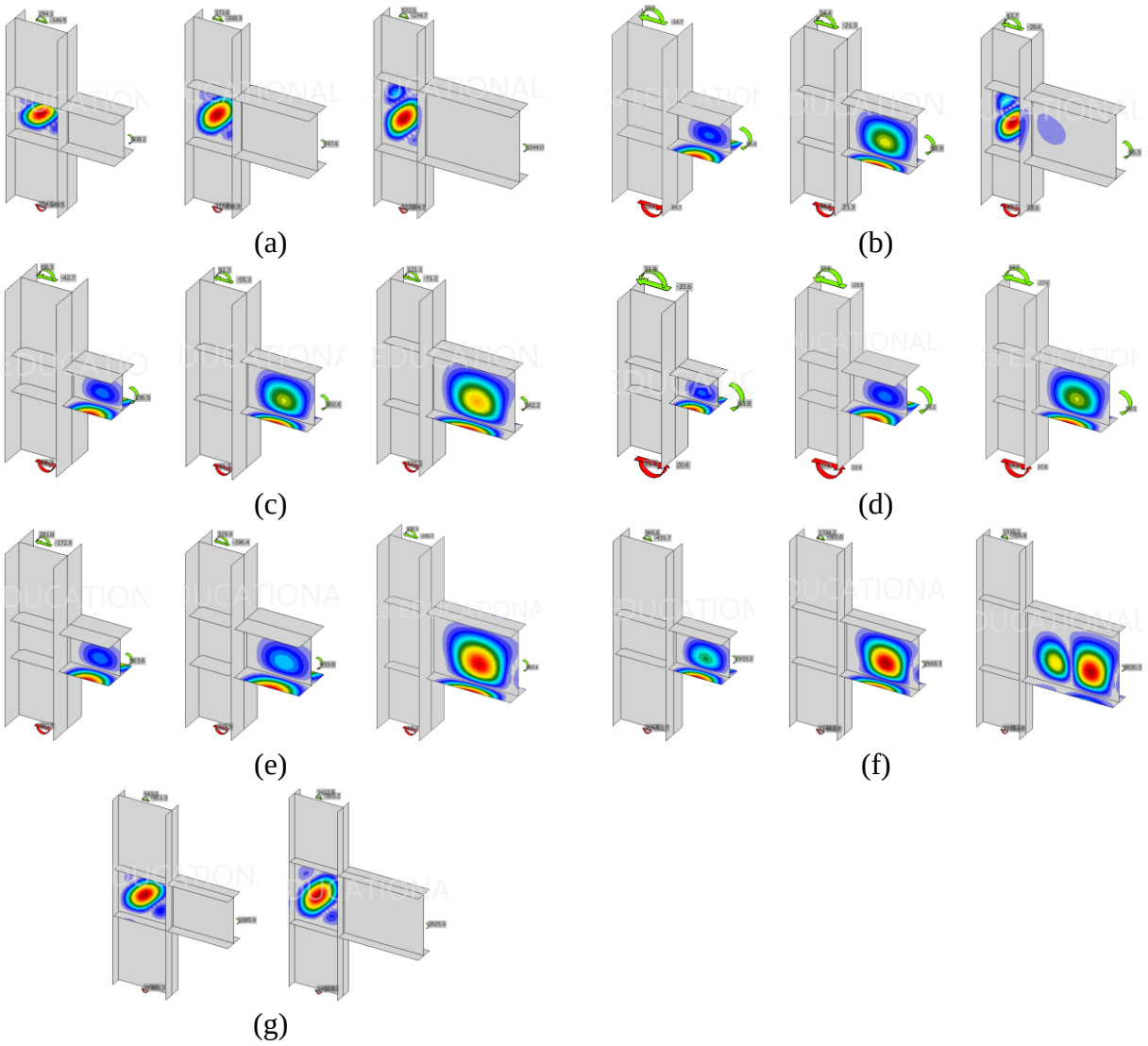

Fig. 3.4 – SET03 - buckling shapes.
(a) HEA500; (b) UC203x203x46; (c) HEB280; (d) HEM140; (e) UC305x305x240; (f) HE600x399; (g) HEB800.

ACIV - Associação para o Desenvolvimento da Engenharia Civil - **UNIVERSIDADE DE COIMBRA** – NIF 505448173
Departament of Civil Engineering - FCTUC * Rua Luís Reis Santos | Pólo II da Univ. Coimbra | 3030-788 COIMBRA
ISISE UC – Institute for Sustainability and Innovation in Structural Engineering

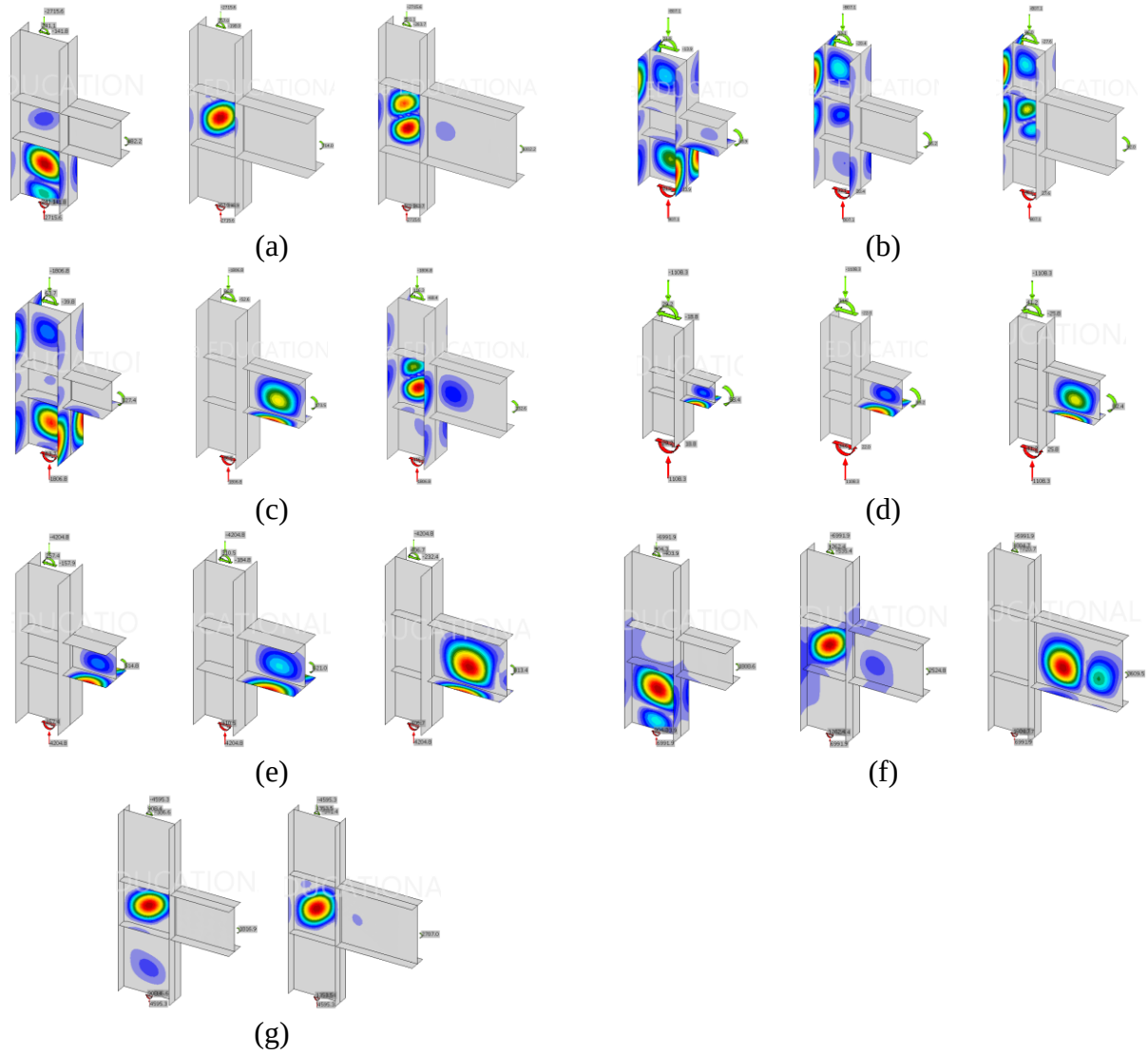

Fig. 3.5 – SET04 (n = 50%) - buckling shapes.
(a) HEA500; (b) UC203x203x46; (c) HEB280; (d) HEM140; (e) UC305x305x240; (f) HE600x399; (g) HEB800.

Table 3.21. Time ratios (GMNA/MNA).

Joint group	DEFAULT MESH		REFINED MESH		Average
	Unstiffened	Stiffened	Unstiffened	Stiffened	
One-sided internal	2.95	1.32	1.27	1.29	1.71
Two-sided internal	2.82	1.78	1.91	2.30	2.20
One-sided roof	1.20	1.00	2.09	1.50	1.45
Two-sided roof	4.13	4.37	3.57	3.51	3.90

Table 3.22. Time ratios (Refined/Default).

Joint group	MNA		GMNA		Average
	Unstiffened	Stiffened	Unstiffened	Stiffened	
One-sided internal	5.94	3.83	2.36	3.76	3.85
Two-sided internal	3.60	1.89	2.44	2.44	2.59
One-sided roof	2.20	3.33	3.83	5.00	3.59
Two-sided roof	2.47	3.06	2.13	2.46	2.53

3.3 RESULTS FOR WELDED COLUMNS (CLUSTERS BB AND BF)

3.3.1 Influence of joint configuration

The failure modes for welded columns in S275 steel (cluster BB-S275) are shown in **Table 3.23**. These results can be compared to those of rolled columns (**Table 3.5**).
Trends similar to those of rolled columns:

- CWS and BCW are the only failure modes for stiffened cases.
- CWT only happens on unstiffened roof joints.
- CWC is dominant on one-sided unstiffened joints. CWS and BCW only happen in cases 10 to 15 that correspond to stocky columns.
- CWC and BCW are the only failure modes on two-sided unstiffened joints with $m_r = 0.5$.

Trends that differ from those of rolled columns:

- Two-sided unstiffened joints with negative m_r present a mixture of CWC, CWS, and BCW, but CWC is predominant (whereas in rolled columns, CWS was predominant).
- Overall, a smaller proportion of cases fail by BCW compared to rolled columns.

3.3.1.a Unstiffened welded columns with no axial load

Statistics of the ratios for unstiffened columns without axial load (1S-U-n0, 2S-U-n0) are shown in **Table 3.24**. The following conclusions are derived:
For EN and FprEN:

- Both methods result in highly conservative results, with mean ratios well below 0.9 for all configurations. No unconservative individual results are obtained.
- The CoV with both EN and FprEN is generally moderate to high.
- With EN, for two-sided joints, the CoV is always high (> 16%) and, for one-sided joints, it is moderate to high.
- FprEN improves the scatter for cases with CWS failure mode, to about 5.5% for one-sided and 8.7% for two-sided. However, the scatter for CWC failure mode is slightly larger than with EN.

For IDEA StatiCa:

- With the default program options (default mesh, MNA) mean results are highly unconservative for CWC and CWS failure modes, and moderately unconservative for CWT. For CWC and CWS, all individual results are unconservative. For CWT, about 60% of individual results are

unconservative. For CWS, the results for one-sided unstiffened joints are more unconservative than for two-sided unstiffened joints.

- Refining the mesh with MNA results in moderately unconservative mean results for CWC and CWS, but still a large proportion of individual results (up to 81% for CWC, up to 95% for CWS) are unconservative.
- Refining the mesh with MNA results in moderately conservative results (< 1) for CWT, with a small proportion of unconservative individual cases (up to 20%).
- There is virtually no difference between the results obtained with GMNA and MNA.
- The CoV with both MNA and GMNA and the default mesh is low, except for 2S joints that fail by CWT, where it is moderate, about 9.1%. Refining the mesh results in moderate CoV below 7.5%.

3.3.1.b Stiffened welded columns with no axial load

For stiffened welded columns without axial load, results are provided in **Table 3.25**. The only failure mode for stiffened columns is CWS. The results show that:
For EN and FprEN:

- Both methods result in highly conservative results, with mean ratios well below 0.9 for all configurations.
- No unconservative individual results are obtained, except a small proportion for 2S-R joints with FprEN.
- The CoV is low to medium. FprEN improves slightly the scatter.

For IDEA StatiCa:

- With the default options (MNA, default mesh), mean ratios are slightly unconservative for internal joints (I) and slightly conservative for roof joints (R). A large proportion of individual cases is unconservative for internal joints. For roof joints, a moderate proportion of individual cases is unconservative. The CoV is low to moderate.
- Improvement of the mesh with MNA results only in marginal improvements of results. A large proportion of individual cases is unconservative even with the Richardson extrapolation.
- There are no significant differences between MNA and GMNA.
- The CoV is similar regardless of method and mesh.

3.3.2 Influence of axial load

For stiffened welded columns without axial load, results are provided in **Table 3.26** (EN and FprEN), **Table 3.27** (IDEA StatiCa, MNA), and **Table 3.28** (IDEA STATICA, GMNA). The results show that:
For EN and FprEN:

- Both methods result in highly conservative results, with mean ratios below 0.9 for all configurations, except for one-sided joints with high axial load $n = 0.7$ and, for FprEN only, for two-sided joints with high axial load. FprEN leads to more unconservative results than EN.
- With EN, no unconservative individual results are obtained, except for high axial load.
- With FprEN, for high axial load, a large proportion (> 80%) of unconservative individual results is obtained for stiffened columns, and a moderate proportion (< 9%) for two-sided unstiffened.

- The CoV with EN is typically moderate, except for two-sided unstiffened, where it is high.
- The CoV with FprEN is low, except for unstiffened joints, where it is moderate for one-sided joints with CWC or CWS, and high for two-sided joints with CWC or CWS failure mode.
- FprEN reduces the scatter for CWT and CWS but increases slightly the scatter for CWC.

For IDEA StatiCa:

- With the default options (MNA, default mesh), mean ratios are highly unconservative. 100% of individual results are unconservative. The CoV is low. Increasing axial load results in increasing mean ratios.
- Improvement of the mesh with MNA lowers slightly the mean results, but the proportion of unconservative individual cases is almost constant. For high values of axial load, highly unconservative mean results are obtained.
- GMNA with the default mesh reduces the mean ratios for cases with axial load. However, most of the individual results are unconservative.
- GMNA with an improvement of the mesh results in moderate to low unconservativeness. Similar mean ratios are obtained for increasing values of axial load. However, the proportion of unconservative individual cases is very high (> 59% and above).
- The CoV is low and remains constant regardless of mesh, method, and level of axial load.
- It can be concluded that GMNA with a refined mesh is the best option for joints with axial load, but still IDEA Statica will typically produce a large proportion of slightly unconservative results.

Table 3.23. Welded columns, S275 (cluster BB-S275), EPPL material model. Failure modes

S275						Case																		
	1S/2S	I/R	U/T	*n*	*mr*	1	2	3	4	5	6	7	8	9	10	11	12	13	14	15	16	17	18	19	20
set_01	1S	I	U	0	0	CWC	CWC	CWC	CWC	CWC	CWC	CWC	CWC	CWC	CWS	CWS	CWS	CWS	CWC	CWC	CWC	CWC	CWC	CWC	CWC
set_02_N30	1S	I	U	0.3	0	CWC	CWC	CWC	CWC	CWC	CWC	CWC	CWC	CWC	CWS	CWS	CWS	CWS	CWC	CWC	CWC	CWC	CWC	CWC	CWC
set_02_N50	1S	I	U	0.5	0	CWC	CWC	CWC	CWC	CWC	CWC	CWC	CWC	CWC	CWS	CWS	CWS	CWS	CWC	CWC	CWC	CWC	CWC	CWC	CWC
set_02_N70	1S	I	U	0.7	0	CWC	CWC	CWC	CWC	CWC	CWC	CWC	CWC	CWC	CWS	CWS	CWS	CWS	CWC	CWC	CWC	CWC	CWC	CWC	CWC
set_03	1S	I	T	0	0	CWS	CWS	CWS	CWS	CWS	CWS	CWS	CWS	CWS	BCW	CWS	CWS	CWS	CWS	BCW	CWS	CWS	CWS	CWS	CWS
set_04_N30	1S	I	T	0.3	0	CWS	CWS	CWS	CWS	CWS	CWS	CWS	CWS	CWS	BCW	CWS	CWS	CWS	CWS	BCW	CWS	CWS	CWS	CWS	CWS
set_04_N50	1S	I	T	0.5	0	CWS	CWS	CWS	CWS	CWS	CWS	CWS	CWS	CWS	BCW	CWS	CWS	CWS	CWS	BCW	CWS	CWS	CWS	CWS	CWS
set_04_N70	1S	I	T	0.7	0	CWS	CWS	CWS	CWS	CWS	CWS	CWS	CWS	CWS	BCW	CWS	CWS	CWS	CWS	BCW	CWS	CWS	CWS	CWS	CWS
set_05_MR050	2S	I	U	0	0.5	CWC	CWC	CWC	CWC	CWC	CWC	CWC	CWC	CWC	BCW	CWC	BCW	CWC	CWC	BCW	CWC	CWC	CWC	CWC	CWC
set_05_MR-050	2S	I	U	0	-0.5	CWC	CWC	CWC	CWC	CWC	CWC	CWC	CWC	CWC	CWS	CWS	CWS	CWS	CWS	CWS	CWS	CWS	CWS	CWC	CWC
set_05_MR-100	2S	I	U	0	-1	CWC	CWC	CWC	CWS	CWC	CWC	CWS	CWS	CWS	CWS	CWS	CWS	CWS	CWS	CWS	CWS	CWS	CWS	CWC	CWC
set_06_N30_MR050	2S	I	U	0.3	0.5	CWC	CWC	CWC	CWC	CWC	CWC	CWC	CWC	CWC	BCW	CWC	BCW	CWC	CWC	BCW	CWC	CWC	CWC	CWC	CWC
set_06_N30_MR-050	2S	I	U	0.3	-0.5	CWC	CWC	CWC	CWC	CWC	CWC	CWC	CWC	CWC	CWS	CWS	CWS	CWS	CWS	CWS	CWS	CWS	CWS	CWC	CWC
set_06_N30_MR-100	2S	I	U	0.3	-1	CWC	CWC	CWC	CWS	CWC	CWC	CWS	CWS	CWS	CWS	CWS	CWS	CWS	CWS	CWS	CWS	CWS	CWS	CWC	CWC
set_06_MR050	2S	I	U	0.5	0.5	CWC	CWC	CWC	CWC	CWC	CWC	CWC	CWC	CWC	BCW	CWC	BCW	CWC	CWC	BCW	CWC	CWC	CWC	CWC	CWC
set_06_MR-050	2S	I	U	0.5	-0.5	CWC	CWC	CWC	CWC	CWC	CWC	CWC	CWC	CWC	CWS	CWS	CWS	CWS	CWS	CWS	CWS	CWS	CWS	CWC	CWC
set_06_MR-100	2S	I	U	0.5	-1	CWC	CWC	CWC	CWS	CWC	CWC	CWS	CWS	CWS	CWS	CWS	CWS	CWS	CWS	CWS	CWS	CWS	CWS	CWC	CWC
set_06_N70_MR050	2S	I	U	0.7	0.5	CWC	CWC	CWC	CWC	CWC	CWC	CWC	CWC	CWC	BCW	CWC	BCW	CWC	CWC	BCW	CWC	CWC	CWC	CWC	CWC
set_06_N70_MR-050	2S	I	U	0.7	-0.5	CWC	CWC	CWC	CWC	CWC	CWC	CWC	CWC	CWC	CWS	CWS	CWS	CWS	CWS	CWS	CWS	CWS	CWS	CWC	CWC
set_06_N70_MR-100	2S	I	U	0.7	-1	CWC	CWC	CWC	CWS	CWC	CWC	CWS	CWS	CWS	CWS	CWS	CWS	CWS	CWS	CWS	CWS	CWS	CWS	CWC	CWC
set_07_MR050	2S	I	T	0	0.5	CWS	CWS	CWS	BCW	BCW	CWS	BCW	BCW	BCW	BCW	BCW	BCW	BCW	BCW	BCW	BCW	BCW	BCW	BCW	BCW
set_07_MR-050	2S	I	T	0	-0.5	CWS	CWS	CWS	CWS	CWS	CWS	CWS	CWS	CWS	CWS	CWS	CWS	CWS	CWS	CWS	CWS	CWS	CWS	CWS	CWS
set_07_MR-100	2S	I	T	0	-1	CWS	CWS	CWS	CWS	CWS	CWS	CWS	CWS	CWS	CWS	CWS	CWS	CWS	CWS	CWS	CWS	CWS	CWS	CWS	CWS
set_08_N30_MR050	2S	I	T	0.3	0.5	CWS	CWS	CWS	BCW	BCW	CWS	BCW	BCW	BCW	BCW	BCW	BCW	BCW	BCW	BCW	BCW	BCW	BCW	BCW	BCW
set_08_N30_MR-050	2S	I	T	0.3	-0.5	CWS	CWS	CWS	CWS	CWS	CWS	CWS	CWS	CWS	CWS	CWS	CWS	CWS	CWS	CWS	CWS	CWS	CWS	CWS	CWS
set_08_N30_MR-100	2S	I	T	0.3	-1	CWS	CWS	CWS	CWS	CWS	CWS	CWS	CWS	CWS	CWS	CWS	CWS	CWS	CWS	CWS	CWS	CWS	CWS	CWS	CWS
set_08_MR050	2S	I	T	0.5	0.5	CWS	CWS	CWS	BCW	BCW	CWS	BCW	BCW	BCW	BCW	BCW	BCW	BCW	BCW	BCW	BCW	BCW	BCW	BCW	BCW
set_08_MR-050	2S	I	T	0.5	-0.5	CWS	CWS	CWS	CWS	CWS	CWS	CWS	CWS	CWS	CWS	CWS	CWS	CWS	CWS	CWS	CWS	CWS	CWS	CWS	CWS
set_08_MR-100	2S	I	T	0.5	-1	CWS	CWS	CWS	CWS	CWS	CWS	CWS	CWS	CWS	CWS	CWS	CWS	CWS	CWS	CWS	CWS	CWS	CWS	CWS	CWS
set_08_N70_MR050	2S	I	T	0.7	0.5	CWS	CWS	CWS	BCW	BCW	CWS	BCW	BCW	BCW	BCW	BCW	BCW	BCW	BCW	BCW	BCW	BCW	BCW	BCW	BCW
set_08_N70_MR-050	2S	I	T	0.7	-0.5	CWS	CWS	CWS	CWS	CWS	CWS	CWS	CWS	CWS	CWS	CWS	CWS	CWS	CWS	CWS	CWS	CWS	CWS	CWS	CWS
set_08_N70_MR-100	2S	I	T	0.7	-1	CWS	CWS	CWS	CWS	CWS	CWS	CWS	CWS	CWS	CWS	CWS	CWS	CWS	CWS	CWS	CWS	CWS	CWS	CWS	CWS
set_09	1S	R	U	0	0	CWT	CWT	CWT	CWT	CWT	CWT	CWT	CWT	CWT	CWT	CWT	CWT	CWT	CWT	CWT	CWT	CWT	CWT	CWT	CWT
set_11	1S	R	T	0	0	CWS	CWS	CWS	CWS	CWS	CWS	CWS	CWS	CWS	BCW	CWS	CWS	CWS	CWS	CWS	CWS	CWS	CWS	CWS	CWS
set_13_MR050	2S	R	U	0	0.5	CWT	CWT	CWT	CWT	CWT	CWT	CWT	CWT	CWT	CWT	CWT	CWT	CWT	CWT	CWT	CWT	CWT	CWT	CWT	CWT
set_13_MR-050	2S	R	U	0	-0.5	CWT	CWT	CWT	CWT	CWT	CWT	CWT	CWT	CWT	CWT	CWT	CWT	CWT	CWT	CWT	CWT	CWT	CWT	CWT	CWT
set_13_MR-100	2S	R	U	0	-1	CWT	CWT	CWT	CWT	CWT	CWT	CWT	CWT	CWT	CWT	CWT	CWT	CWT	CWT	CWT	CWT	CWT	CWT	CWT	CWT
set_15_MR050	2S	R	T	0	0.5	CWS	CWS	CWS	BCW	BCW	CWS	BCW	BCW	CWS	BCW	BCW	BCW	BCW	BCW	BCW	BCW	BCW	BCW	BCW	CWS
set_15_MR-050	2S	R	T	0	-0.5	CWS	CWS	CWS	CWS	CWS	CWS	CWS	CWS	CWS	CWS	CWS	CWS	CWS	CWS	CWS	CWS	CWS	CWS	CWS	CWS
set_15_MR-100	2S	R	T	0	-1	CWS	CWS	CWS	CWS	CWS	CWS	CWS	CWS	CWS	CWS	CWS	CWS	CWS	CWS	CWS	CWS	CWS	CWS	CWS	CWS

Table 3.24. Ratios, unstiffened welded columns, no axial load, S275 (BB-S275), EPPL.

Method	Cases	CWC				CWT				CWS				ALL (EXCEPT BCW)			
		n	Mean	CoV	(>1)/*n*	*n*	Mean	CoV	(>1)/*n*	*n*	Mean	CoV	(>1)/*n*	*tot*	Mean	CoV	(>1)/tot
r_{EN}	**1S-U, n = 0**	16	0.54	12.5%	0%	20	0.48	*19.8%*	0%	4	0.53	11.3%	0%	40	0.51	*16.8%*	0%
	2S-U, n = 0	36	0.58	*16.5%*	0%	60	0.51	*23.5%*	0%	21	0.55	*18.3%*	0%	117	0.54	*21.0%*	0%
	1S-U-I, n = 0	16	0.54	12.5%	0%					4	0.53	11.3%	0%	20	0.53	12.0%	0%
	2S-U-I, n = 0	36	0.58	*16.5%*	0%					21	0.55	*18.3%*	0%	57	0.57	*17.2%*	0%
	1S-U-R, n = 0					20	0.48	*19.8%*	0%					20	0.48	*19.8%*	0%
	2S-U-R, n = 0					60	0.51	*23.5%*	0%					60	0.51	*23.5%*	0%
r_{FprEN}	**1S-U, n = 0**	16	0.53	13.0%	0%	20	0.48	*19.8%*	0%	4	0.62	5.5%	0%	40	0.51	*17.7%*	0%
	2S-U, n = 0	36	0.58	*17.1%*	0%	60	0.51	*23.5%*	0%	21	0.67	8.7%	0%	117	0.56	*21.5%*	0%
	1S-U-I, n = 0	16	0.53	13.0%	0%					4	0.62	5.5%	0%	20	0.55	13.1%	0%
	2S-U-I, n = 0	36	0.58	*17.1%*	0%					21	0.67	8.7%	0%	57	0.61	*15.9%*	0%
	1S-U-R, n = 0					20	0.48	*19.8%*	0%					20	0.48	*19.8%*	0%
	2S-U-R, n = 0					60	0.51	*23.5%*	0%					60	0.51	*23.5%*	0%
$r_{IS,MNA,def}$	**1S-U, n = 0**	16	*1.11*	3.3%	100%	20	1.04	6.2%	70%	4	*1.16*	6.8%	100%	40	1.08	6.3%	85%
	2S-U, n = 0	36	*1.11*	3.8%	100%	60	1.03	9.1%	60%	21	1.06	1.7%	100%	117	1.06	7.5%	79%
	1S-U-I, n = 0	16	*1.11*	3.3%	100%					4	*1.16*	6.8%	100%	20	*1.12*	4.5%	100%
	2S-U-I, n = 0	36	*1.11*	3.8%	100%					21	1.06	1.7%	100%	57	1.09	4.0%	100%
	1S-U-R, n = 0					20	1.04	6.2%	70%					20	1.04	6.2%	70%
	2S-U-R, n = 0					60	1.03	9.1%	60%					60	1.03	9.1%	60%
$r_{IS,MNA,ref}$	**1S-U, n = 0**	16	1.04	1.9%	100%	20	0.96	4.6%	20%	4	*1.11*	6.3%	100%	40	1.00	6.3%	60%
	2S-U, n = 0	36	1.05	2.1%	100%	60	0.96	6.8%	27%	21	1.03	1.6%	100%	117	1.00	6.4%	62%
	1S-U-I, n = 0	16	1.04	1.9%	100%					4	*1.11*	6.3%	100%	20	1.05	4.2%	100%
	2S-U-I, n = 0	36	1.05	2.1%	100%					21	1.03	1.6%	100%	57	1.04	2.1%	100%
	1S-U-R, n = 0					20	0.96	4.6%	20%					20	0.96	4.6%	20%
	2S-U-R, n = 0					60	0.96	6.8%	27%					60	0.96	6.8%	27%
$r_{IS,MNA,rich}$	**1S-U, n = 0**	16	1.01	1.6%	81%	20	0.93	4.6%	0%	4	1.09	6.3%	100%	40	0.98	6.7%	43%
	2S-U, n = 0	36	1.03	2.0%	94%	60	0.93	6.2%	20%	21	1.02	1.6%	95%	117	0.98	6.4%	56%
	1S-U-I, n = 0	16	1.01	1.6%	81%					4	1.09	6.3%	100%	20	1.03	4.2%	85%
	2S-U-I, n = 0	36	1.03	2.0%	94%					21	1.02	1.6%	95%	57	1.02	1.9%	95%
	1S-U-R, n = 0					20	0.93	4.6%	0%					20	0.93	4.6%	0%
	2S-U-R, n = 0					60	0.93	6.2%	20%					60	0.93	6.2%	20%
$r_{IS,GMNA,def}$	**1S-U, n = 0**	16	*1.11*	3.4%	100%	20	1.04	6.2%	70%	4	*1.15*	6.9%	100%	40	1.08	6.3%	85%
	2S-U, n = 0	36	*1.11*	3.9%	100%	60	1.03	9.0%	60%	21	1.06	1.7%	100%	117	1.06	7.5%	79%
	1S-U-I, n = 0	16	*1.11*	3.4%	100%					4	*1.15*	6.9%	100%	20	*1.11*	4.4%	100%
	2S-U-I, n = 0	36	*1.11*	3.9%	100%					21	1.06	1.7%	100%	57	1.09	4.0%	100%
	1S-U-R, n = 0					20	1.04	6.2%	70%					20	1.04	6.2%	70%
	2S-U-R, n = 0					60	1.03	9.0%	60%					60	1.03	9.0%	60%
$r_{IS,GMNA,ref}$	**1S-U, n = 0**	16	1.04	2.0%	94%	20	0.96	4.5%	15%	4	1.10	5.9%	100%	40	1.00	6.2%	55%
	2S-U, n = 0	36	1.04	2.3%	100%	60	0.96	6.7%	27%	21	1.03	1.7%	100%	117	1.00	6.3%	62%
	1S-U-I, n = 0	16	1.04	2.0%	94%					4	1.10	5.9%	100%	20	1.05	3.9%	95%
	2S-U-I, n = 0	36	1.04	2.3%	100%					21	1.03	1.7%	100%	57	1.04	2.2%	100%
	1S-U-R, n = 0					20	0.96	4.5%	15%					20	0.96	4.5%	15%
	2S-U-R, n = 0					60	0.96	6.7%	27%					60	0.96	6.7%	27%
$r_{IS,GMNA,rich}$	**1S-U, n = 0**	16	1.01	1.6%	81%	20	0.93	4.5%	0%	4	1.08	5.7%	100%	40	0.98	6.6%	43%
	2S-U, n = 0	36	1.02	2.0%	86%	60	0.93	6.1%	17%	21	1.02	1.7%	81%	117	0.97	6.3%	50%
	1S-U-I, n = 0	16	1.01	1.6%	81%					4	1.08	5.7%	100%	20	1.03	3.9%	85%
	2S-U-I, n = 0	36	1.02	2.0%	86%					21	1.02	1.7%	81%	57	1.02	1.9%	84%
	1S-U-R, n = 0					20	0.93	4.5%	0%					20	0.93	4.5%	0%
	2S-U-R, n = 0					60	0.93	6.1%	17%					60	0.93	6.1%	17%

Table 3.25. Ratios, stiffened welded columns, no axial load, S275 (cluster BB-S275), EPPL.

Method	Cases	CWS			
		n	Mean	CoV	(>1)/*n*
r_{EN}	**1S-T, n = 0**	37	**0.76**	6.2%	0%
	2S-T, n = 0	90	**0.71**	9.9%	0%
	1S-T-I, n = 0	18	**0.76**	7.7%	0%
	2S-T-I, n = 0	44	**0.71**	9.8%	0%
	1S-T-R, n = 0	19	**0.76**	4.6%	0%
	2S-T-R, n = 0	46	**0.71**	10.1%	0%
r_{FprEN}	**1S-T, n = 0**	37	**0.82**	6.4%	0%
	2S-T, n = 0	90	**0.81**	8.7%	2%
	1S-T-I, n = 0	18	**0.82**	6.0%	0%
	2S-T-I, n = 0	44	**0.81**	5.6%	0%
	1S-T-R, n = 0	19	**0.83**	6.9%	0%
	2S-T-R, n = 0	46	**0.82**	10.9%	4%
$r_{IS,MNA,def}$	**1S-T, n = 0**	37	1.01	7.4%	59%
	2S-T, n = 0	90	1.01	9.9%	58%
	1S-T-I, n = 0	18	1.06	4.3%	89%
	2S-T-I, n = 0	44	1.08	3.2%	100%
	1S-T-R, n = 0	19	0.97	7.4%	32%
	2S-T-R, n = 0	46	0.95	10.3%	17%
$r_{IS,MNA,ref}$	**1S-T, n = 0**	37	0.98	7.1%	54%
	2S-T, n = 0	90	0.98	9.3%	54%
	1S-T-I, n = 0	18	1.03	3.8%	89%
	2S-T-I, n = 0	44	1.04	2.8%	95%
	1S-T-R, n = 0	19	0.94	7.4%	21%
	2S-T-R, n = 0	46	0.92	10.2%	15%
$r_{IS,MNA,rich}$	**1S-T, n = 0**	37	0.98	7.0%	49%
	2S-T, n = 0	90	0.97	9.2%	51%
	1S-T-I, n = 0	18	1.02	3.6%	78%
	2S-T-I, n = 0	44	1.03	2.7%	89%
	1S-T-R, n = 0	19	0.94	7.5%	21%
	2S-T-R, n = 0	46	0.92	10.2%	15%
$r_{IS,GMNA,def}$	**1S-T, n = 0**	37	1.01	7.1%	59%
	2S-T, n = 0	90	1.01	9.6%	58%
	1S-T-I, n = 0	18	1.06	4.2%	89%
	2S-T-I, n = 0	44	1.08	3.2%	100%
	1S-T-R, n = 0	19	0.97	7.1%	32%
	2S-T-R, n = 0	46	0.95	10.0%	17%
$r_{IS,GMNA,ref}$	**1S-T, n = 0**	37	0.98	7.0%	46%
	2S-T, n = 0	90	0.97	9.6%	51%
	1S-T-I, n = 0	18	1.01	4.5%	72%
	2S-T-I, n = 0	44	1.02	4.0%	89%
	1S-T-R, n = 0	19	0.94	7.4%	21%
	2S-T-R, n = 0	46	0.91	10.3%	15%
$r_{IS,GMNA,rich}$	**1S-T, n = 0**	37	0.97	7.1%	35%
	2S-T, n = 0	90	0.95	9.7%	37%
	1S-T-I, n = 0	18	1.00	4.8%	50%
	2S-T-I, n = 0	44	1.01	4.5%	59%
	1S-T-R, n = 0	19	0.93	7.5%	21%
	2S-T-R, n = 0	46	**0.90**	10.5%	15%

Table 3.26. Ratios, welded columns, axial load, S275 (cluster BB-S275), EPPL. EN, FprEN.

Method	Cases	CWC				CWS				ALL (EXCEPT BCW)			
		n	Mean	CoV	(>1)/*n*	*n*	Mean	CoV	(>1)/*n*	*tot*	Mean	CoV	(>1)/tot
r_{EN}	**1S Interior Unstiffened**												
	1S-U-I, n = 0	16	**0.54**	12.5%	0%	4	**0.53**	11.3%	0%	20	**0.53**	12.0%	0%
	1S-U-I, n = 0.3	16	**0.56**	12.8%	0%	4	**0.56**	11.4%	0%	20	**0.56**	12.3%	0%
	1S-U-I, n = 0.5	16	**0.61**	13.4%	0%	4	**0.61**	11.2%	0%	20	**0.61**	12.7%	0%
	1S-U-I, n = 0.7	16	**0.71**	***15.2%***	0%	4	**0.72**	10.8%	0%	20	**0.71**	14.2%	0%
	1S Interior Stiffened												
	1S-T-I, n = 0					18	**0.76**	7.7%	0%	18	**0.76**	7.7%	0%
	1S-T-I, n = 0.3					18	**0.81**	7.0%	0%	18	**0.81**	7.0%	0%
	1S-T-I, n = 0.5					18	**0.87**	5.9%	0%	18	**0.87**	5.9%	0%
	1S-T-I, n = 0.7					18	1.02	9.6%	44%	18	1.02	9.6%	44%
	2S Interior Unstiffened												
	2S-U-I, n = 0	36	**0.58**	***16.5%***	0%	21	**0.55**	***18.3%***	0%	57	**0.57**	***17.2%***	0%
	2S-U-I, n = 0.3	36	**0.61**	***16.9%***	0%	21	**0.59**	***17.9%***	0%	57	**0.60**	***17.2%***	0%
	2S-U-I, n = 0.5	36	**0.65**	***17.2%***	0%	21	**0.64**	***17.0%***	0%	57	**0.65**	***17.1%***	0%
	2S-U-I, n = 0.7	36	**0.77**	***19.1%***	8%	21	**0.75**	***18.6%***	5%	57	**0.76**	***18.8%***	7%
	2S Interior Stiffened												
	2S-T-I, n = 0					44	**0.71**	9.8%	0%	44	**0.71**	9.8%	0%
	2S-T-I, n = 0.3					44	**0.76**	9.3%	0%	44	**0.76**	9.3%	0%
	2S-T-I, n = 0.5					44	**0.82**	8.4%	0%	44	**0.82**	8.4%	0%
	2S-T-I, n = 0.7					44	0.94	9.4%	18%	44	0.94	9.4%	18%
r_{FprEN}	**1S Interior Unstiffened**												
	1S-U-I, n = 0	16	**0.53**	13.0%	0%	4	**0.62**	5.5%	0%	20	**0.55**	13.1%	0%
	1S-U-I, n = 0.3	16	**0.56**	13.3%	0%	4	**0.65**	6.0%	0%	20	**0.58**	13.4%	0%
	1S-U-I, n = 0.5	16	**0.60**	13.9%	0%	4	**0.71**	5.8%	0%	20	**0.63**	14.1%	0%
	1S-U-I, n = 0.7	16	**0.70**	***15.6%***	0%	4	**0.84**	6.0%	0%	20	**0.73**	***15.7%***	0%
	1S Interior Stiffened												
	1S-T-I, n = 0					18	**0.82**	6.0%	0%	18	**0.82**	6.0%	0%
	1S-T-I, n = 0.3					18	**0.87**	5.5%	0%	18	**0.87**	5.5%	0%
	1S-T-I, n = 0.5					18	0.94	5.0%	0%	18	0.94	5.0%	0%
	1S-T-I, n = 0.7					18	***1.11***	7.8%	89%	18	***1.11***	7.8%	89%
	2S Interior Unstiffened												
	2S-U-I, n = 0	36	**0.58**	***17.1%***	0%	21	**0.67**	8.7%	0%	57	**0.61**	***15.9%***	0%
	2S-U-I, n = 0.3	36	**0.61**	***17.4%***	0%	21	**0.72**	8.2%	0%	57	**0.65**	***16.4%***	0%
	2S-U-I, n = 0.5	36	**0.65**	***17.8%***	0%	21	**0.78**	7.6%	0%	57	**0.70**	***16.6%***	0%
	2S-U-I, n = 0.7	36	**0.77**	***19.6%***	8%	21	0.91	9.5%	10%	57	**0.82**	***18.0%***	9%
	2S Interior Stiffened												
	2S-T-I, n = 0					44	**0.81**	5.6%	0%	44	**0.81**	5.6%	0%
	2S-T-I, n = 0.3					44	**0.87**	5.0%	2%	44	**0.87**	5.0%	2%
	2S-T-I, n = 0.5					44	0.94	4.8%	5%	44	0.94	4.8%	5%
	2S-T-I, n = 0.7					44	1.08	6.4%	100%	44	1.08	6.4%	100%

Table 3.27. Ratios, welded columns, axial load, S275 (cluster BB-S275), EPPL. IS MNA.

Method	Cases	CWC				CWS				ALL (EXCEPT BCW)			
		n	Mean	CoV	(>1)/*n*	*n*	Mean	CoV	(>1)/*n*	*tot*	Mean	CoV	(>1)/tot
$r_{IS,MNA,def}$	**1S Interior Unstiffened**												
	1S-U-I, n = 0	16	*1.11*	3.3%	100%	4	*1.16*	6.8%	100%	20	*1.12*	4.5%	100%
	1S-U-I, n = 0.3	16	*1.14*	4.0%	100%	4	*1.20*	6.5%	100%	20	*1.15*	4.9%	100%
	1S-U-I, n = 0.5	16	*1.15*	4.2%	100%	4	*1.22*	4.7%	100%	20	*1.17*	4.8%	100%
	1S-U-I, n = 0.7	16	*1.18*	5.1%	100%	4	*1.25*	4.8%	100%	20	*1.19*	5.6%	100%
	1S Interior Stiffened												
	1S-T-I, n = 0					18	1.06	4.3%	89%	18	1.06	4.3%	89%
	1S-T-I, n = 0.3					18	*1.11*	4.4%	100%	18	*1.11*	4.4%	100%
	1S-T-I, n = 0.5					18	*1.15*	4.2%	100%	18	*1.15*	4.2%	100%
	1S-T-I, n = 0.7					18	*1.20*	4.0%	100%	18	*1.20*	4.0%	100%
	2S Interior Unstiffened												
	2S-U-I, n = 0	36	*1.11*	3.8%	100%	21	1.06	1.7%	100%	57	1.09	4.0%	100%
	2S-U-I, n = 0.3	36	*1.15*	3.5%	100%	21	*1.11*	2.3%	100%	57	*1.13*	3.5%	100%
	2S-U-I, n = 0.5	36	*1.17*	3.4%	100%	21	*1.14*	2.6%	100%	57	*1.16*	3.4%	100%
	2S-U-I, n = 0.7	36	*1.22*	4.6%	100%	21	*1.17*	3.2%	100%	57	*1.20*	4.5%	100%
	2S Interior Stiffened												
	2S-T-I, n = 0					44	1.08	3.2%	100%	44	1.08	3.2%	100%
	2S-T-I, n = 0.3					44	*1.14*	3.1%	100%	44	*1.14*	3.1%	100%
	2S-T-I, n = 0.5					44	*1.18*	4.1%	100%	44	*1.18*	4.1%	100%
	2S-T-I, n = 0.7					44	*1.22*	6.6%	100%	44	*1.22*	6.6%	100%
$r_{IS,MNA,ref}$	**1S Interior Unstiffened**												
	1S-U-I, n = 0	16	1.04	1.9%	100%	4	*1.11*	6.3%	100%	20	1.05	4.2%	100%
	1S-U-I, n = 0.3	16	1.06	2.5%	94%	4	*1.15*	6.1%	100%	20	1.07	4.9%	95%
	1S-U-I, n = 0.5	16	1.07	2.7%	100%	4	*1.16*	4.8%	100%	20	1.08	4.7%	100%
	1S-U-I, n = 0.7	16	1.09	3.2%	100%	4	*1.20*	4.6%	100%	20	*1.11*	5.1%	100%
	1S Interior Stiffened												
	1S-T-I, n = 0					18	1.03	3.8%	89%	18	1.03	3.8%	89%
	1S-T-I, n = 0.3					18	1.08	3.9%	100%	18	1.08	3.9%	100%
	1S-T-I, n = 0.5					18	*1.11*	3.9%	100%	18	*1.11*	3.9%	100%
	1S-T-I, n = 0.7					18	*1.16*	3.9%	100%	18	*1.16*	3.9%	100%
	2S Interior Unstiffened												
	2S-U-I, n = 0	36	1.05	2.1%	100%	21	1.03	1.6%	100%	57	1.04	2.1%	100%
	2S-U-I, n = 0.3	36	1.07	3.0%	100%	21	1.08	2.2%	100%	57	1.07	2.7%	100%
	2S-U-I, n = 0.5	36	1.09	3.2%	100%	21	*1.11*	2.5%	100%	57	1.09	3.1%	100%
	2S-U-I, n = 0.7	36	*1.13*	5.1%	100%	21	*1.14*	3.5%	100%	57	*1.13*	4.5%	100%
	2S Interior Stiffened												
	2S-T-I, n = 0					44	1.04	2.8%	95%	44	1.04	2.8%	95%
	2S-T-I, n = 0.3					44	1.09	3.0%	100%	44	1.09	3.0%	100%
	2S-T-I, n = 0.5					44	*1.13*	3.8%	100%	44	*1.13*	3.8%	100%
	2S-T-I, n = 0.7					44	*1.17*	6.5%	95%	44	*1.17*	6.5%	95%
$r_{IS,MNA,rich}$	**1S Interior Unstiffened**												
	1S-U-I, n = 0	16	1.01	1.6%	81%	4	1.09	6.3%	100%	20	1.03	4.2%	85%
	1S-U-I, n = 0.3	16	1.03	2.0%	88%	4	*1.13*	6.1%	100%	20	1.05	5.0%	90%
	1S-U-I, n = 0.5	16	1.04	2.2%	94%	4	*1.14*	5.1%	100%	20	1.06	4.9%	95%
	1S-U-I, n = 0.7	16	1.07	2.8%	100%	4	*1.18*	4.9%	100%	20	1.09	5.2%	100%
	1S Interior Stiffened												
	1S-T-I, n = 0					18	1.02	3.6%	78%	18	1.02	3.6%	78%
	1S-T-I, n = 0.3					18	1.07	3.7%	89%	18	1.07	3.7%	89%
	1S-T-I, n = 0.5					18	*1.10*	3.8%	100%	18	*1.10*	3.8%	100%
	1S-T-I, n = 0.7					18	*1.15*	3.9%	100%	18	*1.15*	3.9%	100%
	2S Interior Unstiffened												
	2S-U-I, n = 0	36	1.03	2.0%	94%	21	1.02	1.6%	95%	57	1.02	1.9%	95%
	2S-U-I, n = 0.3	36	1.05	3.5%	89%	21	1.07	2.2%	100%	57	1.05	3.2%	93%
	2S-U-I, n = 0.5	36	1.06	3.8%	92%	21	1.09	2.6%	100%	57	1.07	3.7%	95%
	2S-U-I, n = 0.7	36	1.10	5.5%	97%	21	*1.12*	3.7%	100%	57	*1.11*	5.0%	98%
	2S Interior Stiffened												
	2S-T-I, n = 0					44	1.03	2.7%	89%	44	1.03	2.7%	89%
	2S-T-I, n = 0.3					44	1.08	3.0%	100%	44	1.08	3.0%	100%
	2S-T-I, n = 0.5					44	*1.12*	3.7%	100%	44	*1.12*	3.7%	100%
	2S-T-I, n = 0.7					44	*1.15*	6.6%	95%	44	*1.15*	6.6%	95%

Table 3.28. Ratios, welded columns, axial load, S275 (cluster BB-S275), EPPL. IS GMNA

Method	Cases	CWC				CWS				ALL (EXCEPT BCW)			
		n	Mean	CoV	(>1)/*n*	*n*	Mean	CoV	(>1)/*n*	*tot*	Mean	CoV	(>1)/tot
$r_{IS,GMNA,def}$	**1S Interior Unstiffened**												
	1S-U-I, n = 0	16	***1.11***	3.4%	100%	4	***1.15***	6.9%	100%	20	***1.11***	4.4%	100%
	1S-U-I, n = 0.3	16	1.10	4.2%	100%	4	***1.14***	7.1%	100%	20	***1.11***	4.9%	100%
	1S-U-I, n = 0.5	16	1.09	4.4%	100%	4	***1.12***	6.0%	100%	20	1.10	4.7%	100%
	1S-U-I, n = 0.7	16	1.08	5.2%	100%	4	***1.12***	5.1%	100%	20	1.09	5.2%	100%
	1S Interior Stiffened												
	1S-T-I, n = 0					18	1.06	4.2%	89%	18	1.06	4.2%	89%
	1S-T-I, n = 0.3					18	1.04	3.8%	89%	18	1.04	3.8%	89%
	1S-T-I, n = 0.5					18	1.04	3.7%	89%	18	1.04	3.7%	89%
	1S-T-I, n = 0.7					18	1.06	4.6%	94%	18	1.06	4.6%	94%
	2S Interior Unstiffened												
	2S-U-I, n = 0	36	***1.11***	3.9%	100%	21	1.06	1.7%	100%	57	1.09	4.0%	100%
	2S-U-I, n = 0.3	36	***1.10***	5.3%	100%	21	1.04	2.3%	100%	57	1.08	5.2%	100%
	2S-U-I, n = 0.5	36	1.10	5.5%	97%	21	1.04	2.1%	95%	57	1.08	5.3%	96%
	2S-U-I, n = 0.7	36	***1.11***	6.2%	97%	21	1.03	2.6%	90%	57	1.08	6.4%	95%
	2S Interior Stiffened												
	2S-T-I, n = 0					44	1.08	3.2%	100%	44	1.08	3.2%	100%
	2S-T-I, n = 0.3					44	1.06	3.3%	100%	44	1.06	3.3%	100%
	2S-T-I, n = 0.5					44	1.06	3.9%	95%	44	1.06	3.9%	95%
	2S-T-I, n = 0.7					44	1.06	7.3%	89%	44	1.06	7.3%	89%
$r_{IS,GMNA,ref}$	**1S Interior Unstiffened**												
	1S-U-I, n = 0	16	1.04	2.0%	94%	4	1.10	5.9%	100%	20	1.05	3.9%	95%
	1S-U-I, n = 0.3	16	1.03	2.4%	94%	4	***1.11***	6.2%	100%	20	1.05	4.4%	95%
	1S-U-I, n = 0.5	16	1.03	2.7%	88%	4	1.09	5.3%	100%	20	1.04	3.9%	90%
	1S-U-I, n = 0.7	16	1.04	3.7%	88%	4	1.10	4.5%	100%	20	1.05	4.4%	90%
	1S Interior Stiffened												
	1S-T-I, n = 0					18	1.01	4.5%	72%	18	1.01	4.5%	72%
	1S-T-I, n = 0.3					18	1.02	3.5%	67%	18	1.02	3.5%	67%
	1S-T-I, n = 0.5					18	1.02	3.4%	78%	18	1.02	3.4%	78%
	1S-T-I, n = 0.7					18	1.03	4.3%	78%	18	1.03	4.3%	78%
	2S Interior Unstiffened												
	2S-U-I, n = 0	36	1.04	2.3%	100%	21	1.03	1.7%	100%	57	1.04	2.2%	100%
	2S-U-I, n = 0.3	36	1.04	3.0%	94%	21	1.02	2.3%	90%	57	1.03	2.9%	93%
	2S-U-I, n = 0.5	36	1.04	3.0%	97%	21	1.02	1.9%	90%	57	1.03	2.8%	95%
	2S-U-I, n = 0.7	36	1.06	5.2%	92%	21	1.01	2.4%	71%	57	1.04	4.8%	84%
	2S Interior Stiffened												
	2S-T-I, n = 0					44	1.02	4.0%	89%	44	1.02	4.0%	89%
	2S-T-I, n = 0.3					44	1.03	3.0%	86%	44	1.03	3.0%	86%
	2S-T-I, n = 0.5					44	1.03	3.3%	93%	44	1.03	3.3%	93%
	2S-T-I, n = 0.7					44	1.03	6.7%	82%	44	1.03	6.7%	82%
$r_{IS,GMNA,rich}$	**1S Interior Unstiffened**												
	1S-U-I, n = 0	16	1.01	1.6%	81%	4	1.08	5.7%	100%	20	1.03	3.9%	85%
	1S-U-I, n = 0.3	16	1.01	1.9%	81%	4	1.10	6.0%	100%	20	1.03	4.5%	85%
	1S-U-I, n = 0.5	16	1.01	2.2%	69%	4	1.08	5.2%	100%	20	1.03	3.9%	75%
	1S-U-I, n = 0.7	16	1.02	3.2%	81%	4	1.09	4.3%	100%	20	1.04	4.2%	85%
	1S Interior Stiffened												
	1S-T-I, n = 0					18	1.00	4.8%	50%	18	1.00	4.8%	50%
	1S-T-I, n = 0.3					18	1.01	3.5%	67%	18	1.01	3.5%	67%
	1S-T-I, n = 0.5					18	1.02	3.3%	61%	18	1.02	3.3%	61%
	1S-T-I, n = 0.7					18	1.03	4.2%	61%	18	1.03	4.2%	61%
	2S Interior Unstiffened												
	2S-U-I, n = 0	36	1.02	2.0%	86%	21	1.02	1.7%	81%	57	1.02	1.9%	84%
	2S-U-I, n = 0.3	36	1.02	2.9%	78%	21	1.02	2.4%	62%	57	1.02	2.7%	72%
	2S-U-I, n = 0.5	36	1.02	2.7%	78%	21	1.01	1.9%	81%	57	1.02	2.4%	79%
	2S-U-I, n = 0.7	36	1.04	5.2%	81%	21	1.00	2.3%	67%	57	1.02	4.6%	75%
	2S Interior Stiffened												
	2S-T-I, n = 0					44	1.01	4.5%	59%	44	1.01	4.5%	59%
	2S-T-I, n = 0.3					44	1.02	2.9%	61%	44	1.02	2.9%	61%
	2S-T-I, n = 0.5					44	1.02	3.1%	82%	44	1.02	3.1%	82%
	2S-T-I, n = 0.7					44	1.02	6.6%	75%	44	1.02	6.6%	75%

3.3.3 Influence of fillet welds

The failure modes for welded columns with column-web-to-column-flange fillet welds are shown in **Table 3.29**. The following conclusions can be drawn:

- As expected, all stiffened cases fail by CWS.
- Only stocky unstiffened columns (cases 10 to 16) fail by CWS.
- Only very stocky columns fail by BCW.
- Comparing **Table 3.29** (cluster BF, welded columns with column-web-to-column-flange fillet welds) with **Table 3.23** (cluster BB, welded columns with column-web-to-column-flange butt welds), the only difference is for models 14, 15 in sets 01 - 02 (1S-U without and with axial load) and model 16, in set 02 (1S-U with axial load).

Table 3.29. Failure modes for welded columns with fillet welds, S275 (cluster BF-S275).

S275						Case																			
	1S/2S	I/R	U/T	*n*	*mr*	1	2	3	4	5	6	7	8	9	10	11	12	13	14	15	16	17	18	19	20
set_01	1S	I	U	0	0	CWC	CWC	CWC	CWC	CWC	CWC	CWC	CWC	CWC	CWS	CWS	CWS	CWS	CWS	CWS	CWC	CWC	CWC	CWC	CWC
set_02_N30	1S	I	U	0.3	0	CWC	CWC	CWC	CWC	CWC	CWC	CWC	CWC	CWC	CWS	CWS	CWS	CWS	CWS	CWS	CWS	CWC	CWC	CWC	CWC
set_02_N50	1S	I	U	0.5	0	CWC	CWC	CWC	CWC	CWC	CWC	CWC	CWC	CWC	CWS	CWS	CWS	CWS	CWS	CWS	CWS	CWC	CWC	CWC	CWC
set_02_N70	1S	I	U	0.7	0	CWC	CWC	CWC	CWC	CWC	CWC	CWC	CWC	CWC	CWS	CWS	CWS	CWS	CWS	CWS	CWS	CWC	CWC	CWC	CWC
set_03	1S	I	T	0	0	CWS	CWS	CWS	CWS	CWS	CWS	CWS	CWS	CWS	BCW	CWS	CWS	CWS	CWS	BCW	CWS	CWS	CWS	CWS	CWS
set_04_N30	1S	I	T	0.3	0	CWS	CWS	CWS	CWS	CWS	CWS	CWS	CWS	CWS	BCW	CWS	CWS	CWS	CWS	BCW	CWS	CWS	CWS	CWS	CWS
set_04_N50	1S	I	T	0.5	0	CWS	CWS	CWS	CWS	CWS	CWS	CWS	CWS	CWS	BCW	CWS	CWS	CWS	CWS	BCW	CWS	CWS	CWS	CWS	CWS
set_04_N70	1S	I	T	0.7	0	CWS	CWS	CWS	CWS	CWS	CWS	CWS	CWS	CWS	BCW	CWS	CWS	CWS	CWS	BCW	CWS	CWS	CWS	CWS	CWS

The ratios for welded columns with column-web-to-column-flange fillet welds are shown in **Table 3.30** (EN, FprEN), **Table 3.31** (IS, MNA) and **Table 3.32** (IS, GMNA). The trends follow those of the welded column with butt welds, but some ratios change slightly. The following conclusions can be drawn:

For EN and FprEN:

- Highly conservative mean ratios with no unconservative individual cases are systematically obtained with all methods, except for high levels of axial load (n = 0.7) for stiffened joints, for which FprEN is moderately unconservative.
- With EN, the CoV is generally moderate; however, for axially loaded unstiffened joints with CWS failure it is high.
- With FprEN, the CoV is generally low, except for CWC and for stiffened joints with very high levels of axial load, where it is moderate.

For IDEA StatiCa:

- With the default options (default mesh, MNA), moderate to high unconservative mean ratios are obtained for all configurations, except 1S-T without axial load. Almost all individual results are unconservative.
- With the default options, increasing axial load results on increasing mean ratios. Even for low values of axial load the mean ratios are highly unconservative.
- Increasing the mesh size but keeping MNA analysis slightly improves the results, but the general trend is still unconservativeness. For CWC failure modes, the mean ratios are only slightly conservative, except for high level of axial load (n = 0.7), for which the mean ratio is slightly conservative. For CWS failure modes, all mean ratios with axial load are moderately unconservative, but almost all individual ratios are above 1. The unconservativeness increases with axial load.

- Keeping the mesh size but using GMNA analysis results slightly improves the results. For all configurations, the mean ratios are moderately unconservative, with a high proportion of unconservative individual cases. However, the dependency of the ratios with axial load is removed.
- Improving the mesh size and using GMNA analysis results in slightly conservative mean ratios for all configurations with CWC failure mode, and for all stiffened joints. The ratios are only slightly unconservative for unstiffened joints with CWS failure mode. The proportion of unconservative cases is still high for all configurations, except unstiffened with low values of axial load and CWC failure, for which no unconservative individual results are obtained.
- The CoV is low and rather stable regardless of the mesh and analysis type.

Table 3.30. Ratios, welded columns, fillet welds, S275 (BF-S275), EPPL. EN, FprEN.

Method	Cases	CWC				CWS				ALL (EXCEPT BCW)			
		n	Mean	CoV	(>1)/*n*	*n*	Mean	CoV	(>1)/*n*	*tot*	Mean	CoV	(>1)/tot
r_{EN}	**1S-I**	53	**0.69**	***16.5%***	2%	99	**0.80**	***19.1%***	8%	152	**0.76**	***19.6%***	6%
	1S-I-U	53	**0.69**	***16.5%***	2%	27	**0.65**	***20.9%***	4%	80	**0.67**	***18.1%***	3%
	1S-I-T					72	**0.85**	13.9%	10%	72	**0.85**	13.9%	10%
	1S-U-I, n = 0	14	**0.62**	13.0%	0%	6	**0.55**	14.0%	0%	20	**0.60**	14.1%	0%
	1S-U-I, n = 0.3	13	**0.64**	12.2%	0%	7	**0.61**	***18.6%***	0%	20	**0.63**	14.4%	0%
	1S-U-I, n = 0.5	13	**0.69**	12.5%	0%	7	**0.66**	***18.0%***	0%	20	**0.68**	14.3%	0%
	1S-U-I, n = 0.7	13	**0.80**	14.1%	8%	7	**0.77**	***18.1%***	14%	20	**0.79**	***15.2%***	10%
	1S-T-I, n = 0					18	**0.75**	8.6%	0%	18	**0.75**	8.6%	0%
	1S-T-I, n = 0.3					18	**0.80**	8.0%	0%	18	**0.80**	8.0%	0%
	1S-T-I, n = 0.5					18	**0.86**	6.9%	0%	18	**0.86**	6.9%	0%
	1S-T-I, n = 0.7					18	1.00	9.8%	39%	18	1.00	9.8%	39%
r_{FprEN}	**1S-I**	53	**0.69**	***16.6%***	2%	99	**0.88**	14.7%	17%	152	**0.81**	***19.1%***	12%
	1S-I-U	53	**0.69**	***16.6%***	2%	27	**0.78**	13.2%	4%	80	**0.72**	***16.6%***	3%
	1S-I-T					72	0.92	13.0%	22%	72	0.92	13.0%	22%
	1S-U-I, n = 0	14	**0.62**	13.2%	0%	6	**0.68**	5.6%	0%	20	**0.64**	12.0%	0%
	1S-U-I, n = 0.3	13	**0.64**	12.4%	0%	7	**0.73**	7.0%	0%	20	**0.67**	12.0%	0%
	1S-U-I, n = 0.5	13	**0.69**	12.7%	0%	7	**0.79**	6.5%	0%	20	**0.73**	12.4%	0%
	1S-U-I, n = 0.7	13	**0.80**	14.3%	8%	7	0.92	6.6%	14%	20	**0.84**	13.4%	10%
	1S-T-I, n = 0					18	**0.81**	6.9%	0%	18	**0.81**	6.9%	0%
	1S-T-I, n = 0.3					18	**0.86**	6.6%	0%	18	**0.86**	6.6%	0%
	1S-T-I, n = 0.5					18	0.93	5.8%	0%	18	0.93	5.8%	0%
	1S-T-I, n = 0.7					18	1.08	7.9%	89%	18	1.08	7.9%	89%

Table 3.31. Ratios, welded columns, fillet welds, S275 (BF-S275), EPPL. IS MNA.

Method	Cases	CWC				CWS				ALL (EXCEPT BCW)			
		n	Mean	CoV	(>1)/*n*	*n*	Mean	CoV	(>1)/*n*	*tot*	Mean	CoV	(>1)/tot
$r_{IS,MNA,def}$	**1S-I**	53	1.10	4.3%	98%	99	***1.11***	5.1%	98%	152	***1.10***	4.9%	98%
	1S-I-U	53	1.10	4.3%	98%	27	***1.13***	5.1%	100%	80	***1.11***	4.8%	99%
	1S-I-T					72	1.10	5.0%	97%	72	1.10	5.0%	97%
	1S-U-I, n = 0	14	1.06	2.9%	93%	6	1.08	5.1%	100%	20	1.06	3.7%	95%
	1S-U-I, n = 0.3	13	1.09	3.0%	100%	7	***1.12***	5.2%	100%	20	***1.10***	4.0%	100%
	1S-U-I, n = 0.5	13	***1.11***	3.4%	100%	7	***1.14***	4.2%	100%	20	***1.12***	3.8%	100%
	1S-U-I, n = 0.7	13	***1.13***	4.9%	100%	7	***1.16***	4.7%	100%	20	***1.14***	4.9%	100%
	1S-T-I, n = 0					18	1.04	2.6%	89%	18	1.04	2.6%	89%
	1S-T-I, n = 0.3					18	1.08	2.9%	100%	18	1.08	2.9%	100%
	1S-T-I, n = 0.5					18	***1.12***	2.9%	100%	18	***1.12***	2.9%	100%
	1S-T-I, n = 0.7					18	***1.16***	3.2%	100%	18	***1.16***	3.2%	100%
$r_{IS,MNA,ref}$	**1S-I**	53	1.02	3.3%	70%	99	1.07	4.8%	90%	152	1.05	4.9%	83%
	1S-I-U	53	1.02	3.3%	70%	27	1.07	5.4%	96%	80	1.04	4.9%	79%
	1S-I-T					72	1.07	4.6%	88%	72	1.07	4.6%	88%
	1S-U-I, n = 0	14	0.99	2.1%	29%	6	1.04	5.4%	83%	20	1.00	4.2%	45%
	1S-U-I, n = 0.3	13	1.01	1.8%	85%	7	1.07	5.5%	100%	20	1.03	4.5%	90%
	1S-U-I, n = 0.5	13	1.02	2.0%	85%	7	1.08	5.1%	100%	20	1.04	4.2%	90%
	1S-U-I, n = 0.7	13	1.05	3.3%	85%	7	***1.10***	5.4%	100%	20	1.07	4.6%	90%
	1S-T-I, n = 0					18	1.01	2.2%	56%	18	1.01	2.2%	56%
	1S-T-I, n = 0.3					18	1.06	2.5%	94%	18	1.06	2.5%	94%
	1S-T-I, n = 0.5					18	1.08	2.6%	100%	18	1.08	2.6%	100%
	1S-T-I, n = 0.7					18	***1.12***	3.2%	100%	18	***1.12***	3.2%	100%
$r_{IS,MNA,rich}$	**1S-I**	53	0.99	3.1%	40%	99	1.06	4.8%	86%	152	1.03	5.3%	70%
	1S-I-U	53	0.99	3.1%	40%	27	1.06	5.8%	89%	80	1.01	5.2%	56%
	1S-I-T					72	1.06	4.5%	85%	72	1.06	4.5%	85%
	1S-U-I, n = 0	14	0.96	2.0%	0%	6	1.03	5.8%	83%	20	0.98	4.7%	25%
	1S-U-I, n = 0.3	13	0.99	1.7%	31%	7	1.05	5.9%	86%	20	1.01	4.9%	50%
	1S-U-I, n = 0.5	13	1.00	1.6%	46%	7	1.06	5.8%	86%	20	1.02	4.7%	60%
	1S-U-I, n = 0.7	13	1.02	2.9%	85%	7	1.08	5.8%	100%	20	1.04	4.9%	90%
	1S-T-I, n = 0					18	1.00	2.0%	50%	18	1.00	2.0%	50%
	1S-T-I, n = 0.3					18	1.05	2.4%	89%	18	1.05	2.4%	89%
	1S-T-I, n = 0.5					18	1.07	2.5%	100%	18	1.07	2.5%	100%
	1S-T-I, n = 0.7					18	***1.10***	3.3%	100%	18	***1.10***	3.3%	100%

ACIV - Associação para o Desenvolvimento da Engenharia Civil - **UNIVERSIDADE DE COIMBRA** – NIF 505448173
Departament of Civil Engineering - FCTUC * Rua Luís Reis Santos | Pólo II da Univ. Coimbra | 3030-788 COIMBRA
ISISE UC – Institute for Sustainability and Innovation in Structural Engineering

Table 3.32. Ratios welded columns, fillet welds, S275 (BF-S275), EPPL. IS GMNA.

Method	Cases	CWC				CWS				ALL (EXCEPT BCW)			
		n	Mean	CoV	(>1)/*n*	*n*	Mean	CoV	(>1)/*n*	*tot*	Mean	CoV	(>1)/tot
$r_{IS,GMNA,def}$	**1S-I**	53	1.05	3.7%	89%	99	1.03	3.9%	83%	152	1.04	3.9%	85%
	1S-I-U	53	1.05	3.7%	89%	27	1.06	5.2%	85%	80	1.05	4.2%	88%
	1S-I-T					72	1.02	2.8%	82%	72	1.02	2.8%	82%
	1S-U-I, n = 0	14	1.05	2.9%	93%	6	1.07	5.2%	100%	20	1.06	3.7%	95%
	1S-U-I, n = 0.3	13	1.06	3.2%	100%	7	1.07	6.2%	100%	20	1.06	4.3%	100%
	1S-U-I, n = 0.5	13	1.05	3.7%	92%	7	1.05	5.2%	71%	20	1.05	4.1%	85%
	1S-U-I, n = 0.7	13	1.04	4.9%	69%	7	1.04	4.4%	71%	20	1.04	4.6%	70%
	1S-T-I, n = 0					18	1.03	2.6%	89%	18	1.03	2.6%	89%
	1S-T-I, n = 0.3					18	1.02	2.3%	89%	18	1.02	2.3%	89%
	1S-T-I, n = 0.5					18	1.02	2.2%	89%	18	1.02	2.2%	89%
	1S-T-I, n = 0.7					18	1.02	3.9%	61%	18	1.02	3.9%	61%
$r_{IS,GMNA,ref}$	**1S-I**	53	0.99	2.6%	42%	99	1.01	3.6%	47%	152	1.00	3.4%	45%
	1S-I-U	53	0.99	2.6%	42%	27	1.03	4.8%	63%	80	1.00	3.8%	49%
	1S-I-T					72	1.00	2.8%	42%	72	1.00	2.8%	42%
	1S-U-I, n = 0	14	0.99	2.1%	29%	6	1.04	5.2%	83%	20	1.00	4.0%	45%
	1S-U-I, n = 0.3	13	1.00	2.0%	46%	7	1.04	5.7%	57%	20	1.01	4.1%	50%
	1S-U-I, n = 0.5	13	0.99	2.2%	38%	7	1.02	4.7%	57%	20	1.00	3.4%	45%
	1S-U-I, n = 0.7	13	1.00	3.8%	54%	7	1.02	4.1%	57%	20	1.00	3.9%	55%
	1S-T-I, n = 0					18	0.99	3.3%	39%	18	0.99	3.3%	39%
	1S-T-I, n = 0.3					18	1.00	2.0%	44%	18	1.00	2.0%	44%
	1S-T-I, n = 0.5					18	1.00	1.9%	44%	18	1.00	1.9%	44%
	1S-T-I, n = 0.7					18	1.00	3.6%	39%	18	1.00	3.6%	39%
$r_{IS,GMNA,rich}$	**1S-I**	53	0.97	2.4%	8%	99	1.00	3.7%	35%	152	0.99	3.5%	26%
	1S-I-U	53	0.97	2.4%	8%	27	1.02	4.7%	48%	80	0.99	4.0%	21%
	1S-I-T					72	0.99	2.9%	31%	72	0.99	2.9%	31%
	1S-U-I, n = 0	14	0.96	2.0%	0%	6	1.03	5.4%	67%	20	0.98	4.4%	20%
	1S-U-I, n = 0.3	13	0.98	1.8%	0%	7	1.02	5.7%	57%	20	0.99	4.3%	20%
	1S-U-I, n = 0.5	13	0.98	1.8%	8%	7	1.01	4.6%	43%	20	0.99	3.5%	20%
	1S-U-I, n = 0.7	13	0.98	3.5%	23%	7	1.01	4.1%	29%	20	0.99	3.8%	25%
	1S-T-I, n = 0					18	0.98	3.8%	28%	18	0.98	3.8%	28%
	1S-T-I, n = 0.3					18	0.99	2.0%	28%	18	0.99	2.0%	28%
	1S-T-I, n = 0.5					18	1.00	1.9%	33%	18	1.00	1.9%	33%
	1S-T-I, n = 0.7					18	1.00	3.5%	33%	18	1.00	3.5%	33%

3.3.4 Stiffness

Table 3.33 shows statistics of ratios for initial stiffness for welded columns (cluster BB-S275) with EPPL material model, for different joint configurations, but only for EN and FprEN (as

discussed in Section 2.3.3, the stiffness ratios are not meaningful for IDEA StatiCa). The results show that:

- For welded columns with column-web-to-column-flange fillet welds there is no difference in the stiffness predictions with EN or FprEN. Thus, FprEN results in no improvement with respect to EN.
- By comparison with **Table 3.15**, the trends for stiffness ratios on welded columns with both EN and FprEN are similar to those of rolled columns, but slightly less unconservative (that is, for welded columns the mean ratios are slightly below those for rolled columns, and a smaller proportion of individual cases are unconservative).
- Both EN and FprEN are unconservative for stiffened joints and conservative for unstiffened joints.
- A large percentage of individual cases (40%) is unconservative (ratios above 1).
- Large max ratios are obtained, up to 2.12.
- The ratios present a high CoV of 43.2%.

Focusing on the influence of joint typology, the following trends can be observed:

- The mean ratios for unstiffened joints with no axial load are highly conservative (about 0.59 < 1), with a high CoV (22.6%), and with only a small proportion of unconservative individual results (0% for 1S and 1% for 2S).
- The mean ratios for stiffened joints with no axial load are highly unconservative (1.3).
- For one-sided stiffened joints with no axial load, the scatter is high (16.4%), and basically all individual results (98%) are unconservative.
- For two-sided stiffened joints with no axial load, the scatter is high (25.4%), 81% of individual cases are unconservative, featuring high individual ratios (up to 2.12).
- The increase of axial load does not affect the results.

Table 3.34 shows the stiffness values for the sub-set of one-sided internal joints, including the effect of column-web-to-column-flange fillet weld. All trends are like those of **Table 3.33** but the inclusion of fillet welds in the model results in higher ratios for unstiffened joints and lower ratios for stiffened joints. Consequently, the mean ratios and proportion of unconservative cases increase for unstiffened joints and decrease for stiffened joints.

Table 3.33. Initial stiffness ratios, welded columns, S275 (BB-S275), EPPL. EN, FprEN.

Cases	s_{EN}							s_{FprEN}						
	tot	Mean	CoV	Max	Min	(>1)	(>1)/tot	*tot*	Mean	CoV	Max	Min	(>1)	(>1)/tot
All	800	**0.89**	***43.2%***	2.12	0.35	320	40%	800	**0.89**	***43.2%***	2.12	0.35	320	40%
No axial force														
1S-U, n = 0	40	**0.58**	***22.6%***	0.88	0.39	0	0%	40	**0.58**	***22.6%***	0.88	0.39	0	0%
1S-T, n = 0	40	***1.30***	***16.4%***	1.81	0.92	39	98%	40	***1.30***	***16.4%***	1.81	0.92	39	98%
2S-U, n = 0	120	**0.59**	***23.7%***	1.00	0.35	1	1%	120	**0.59**	***23.7%***	1.00	0.35	1	1%
2S-T, n = 0	120	***1.30***	***25.4%***	2.12	0.73	97	81%	120	***1.30***	***25.4%***	2.12	0.73	97	81%
Stiffened														
All, T-I, n = 0	80	***1.14***	***19.6%***	1.74	0.73	59	73.8%	80	***1.14***	***19.6%***	1.74	0.73	59	73.8%
All, T-R, n = 0	80	***1.46***	***19.8%***	2.12	0.93	77	96%	80	***1.46***	***19.8%***	2.12	0.93	77	96%
All, T,(I+R), n = 0	160	***1.30***	***23.4%***	2.12	0.73	136	85%	160	***1.30***	***23.4%***	2.12	0.73	136	85%
1S Interior Unstiffened														
1S-U-I, n = 0	20	**0.55**	***19.5%***	0.80	0.39	0	0%	20	**0.55**	***19.5%***	0.80	0.39	0	0%
1S-U-I, n = 0.3	20	**0.54**	***18.7%***	0.71	0.37	0	0%	20	**0.54**	***18.7%***	0.71	0.37	0	0%
1S-U-I, n = 0.5	20	**0.55**	***18.8%***	0.72	0.38	0	0%	20	**0.55**	***18.8%***	0.72	0.38	0	0%
1S-U-I, n = 0.7	20	**0.55**	***18.9%***	0.74	0.38	0	0%	20	**0.55**	***18.9%***	0.74	0.38	0	0%
1S Interior Stiffened														
1S-T-I, n = 0	20	***1.13***	8.1%	1.27	0.92	19	95%	20	***1.13***	8.1%	1.27	0.92	19	95%
1S-T-I, n = 0.3	20	***1.14***	7.9%	1.27	0.93	19	95%	20	***1.14***	7.9%	1.27	0.93	19	95%
1S-T-I, n = 0.5	20	***1.15***	7.8%	1.28	0.94	19	95%	20	***1.15***	7.8%	1.28	0.94	19	95%
1S-T-I, n = 0.7	20	***1.16***	7.8%	1.28	0.96	19	95%	20	***1.16***	7.8%	1.28	0.96	19	95%
2S Interior Unstiffened														
2S-U-I, n = 0	60	**0.54**	***18.7%***	0.73	0.35	0	0%	60	**0.54**	***18.7%***	0.73	0.35	0	0%
2S-U-I, n = 0.3	60	**0.55**	***18.9%***	0.73	0.35	0	0%	60	**0.55**	***18.9%***	0.73	0.35	0	0%
2S-U-I, n = 0.5	60	**0.55**	***19.0%***	0.74	0.36	0	0%	60	**0.55**	***19.0%***	0.74	0.36	0	0%
2S-U-I, n = 0.7	60	**0.56**	***19.1%***	0.75	0.36	0	0%	60	**0.56**	***19.1%***	0.75	0.36	0	0%
2S Interior Stiffened														
2S-T-I, n = 0	60	***1.14***	***22.2%***	1.74	0.73	40	67%	60	***1.14***	***22.2%***	1.74	0.73	40	67%
2S-T-I, n = 0.3	60	***1.15***	***22.0%***	1.75	0.74	42	70%	60	***1.15***	***22.0%***	1.75	0.74	42	70%
2S-T-I, n = 0.5	60	***1.15***	***21.9%***	1.75	0.75	42	70%	60	***1.15***	***21.9%***	1.75	0.75	42	70%
2S-T-I, n = 0.7	60	***1.16***	***21.8%***	1.76	0.76	42	70%	60	***1.16***	***21.8%***	1.76	0.76	42	70%
Roof														
1S-U-R, n = 0	20	**0.61**	***24.3%***	0.88	0.39	0	0%	20	**0.61**	***24.3%***	0.88	0.39	0	0%
2S-U-R, n = 0	60	**0.63**	***25.0%***	1.00	0.39	1	2%	60	**0.63**	***25.0%***	1.00	0.39	1	2%
1S-T-R, n = 0	20	***1.46***	11.5%	1.81	1.13	20	100%	20	***1.46***	11.5%	1.81	1.13	20	100%
2S-T-R, n = 0	60	***1.46***	***21.9%***	2.12	0.93	57	95%	60	***1.46***	***21.9%***	2.12	0.93	57	95%

Table 3.34. Initial stiffness, welded cols., fillet welds, S275 (BF-S275), EPPL. EN, FprEN.

Cases	s_{EN}							s_{FprEN}						
	tot	Mean	CoV	Max	Min	(>1)	(>1)/tot	*tot*	Mean	CoV	Max	Min	(>1)	(>1)/tot
1S-I	160	**0.87**	***30.2%***	1.26	0.45	66	41%	160	**0.87**	***30.2%***	1.26	0.45	66	41%
1S-I-U	80	**0.63**	***15.1%***	0.78	0.45	0	0%	80	**0.63**	***15.1%***	0.78	0.45	0	0%
1S-I-T	80	***1.12***	8.4%	1.26	0.88	66	83%	80	***1.12***	8.4%	1.26	0.88	66	83%
1S-U-I, n = 0	20	**0.62**	***15.1%***	0.77	0.46	0	0%	20	**0.62**	***15.1%***	0.77	0.46	0	0%
1S-U-I, n = 0.3	20	**0.63**	***15.3%***	0.77	0.45	0	0%	20	**0.63**	***15.3%***	0.77	0.45	0	0%
1S-U-I, n = 0.5	20	**0.63**	***15.5%***	0.77	0.45	0	0%	20	**0.63**	***15.5%***	0.77	0.45	0	0%
1S-U-I, n = 0.7	20	**0.63**	***15.6%***	0.78	0.46	0	0%	20	**0.63**	***15.6%***	0.78	0.46	0	0%
1S-T-I, n = 0	20	***1.11***	8.7%	1.25	0.88	16	80%	20	***1.11***	8.7%	1.25	0.88	16	80%
1S-T-I, n = 0.3	20	***1.12***	8.6%	1.25	0.90	16	80%	20	***1.12***	8.6%	1.25	0.90	16	80%
1S-T-I, n = 0.5	20	***1.12***	8.5%	1.26	0.91	17	85%	20	***1.12***	8.5%	1.26	0.91	17	85%
1S-T-I, n = 0.7	20	***1.13***	8.4%	1.26	0.92	17	85%	20	***1.13***	8.4%	1.26	0.92	17	85%

4 Summary and Conclusions

4.1 SUMMARY

This report presents a systematic comparison of the initial stiffness and moment resistance of joints, obtained with the current and upcoming Eurocode procedures, and with the software IDEA StatiCa, for welded, strong-axis, open-section beam-column joints, using high-quality finite element solid models as a comparison benchmark. The FEM results are considered a benchmark in the context of this report, as they have been properly validated with experimental tests, and their numerical convergence has been assessed. The selection of the moment resistance on the moment-rotation curve is based on a 5% plastic equivalent strain criterion, according to what is adopted by IDEA StatiCa.

The joints are designed to fail mainly by components associated with the column. 20 representative cases have been analyzed in different configurations. Each case corresponds to a combination of column and beam. Each configuration corresponds to a type of joint (one-sided, two-sided), a different position of the joint (internal story or roof), transverse stiffeners or not, different levels of axial load in the column and, for the two-sided joints, different ratios of the applied moment at both sides of the joints. Rolled and welded columns are included, and the effect of butt welds vs. fillet welds is analyzed.

The comparison considers several assumptions that directly influence the results. They were listed in Section 2.4.3 and relate to: (i) scope of the assessment (welded joints, strong-axis, no weak axis interaction, European hot-rolled open sections or equivalent welded sections, stiffened and unstiffened joints, one- and two-sided joints, intermediate story, and roof, full penetration butt-welds or fillet welds between beam flanges and column flange and between column flange and column web, maximum sizes of steel profiles); (ii) assumption related to the benchmark numerical models implemented in Abaqus (geometry of the core part of the FE model where solid elements are used, amplitude of the initial geometrical imperfections, no direct consideration of residual stresses, no consideration of strain hardening).

The relevant results are expressed generally in terms of the ratio $r_{method} = M_{R,method} / M_{R,FEM,5\%}$, that is, the ratio between the moment resistance obtained with the given method (EN, prEN, IS,MNA,def; IS,MNA,ref; IS,MNA,rich; IS,GMNA,def; IS,GMNA,ref; IS,GMNA,rich, corresponding, respectively to EN 1993-1-8:2005, FprEN1993-1-8:2023, IDEA StatiCa with MNA and default mesh, IDEA StatiCa with MNA and refined mesh, IDEA Statica with MNA and Richardson extrapolation, IDEA StatiCa with GMNA and default mesh, IDEA StatiCa with GMNA and refined mesh, IDEA Statica with GMNA and Richardson extrapolation,) and the benchmark moment resistance (FEM, obtained from the Abaqus models considering the 5% equivalent plastic strain limit). The cases failing by failure of the welds are excluded from the evaluation, as this failure mode is not properly captured by the FE model.

This assessment should not be understood as a statement of the reliability of the design provisions of the Eurocode or IDEA StatiCa, as no reliability assessment is carried out. Additionally, some assumptions may lead to a safe-sided estimation of the moment resistance that

should be properly analyzed and discussed before coming to objective statements about the reliability of these results.
The results, detailed in the previous Chapter, are summarized hereby.

For rolled columns:

IDEA StatiCa with default options (MNA analysis and default mesh) provides unconservative results: a mean ratio of 1.06, with a proportion of 82% of unconservative individual ratios. However, the scatter is moderate, with a CoV of 7.8%.

Refining the mesh (halving the size of the default mesh) provides a better approximation to the FEM results, in terms of mean ratio (1.01) and a smaller proportion of unconservative individual ratios (59%). However, the computational effort in terms of the accuracy obtained is somehow questionable.

With the default mesh and GMNA analysis, the mean ratio is exactly 1 and the CoV is lowered to 5.2%, yet 60% of individual cases are still unconservative.

With the refined mesh and GMNA analysis, IDEA StatiCa is slightly conservative (mean ratio 0.96), with a moderate CoV (5.6%) and only a small proportion of unconservative cases (20%). With this option, the worst results are obtained for two-sided stiffened joints with or without axial load.

For welded columns:

For welded columns, IDEA StatiCa is generally unconservative.

IDEA StatiCa with default options (MNA analysis and default mesh) provides unconservative results: a mean ratio of 1.12, with a proportion of 88% of unconservative individual ratios. However, the scatter is moderate, with a CoV of 8.6%.

Refining the mesh (halving the size of the default mesh) provides a better approximation to the FEM results, in terms of mean ratio (1.06), but almost the same proportion of unconservative individual ratios (83%). Scatter is similar.

With the default mesh and GMNA analysis, the mean ratio is 1.06 and the CoV is lowered to 6.8%, yet 86% of individual cases are still unconservative.

With the refined mesh and GMNA analysis, IDEA StatiCa is slightly unconservative (mean ratio 1.01), with a moderate CoV (6.2%) but a high proportion of unconservative cases (75%).

Other relevant conclusions

Regarding the 5% equivalent plastic strain criterion, it has been shown that, for this type of joint, it produces resistance results like those obtained with a reduction of secant stiffness to 1/3 of the initial stiffness.

Initial imperfections play a minor role in the behavior of the joints analyzed; however, geometrical non-linearity (2nd order analysis) should be included, particularly in cases where the axial load is present.

The material model used by IDEA StatiCa results in an average of 3% increase in moment resistance.

The moment resistances obtained including strain hardening are slightly higher (about 4%) than those with an elastic-perfectly plastic material.

ACIV - Associação para o Desenvolvimento da Engenharia Civil - **UNIVERSIDADE DE COIMBRA** – NIF 505448173
Departament of Civil Engineering - FCTUC * Rua Luís Reis Santos | Pólo II da Univ. Coimbra | 3030-788 COIMBRA
ISISE UC – Institute for Sustainability and Innovation in Structural Engineering

The inclusion of welds and adjacent plate regions in the evaluation of the plastic equivalent strain leads to overly conservative values of resistance for fillet welds in tension. For this study, the fillet welds and adjacent plate regions were excluded from the evaluation of the 5% plastic equivalent strain.

4.2 Implementations for IDEA StatiCa

The following comments are relevant for implementation in IDEA StatiCa:

1. Initial imperfections are not relevant for this type of joint.
2. Purely material non-linear analysis without second-order effects results in unconservative results. It is therefore recommended that the geometrically non-linear analysis is activated by default in the program. This option, however, is only fully effective for rolled columns.
3. The mesh size plays an essential role in the accuracy of results. A potential approach to estimate the converged value could be based on an automated process that decreases (or maybe increases) the mesh size and applies the Richardson extrapolation to the moment resistance obtained with both values.
4. The cases involving axial force are quite unconservative. The interaction of shear and biaxial force in the shell element in the program probably needs to be revisited.
5. A reliability assessment of program results according to EN 1993-1-14 is necessary but is outside the scope of this report.

References

CEN (2002a). *EN 1990: 2002. Eurocode – Basis of structural design*. European Committee for Standardization, Brussels.

CEN (2002b). *EN 1991-1-1: 2002. Eurocode 1: Actions on structures – Part 1-1: General actions – Densities, self-weight, imposed loads for buildings*. European Committee for Standardization, Brussels.

CEN (2003). *EN 1991-1-3: 2003. Eurocode 1: Actions on structures – Part 1-3: General actions – Snow loads*. European Committee for Standardization, Brussels.

CEN (2004a). *EN 1992-1-1: 2004. Eurocode 2: Design of concrete structures – Part 1-1: General rules and rules for buildings*. European Committee for Standardization, Brussels.

CEN (2004b). *EN 1994-1-1: 2004. Eurocode 4: Design of composite steel and concrete structures – Part 1-1: General rules and rules for buildings*. European Committee for Standardization, Brussels.

CEN (2005a). *EN 1993-1-1: 2005. Eurocode 3: Design of steel structures – Part 1-1: General rules and rules for buildings*. European Committee for Standardization, Brussels.

CEN (2005b). *EN 1993-1-8: 2005. Eurocode 3: Design of steel structures – Part 1-8: Design of joints.* European Committee for Standardization, Brussels.

CEN (2006). *EN 1993-1-5: 2006. Eurocode 3: Design of steel structures – Part 1-5: Plated structural elements.* European Committee for Standardization, Brussels.

CEN (2023). *FprEN 1993-1-8: 2023. Eurocode 3: Design of steel structures – Part 1-8: Design of joints.* European Committee for Standardization, Brussels.

CEN (2022). *prEN 1993-1-14: 2022. Eurocode 3: Design of steel structures – Part 1-14: Design assisted by finite element analysis.* European Committee for Standardization, Brussels.

Corman, A., (2022). Characterization of the full non-linear behavior up to failure of the sheared panel zone under monotonic loading conditions. PhD Thesis.

Jaspart JP, Weynand K, (2016). Design of Joints in Steel and Composite Structures, ECCS Press and Ernst & Sohn, Brussels, Belgium.

Jaspart, J., Corman, A., Demonceau, J. (2022). Mechanical Properties of the Component "Column Web in Compression" in Steel Beam-to-column Joints. Ce/Papers, 5(4), 242–250.

Jordão, S. (2008). Comportamento de juntas soldadas em nó interno com vigas de diferentes alturas e aço de alta resistência (in Portuguese) [PhD thesis]. http://hdl.handle.net/10316/7542

Johnson, G. R., & Cook, W. H. (1983). A Constitutive Model and Data for Metals Subjected to Large Strains, High Strain Rates, and High Temperatures. Proceedings 7th International Symposium on Ballistics, 19-21, 541–547.

Klein, H. (1985). Das elastisch-plastische Last-Verformungsverhalten M-v steifenlose, geschweisster Knoten für die Berechnung von Stahlrahmen mit HEB-Stützen (in German) [PhD thesis].

Oñate, E. (2009). Structural analysis with the finite element method. Linear statics: volume 1: Basis and Solids. Springer Science & Business Media.

Simões da Silva, L. (2008). Towards a consistent design approach for steel joints under generalized loading. Journal of Constructional Steel Research, **64**(9), pp.1059–1075.

Simulia, Abaqus User Manual, Dassault systems Simulia Corp., (2021) [online]. Last accessed 06/01/2023. Available at: https://help.3ds.com/HelpProductsDS.aspx

Yun, X., & Gardner, L. (2017). Stress-strain curves for hot-rolled steels. Journal of Constructional Steel Research, 133, 36-46.

Authors of Report	Responsible for the Institution
Assinado por: **Luís Alberto Proença Simões da Silva** Num. de Identificação: 04411525 Data: 2025.03.19 18:17:15 +0100 Prof. Luís Simões da Silva	Assinado por: **Carlos Alberto da Silva Rebelo** Num. de Identificação: 05621013 Data: 2025.03.19 12:24:32 +0000 CHAVE MÓVEL Prof. Carlos Rebelo
Firmado por CONDE CONDE, JORGE (FIRMA) el día 09/03/2025 con un certificado emitido por AC DNIE 006 Prof. Jorge Conde	
Assinado por: **FILIP LJUBINKOVIC** Num. de Identificação: TR:PT-7K18L9174 Data: 2025.03.05 14:48:56+00'00' Dr. Filip Ljubinković	
Assinado por: **João Pedro Simões Cândido Martins** Num. de Identificação: 12565838 Data: 2025.03.05 14:04:37+00'00' CHAVE MÓVEL Prof. João Pedro Martins	
Assinado por: **Ana Francisca Henriques Parente dos Santos** Num. de Identificação: 14075013 Data: 2025.03.05 12:51:58+00'00' Dra. Francisca Santos	
gov.br Documento assinado digitalmente FERNANDO FREIRE RIBEIRO Data: 05/03/2025 09:29:10-0300 Verifique em https://validar.iti.gov.br Mr. Fernando Freire	
Assinado por: **Juan Emanuel Aguiar da Silva Baptista** Num. de Identificação: 31425677 Data: 2025.03.05 12:15:19+00'00' Mr. Juan Aguiar	